

# **D1.4 – Improved Freshmaker Reference site**

**Improved Freshmaker reference site in  
Ovezande, the Netherlands (TRL8)**





**Title:** Improved Freshmaker Reference site (TRL8)

<b>Grant agreement no:</b>	642228
<b>Work Package:</b>	WP1.2
<b>Deliverable number:</b>	D1.4
<b>Partner responsible:</b>	KWR Watercycle Research Institute
<b>Deliverable author(s):</b>	Dr. Koen Zuurbier, Teun van Dooren MSc, Steven Ros MSc
<b>Quality assurance:</b>	Prof. Dr. Pieter Stuyfzand (KWR), Dr. Klaus Hinsby (GEUS)
<b>Planned delivery date:</b>	30 September 2017
<b>Actual delivery date:</b>	13 August 2018
<b>Dissemination level:</b>	<p>PU</p> <p><i>PU = Public</i></p> <p><i>PP = Restricted to other programme participants (including the Commission Services)</i></p> <p><i>RE = Restricted to a group specified by the consortium (including the Commission Services)</i></p> <p><i>CO = Confidential, only for members of the consortium (including the Commission Services)</i></p>

## Table of contents

Executive Summary .....	2
1. Introduction .....	3
Aims (this report).....	3
Note.....	3
2. Set-up of the Freshmaker system .....	5
2.1. ASR-strategy .....	5
2.2. Study area .....	5
2.3. The ASR-facility .....	8
2.4. Monitoring wells .....	9
2.5. Photographic impression .....	14
3. Characterization of the target aquifer .....	17
3.1. Approach .....	17
3.2. Aquifer characterization .....	17
3.3. Native groundwater characterization .....	17
4. Groundwater flow and transport model .....	21
4.1. Model set-up .....	21
4.2. Modelling strategy.....	22
5. Monitoring during operation.....	23
5.1. Water quantity analysis.....	23
5.2. Water quality analysis.....	23
5.3. Hydrological effects .....	23
5.4. Geophysical measurements .....	24
6. Results: Monitoring.....	25
6.1. Water quantity analysis.....	25
6.2. Water quality analysis: infiltration water .....	28
6.3. Water quality analysis: recovered freshwater (HDDW1).....	31
6.4. Water quality analysis: intercepted brackish groundwater (HDDW2).....	34
6.5. Hydrological effects .....	36
6.6. Geophysical measurements: CVES.....	40

6.6.1.	CVES-1: along the HDDWs (within Cycle 2016) .....	40
6.6.2.	CVES-2: perpendicular to the HDDWs (Cycle 2016) .....	42
6.6.3.	CVES-1: along the HDDWs (long-term effects: 2013-2016).....	43
6.6.4.	CVES-2: perpendicular to the HDDWs (long-term effects: 2013-2016).....	44
6.7.	Geophysical measurements: EM-39.....	45
7.	Results: Modelling .....	49
7.1.	Comparison field data and groundwater modelling.....	49
7.2.	Automated control unit.....	56
	Modelling of the automated control unit.....	56
	Practical implementation of the automated control unit in 2017 .....	58
7.3.	Maximum storage capacity at Ovezande.....	60
8.	Pre-treatment using river-bed filtration .....	63
9.	Low-cost HDDW: experiences with maintenance and replication .....	65
	Mechanical and chemical well regeneration Freshmaker.....	66
	Applied well regenerations, results.....	69
	Installation of new HDDWs at the Groede site .....	72
	Implications for the future use of HDDW technology for the Freshmaker.....	77
10.	Cost analysis Freshmaker Ovezande .....	79
11.	Conclusions .....	81
12.	References.....	83
A.	Appendix .....	85
	Water quality analysis: observed groundwater (MW1) .....	85

## Executive Summary

The Freshmaker Ovezande site has been operating from 2013 until 2017 (5 cycles). Based on the documentation and interpretation of the operation and analyses during these cycles, it was found that:

- The system was able to store and supply around 5 000 m<sup>3</sup> per year.
- The system has an estimated maximum storage and recovery capacity of 6 000 m<sup>3</sup>, based on groundwater modelling.
- Construction and maintenance of HDDWs and pre-treatment was identified as a key aspect for the success of a Freshmaker.
- A more robust and economically viable alternative for the Ovezande HDDWs was developed and successfully tested at the Groede site.
- Clogging of the shallow HDDW at the Freshmaker Ovezande was caused by insufficient pre-treatment (2013-2014) and biological growth in the well (2013-2017). Regeneration was successfully applied, but will (slightly) impact the operational costs.
- Further automation of the Freshmaker's operation via an automated control unit has been designed and is to be implemented in Ovezande and at future Freshmaker sites to automate the process of infiltration and interception.
- It was found based on modelling and field observations that the hydrological impacts of the Freshmaker on the surroundings are limited.
- The measurements and models suggest there is a stand-still situation or even gradual freshening of the groundwater at the Freshmaker site.
- Infiltration of surface water poses water quality risks, mainly related to pesticides in this agricultural region. By limiting the infiltration period to 15 November – 15 April (winter season), potential exceedances of pollutant's maximum concentrations can presumably be prevented.
- Based on the construction costs, operational and energy costs, and spatial claim on agricultural land, the Freshmaker provides an economically very interesting alternative for irrigation water supply, with an estimated cost price of 0.54 eur/m<sup>3</sup>.

## 1. Introduction

The Freshmaker pilot in Ovezande, the Netherlands, started in 2013 and will run until at least 2017. The aim at this SUBSOL reference site is to demonstrate the robustness and to improve the operation of the Freshmaker: maximize the freshwater recovery, while minimizing the saltwater interception and energy consumption. Additional focus is on the intake/pre-treatment of infiltrated stormwater runoff. The Ovezande Freshmaker consists of two 70 meter long horizontal wells (75 mm diameter) for additional infiltration of freshwater (upper well, 7 m depth) and abstraction of saltwater (lower well, 14.5 m depth). During the rainy season, 50 – 100 m<sup>3</sup> of fresh water can be infiltrated per m filter length, resulting in an additional freshwater storage of 3,500 – 7,000 m<sup>3</sup>, enough to provide the local farmer with irrigation water during summer. A pilot was executed in 2013/2014 and prolonged operation and achievement of TRL8 (actual system completed and qualified through test and demonstration) was the aim in the SUBSOL project. Therefore, the following activities were undertaken:

- Additional data collection and monitoring, enabling us to better test and document the efficiency of the Freshmaker under varying hydrological conditions. This extended monitoring also provided the necessary data to conclude on the expected lifespan and maintenance costs of the Freshmaker.
- Development of an automated central controlling unit to control and monitor the pre-treatment, infiltration, and recovery of the freshwater and the interception of the saltwater. This requires conversion of knowledge and knowhow from models and scientific expertise into operation software. This automation of Freshmaker control facilitates end-users in Freshmaker implementation (D1.4).
- Development of appropriate drilling strategies, well design, pre-treatment, and well regeneration to minimize the risk of HDDW failure.
- Modelling of the effects of the use of Freshmaker on the local / regional groundwater system. The Freshmaker may interfere with some of the targets set by the Water Framework Directive due to disposal of deeper, saline groundwater to the surface water system. These analyses provide the necessary input to develop a regulatory framework in close cooperation with local / regional authorities.

### Aims (this report)

The aim is to demonstrate the use of the Freshmaker for storage of seasonal freshwater surpluses in a freshwater lens in Ovezande, The Netherlands.

### Note

Information and description on the set-up and aquifer characterisation from earlier studies and publications was used to compile the first chapters of the report.



## 2. Set-up of the Freshmaker system

### 2.1. ASR-strategy

The Freshmaker in Ovezande was installed to improve freshwater management in coastal areas by aquifer storage and recovery (ASR), using two horizontal directional drilled wells (HDDWs). This technique enlarges, protects, and utilizes shallow fresh groundwater lenses by simultaneous saltwater abstraction and freshwater infiltration/recovery.

### 2.2. Study area

Ovezande is located in the coastal province of Zeeland, in the southwest of the Netherlands (Figure 2.1). Cross-sections through the regional subsurface are given in Figure 2.3 and Figure 2.4. The regional shallow subsurface (0 – 25 m-NAP) is dominated by marine deposits of salt marshes and creek ridges, formed during the Holocene sea level rise (formations NAWA and NWNZ). The shallow sediments can vary locally from clay and peat (mainly in salt marsh deposits) to fine sand (in creek ridges). Consequently, the presence of a permeable shallow subsurface is strongly influenced by this local distribution. The underlying sediments consist mainly of fine sands of aeolian origin (formation BX) and fine to coarse sands with intervening clay layers of fluvial and marine origin (formations EE, PZWA, and MS) that were deposited during the Pleistocene. Marine sands and clays of Pliocene and Miocene age are encountered deeper in the subsurface (formations BR and OO).

Due to the surrounding Scheldt estuaries and saline seepage, freshwater is scarce in the study area. Freshwater resources are limited to precipitation and local fresh groundwater lenses in sandy creek ridges (Figure 2.1).

The annual distribution of precipitation and evaporation is given in Figure 2.5 and is typical for a temperate oceanic climate. There is a clear seasonal variation visible in the net precipitation. This is mainly due to the seasonal variation of evaporation, since precipitation is more randomly distributed throughout the year. The annual sums of precipitation and evaporation amount to approximately 924 mm and 663 mm, respectively, resulting in a net annual precipitation 261 mm.

The Freshmaker pilot site in Ovezande is located on a 5 km wide sandy creek ridge that has a local surface level varying from 0.1 to 0.5 m above sea level (m ASL). Draining water courses on the creek ridge are deep with water levels of 0.6 to 0.7 m below sea level (m BSL). The creek ridge is surrounded by older peat and clay deposits with elevations ranging from 0 to 1.5 m BSL. Due to the higher elevation of the sandy creek ridge, a fresh groundwater lens can form in the subsurface, with groundwater flow being directed from the centre of the lens towards the surrounding peat and clay deposits. The phreatic groundwater level is largely controlled by precipitation and evapotranspiration on the creek ridge and is shown in Figure 2.2.

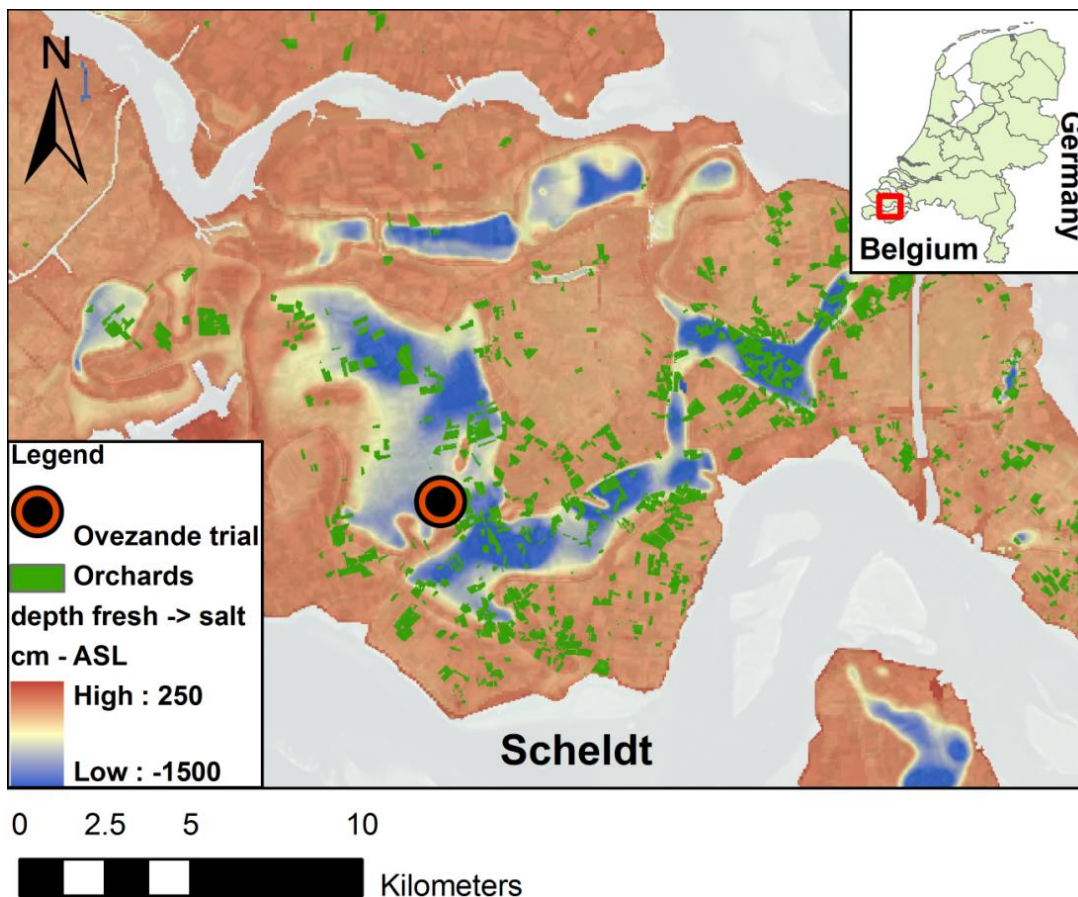


Figure 2.1: Overview of the study area. The depth of the fresh-salt interface that corresponds with a chloride concentration of 1000 mg/L indicates the distribution of natural fresh groundwater lenses around the Freshmaker pilot site in Ovezande.

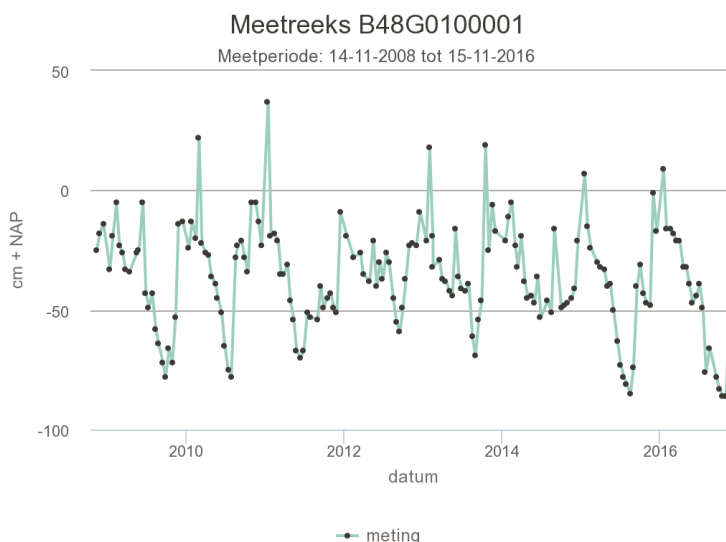


Figure 2.2: Typical phreatic groundwater level on the creek ridge at approximately 1 km southeast of the Freshmaker field site. cm+NAP = cm above sea level. Via: [www.grondwatertools.nl](http://www.grondwatertools.nl)

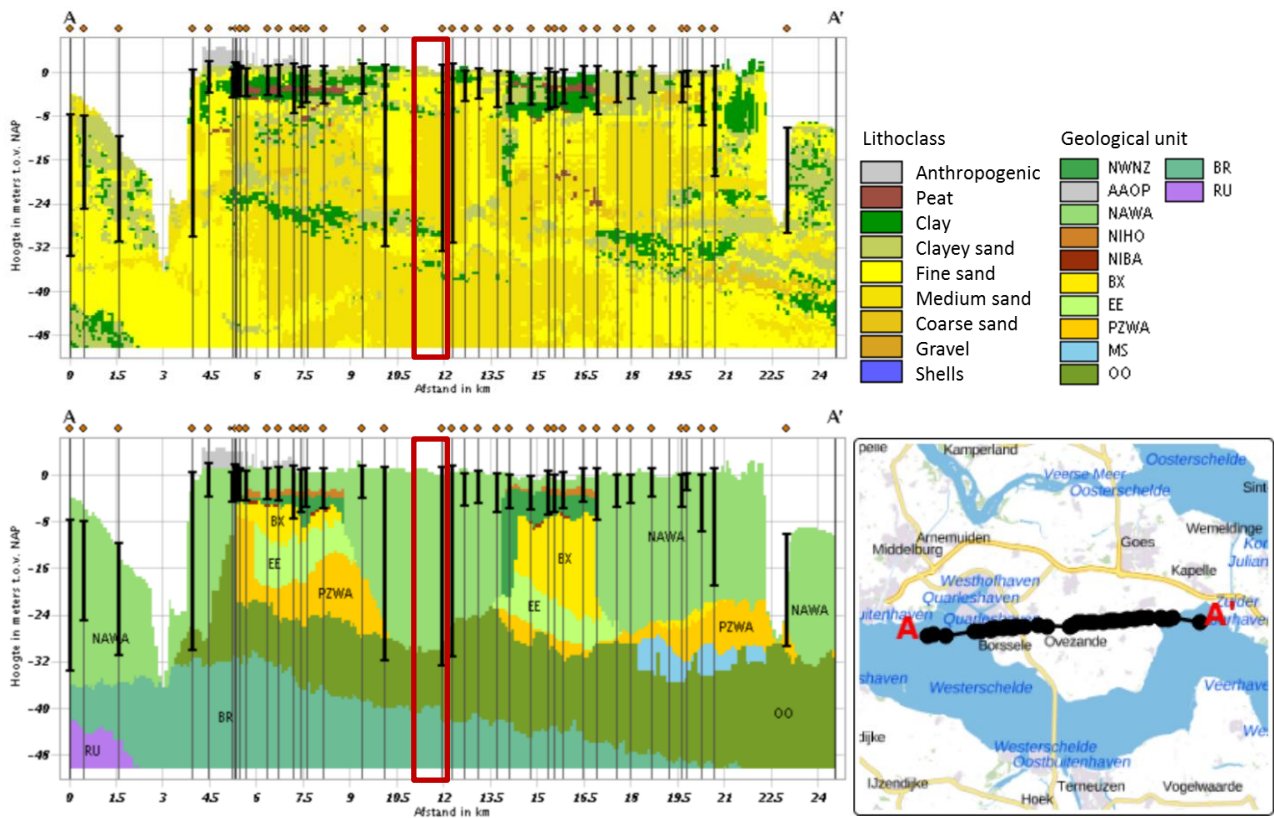


Figure 2.3: E-W cross-section (bottom-right) through the subsurface at Ovezande with most probable lithoclass (top-left) and corresponding geological units (bottom-left). The y-axis represents the depth in meters with respect to the Dutch reference sea level (NAP) and the x-axis represents the distance along the cross-section in kilometers. The red rectangles indicate the approximate location of the Freshmaker in Ovezande. The legend (top-right) represents the formations found within the subsurface, which are elaborated upon in the main text. The vertical line-segments and orange dots represent sediment core-drillings.

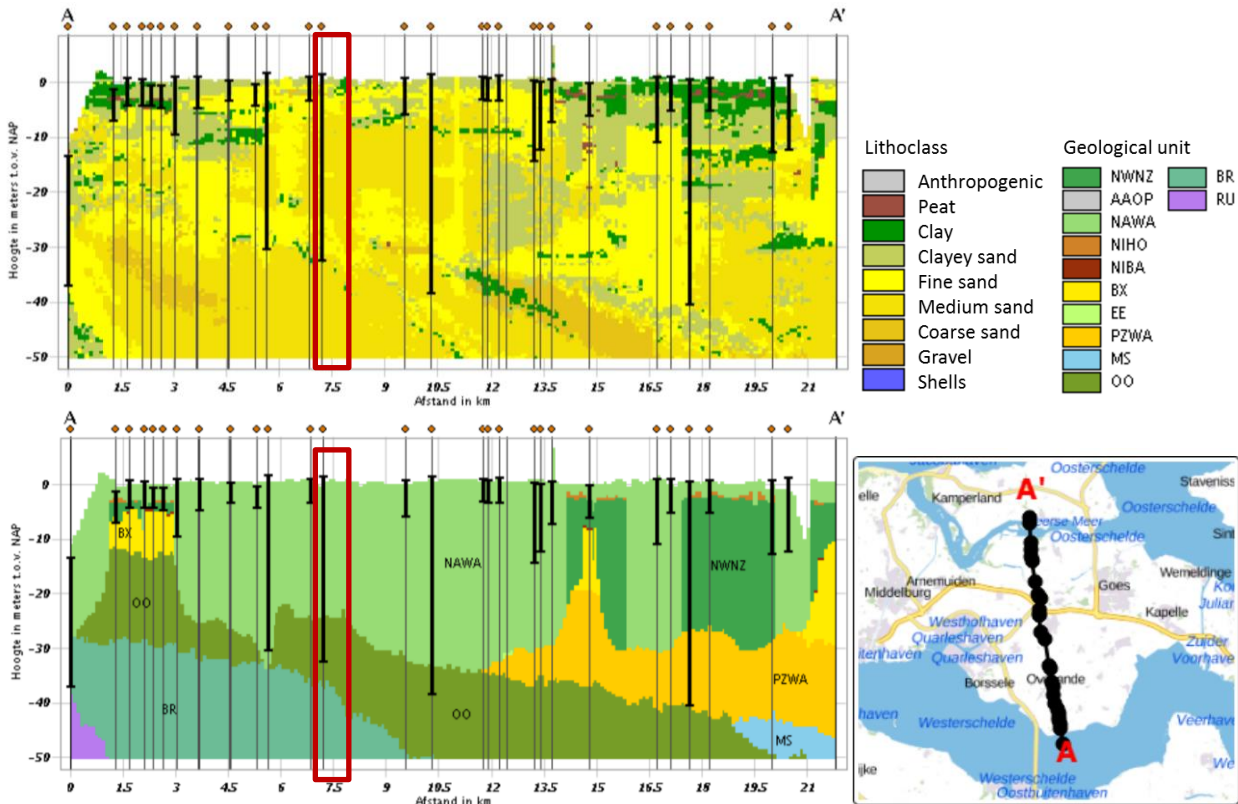


Figure 2.4: S-N cross-section (bottom-right) through the subsurface at Ovezande with most probable lithoclass (top-left) and corresponding geological units (bottom-left). The y-axis represents the depth in meters with respect to the Dutch reference sea level (NAP) and the x-axis represents the distance along the cross-section in kilometers. The red rectangles indicate the approximate location of the Freshmaker in Ovezande. The legend (top-right) represents the formations found within the subsurface, which are elaborated upon in the main text. The vertical line-segments and orange dots represent sediment core-drillings.

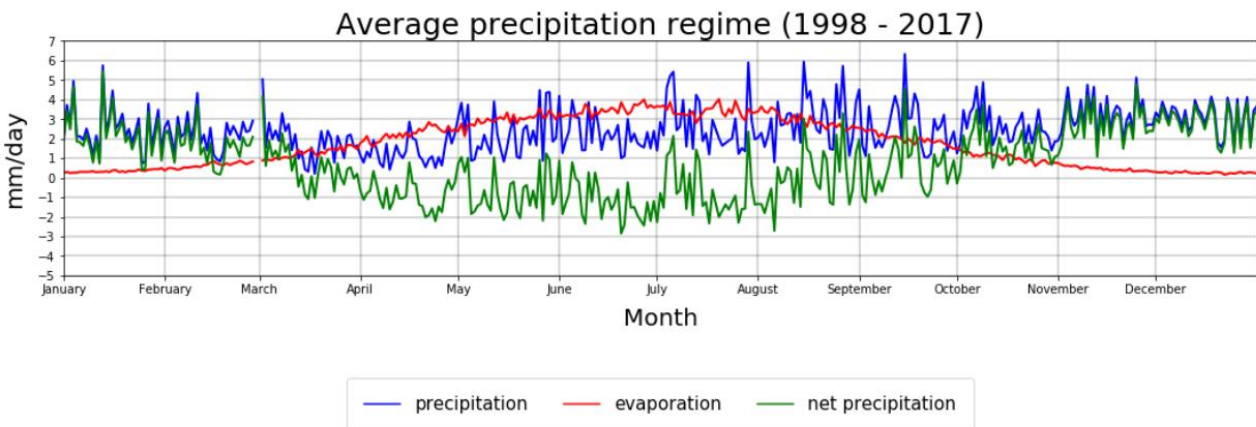


Figure 2.5: Average precipitation regime for Ovezande over the period 1998 - 2017. The net precipitation (precipitation – evaporation) is calculated from precipitation measured in Ovezande and from evaporation measured in Vlissingen.

### 2.3. The ASR-facility

In December 2012 (HDDW1) and March 2013 (HDDW2), horizontal directional drilling was used to create two open boreholes with a diameter of approximately 300 mm. The 70 m long

HDDW2 with a diameter of 75 mm and four rows with 10 mm holes at 10 cm intervals was wrapped with geotextile and installed in the deepest borehole at a depth of ~14.5 m below the land surface (Figure 2.6 and Figure 2.7). A perforated casing with a diameter of 125 mm and 8 rows of open holes of 10 mm at 10 cm intervals over a length of 70 m surrounded this HDDW during placement for protection and was left around the HDDW. The shallow HDDW1 had the same properties and was installed right above the deeper well at a depth of ~7 m below the land surface. At this HDDW, a non-perforated casing was used for protection during placement, which was removed after the HDDW was in place. The depth intervals of the target aquifer for the boreholes were based on cone penetration tests to ensure that the HDDWs were placed in sections with relatively high permeability, without intervening clay layers.

The freshwater surpluses from a nearby water course were stored in a ~4,000 m<sup>3</sup> basin in 2013 and the first half of 2014 (Figure 2.8 and Figure 2.9), to enable intake of large volumes of freshwater in periods with the highest discharge of fresh surface water in the water course, and to deal with potential variation in the supply. After (anticipated) settlement of fine suspended particles in the basin, water pumped from the top of the basin was filtrated with a 50 micron filter and was infiltrated into a freshwater lens through the shallow HDDW, using a 3 m high standpipe to provide a constant pressure for infiltration (Figure 2.9). Since November 2014, this basin settlement was replaced by a river bed-filtration system (Figure 2.8 and Figure 2.10).

The same shallow HDDW is used to recover the freshwater again during periods of water shortage (droughts or summers) (Figure 2.6). The shallow HDDW thus functions as a horizontal ASR well, enlarging and utilizing the shallow fresh groundwater lens. The fresh groundwater recovered by the Freshmaker is used for irrigation in the growing season at an orchard, where a maximum chloride concentration of 250 mg/l is allowed.

The deep HDDW is located below the shallow fresh groundwater lens and intercepts brackish groundwater. This interception well protects the shallow HDDW from salinizing. The intercepted brackish groundwater is discharged to the local watercourse, with a permitted maximum of 40 m<sup>3</sup>/d (Figure 2.9).

#### **2.4. Monitoring wells**

Several monitoring wells were installed around the HDDWs to determine the distribution and dynamics of the freshwater lens during operation of the Freshmaker (Figure 2.7 to Figure 2.9). The main properties of these monitoring wells are included in Table 2.1.

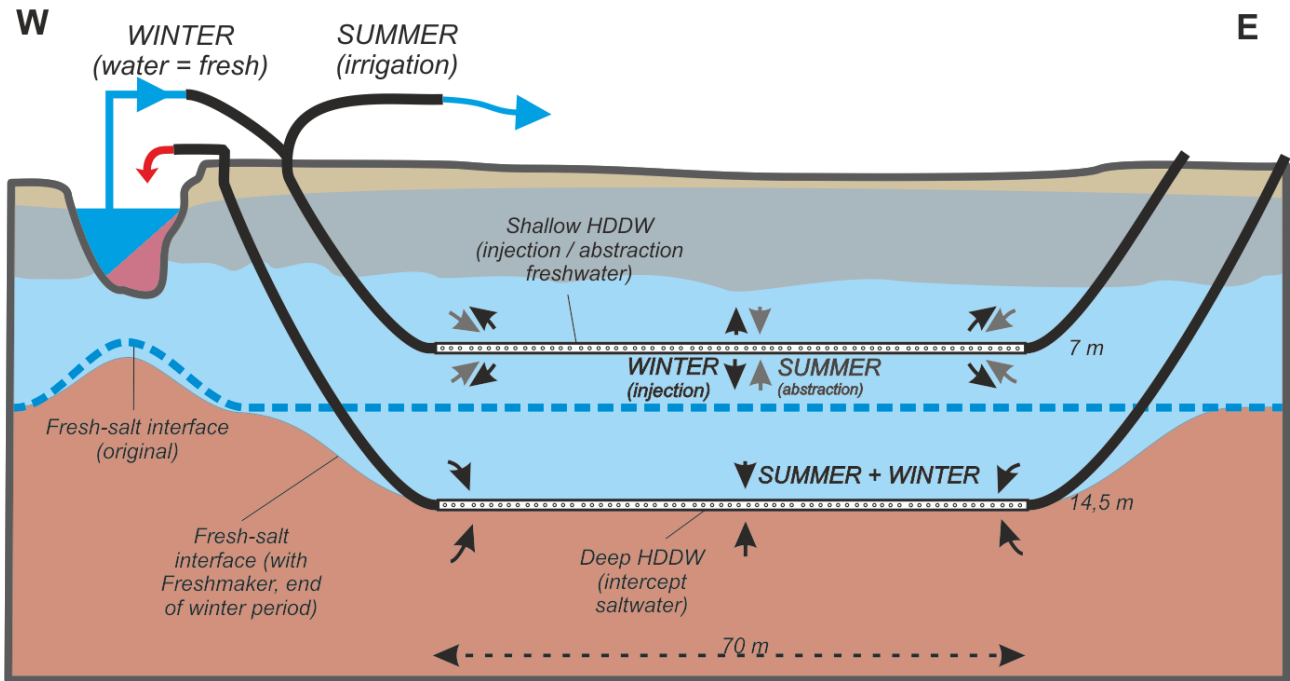


Figure 2.6: W-E cross-section of the Freshmaker set-up and operation at the Ovezande pilot site (MW = monitoring well, HDDW = horizontal directional drilled well).

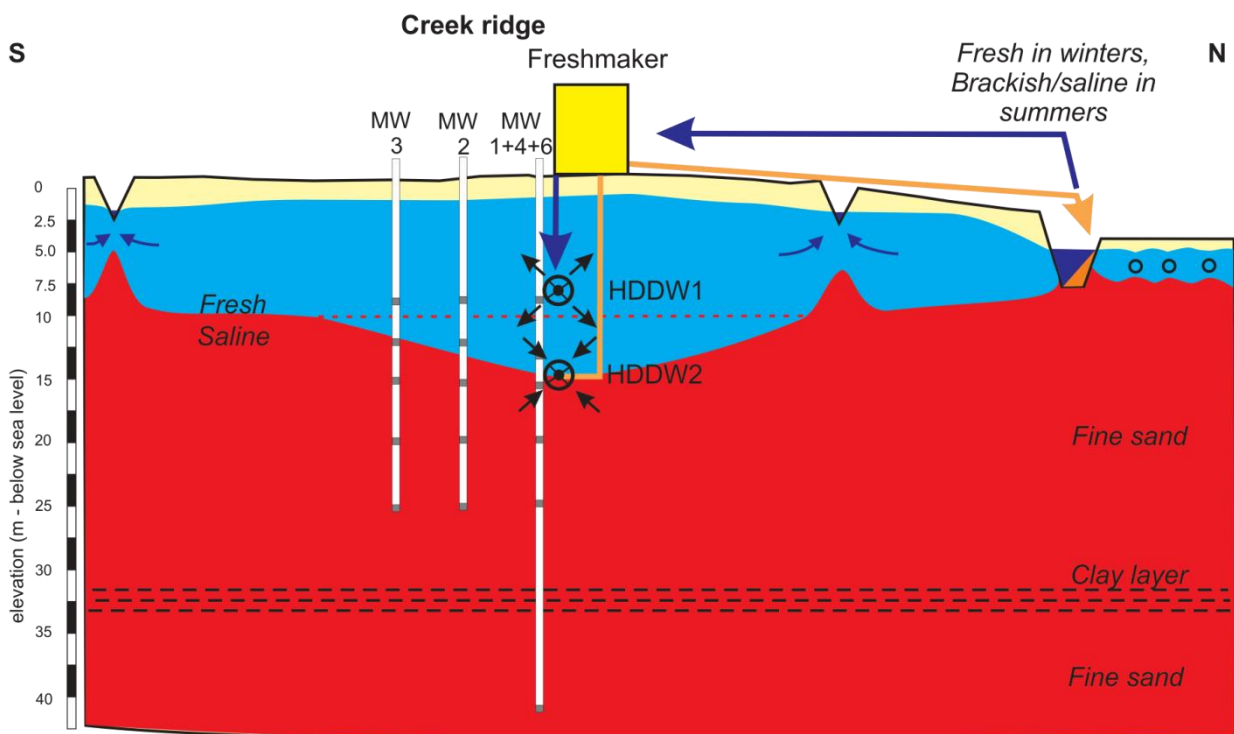


Figure 2.7: S-N cross-section of the Freshmaker set-up and operation at the Ovezande pilot site (MW = monitoring well, HDDW = horizontal directional drilled well).



Figure 2.8: Plan view of the Freshmaker set-up at the Ovezande pilot site. (HDDWs = horizontal directional drilled wells, CVES = continuous vertical electrical soundings, MW = monitoring well).

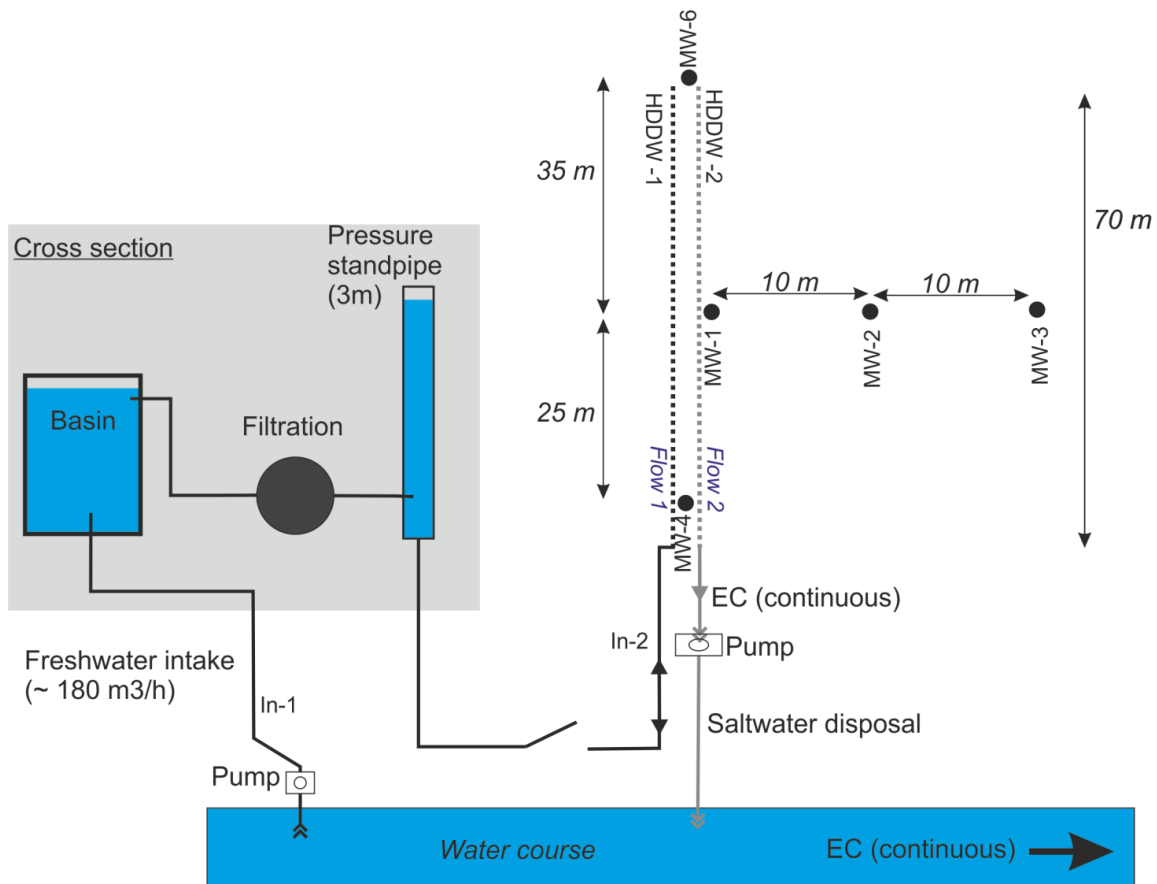
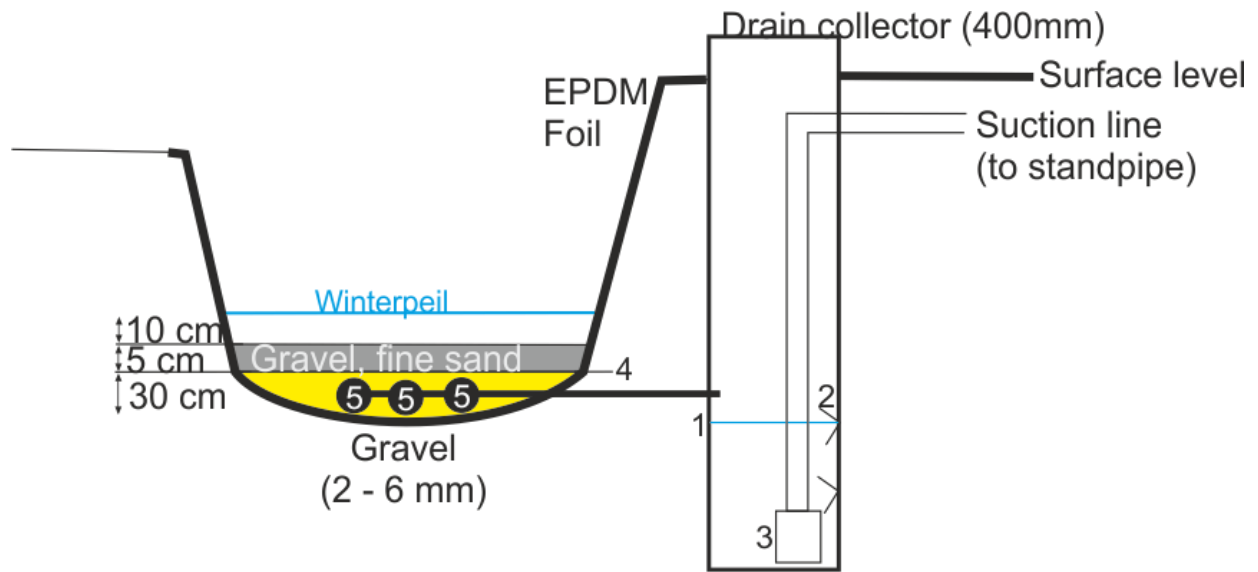


Figure 2.9: Schematic overview of the Freshmaker set-up at the Ovezande pilot site (intake as in 2013-2014).



1. Water level in collector
2. Sensors (max. and min. level)
3. One-way valve
4. Nylon foil
5. PE drains: L = 23 m / D=80 mm / Slots = 1.3 mm

Figure 2.10: Intake via river-bed filtration (since November 2014).

Table 2.1: Properties of the monitoring well screens (MW#-S#) around the Freshmaker system in Ovezande (Figure 2.7 to Figure 2.9).

Monitoring Well-Screens	X-Coordinate	Y-Coordinate	Land surface (m ASL)	Filter Top (m BSL)	Filter Bottom (m BSL)	Drilling method
MW1-S1	45222.59	384884.92	0.39	-7.10	-7.60	Bailer
MW1-S2	45222.64	384884.90	0.39	-12.13	-12.63	
MW1-S3	45222.58	384884.87	0.39	-15.14	-15.64	
MW1-S4	45222.61	384884.82	0.39	-19.14	-19.64	
MW1-S5	45222.70	384884.85	0.39	-24.11	-24.61	
MW1-S6	45222.67	384884.83	0.39	-38.11	-38.61	
MW2-S1	45226.54	384875.71	0.43	-8.11	-8.61	Bailer
MW2-S2	45226.52	384875.71	0.43	-12.11	-12.61	
MW2-S3	45226.56	384875.68	0.43	-15.12	-15.62	
MW2-S4	45226.45	384875.66	0.43	-19.12	-19.62	
MW2-S5	45226.51	384875.63	0.43	-24.11	-24.61	
MW3-S1	45228.78	384866.21	0.53	-8.01	-8.51	Direct push
MW3-S2	45228.91	384866.01	0.52	-12.01	-12.51	
MW3-S3	45229.04	384865.82	0.53	-15.00	-15.50	
MW3-S4	45229.19	384865.59	0.52	-18.99	-19.49	
MW3-S5	45229.32	384865.37	0.52	-23.95	-24.45	
MW4-S1	45193.07	384884.46	0.34	-8.23	-8.73	Bailer
MW4-S2	45193.06	384884.50	0.34	-12.22	-12.72	
MW4-S3	45193.09	384884.48	0.34	-15.21	-15.71	
MW4-S4	45193.05	384884.46	0.34	-19.23	-19.73	
MW4-S5	45193.01	384884.49	0.34	-24.21	-24.71	
MW5-S1	45335.08	384921.56	0.31	-8.24	-8.74	Direct push
MW5-S2	45335.25	384921.32	0.31	-12.23	-12.73	
MW5-S3	45335.36	384921.17	0.31	-15.23	-15.73	
MW5-S4	45335.86	384920.44	0.31	-19.29	-19.79	
MW5-S5	45335.66	384920.79	0.31	-24.21	-24.71	
MW6-S1	45261.96	384895.32	0.17	-8.38	-8.88	Direct push
MW6-S2	45262.11	384895.10	0.19	-12.34	-12.84	
MW6-S3	45262.21	384894.86	0.20	-15.36	-15.86	
MW6-S4	45222.35	384894.64	0.21	-19.35	-19.85	

## 2.5. Photographic impression

A photographic impression of the Freshmaker in Ovezande is presented in Figure 2.11 to Figure 2.14.



Figure 2.11: Drilling of the horizontal borehole (left) and the 75 mm HDPE well screens wrapped in geo-textile (middle) and the reamer used to create the 300 mm borehole (right)



Figure 2.12: Housing and impression of the central control unit.



Figure 2.13: Impression of the basin used for intake (2013-2014) and buffer for recovered water before sprinkler irrigation (left) and the location of the HDDWs (below surface level, right)



Figure 2.14: Realization (left) of the river-bed filtration system and the result (right)



### 3. Characterization of the target aquifer

#### 3.1. Approach

A detailed characterization of the target aquifer was obtained by:

- Using a 40 m deep bailer drilling at the centre of the HDDWs (MW1, Figure 2.8), with samples taken every 1 m.
- Preparing the samples using the method of Konert and Vandenberghe (1997).
- Using a HELOS/KR laser particle sizer (Sympatec GmbH, Germany) to derive the grain size distributions of the prepared samples.
- Using Bear (1972) to determine the hydraulic conductivity of the target aquifer from the measured grain size distribution.

A detailed characterization of the native groundwater in the target aquifer was obtained by:

- Recording the electrical conductivities in the aquifer at three locations (MW1, 2, and 4) prior to operation of the Freshmaker (January 2013) by geophysical borehole logging using a Robertson DIL-39 probe ('EM-39 (McNeill et al., 1990)). This allows to determine the exact location of the fresh-salt interface.
- Conducting continuous vertical electrical soundings (CVES) to map the lateral extent of the freshwater lens prior to operation of the Freshmaker (January 2013).
- Sampling all monitoring well screens prior to operation of the Freshmaker (December 2012), and analysing the samples similar to the water quality analyses during monitoring (see 'Monitoring during operation').

#### 3.2. Aquifer characterization

The target aquifer for the Freshmaker pilot is a relatively homogeneous phreatic aquifer that consists of fine to medium fine sand, with a mean grain size of 150 to 200  $\mu\text{m}$  (Figure 3.1). At a depth of about 30 m BSL, a 2 m thick clay layer separates the upper aquifer from a deeper sandy aquifer. Hydraulic conductivities of the target aquifer were estimated as ~5 to 10 m/d, which matches typical values for local creek ridge sediments.

#### 3.3. Native groundwater characterization

The CVES results indicated the original presence of a freshwater lens with a thickness of 0 to 10 m. This thickness is controlled by the elevation of the surface level and the seepage of saline groundwater towards the draining water course (Figure 3.2). Based on EM-39 measurements, the freshwater lens had a thickness of approximately 9 m and a mixing zone of approximately 6 m at the location of the HDDWs. Below this mixing zone, the high conductivities indicated the presence of groundwater with a salinity equal to local seawater, which has a chloride concentration of approximately 16,800 mg/l. These observations are confirmed by the observed chloride concentration profile at each monitoring well (Figure 3.3).

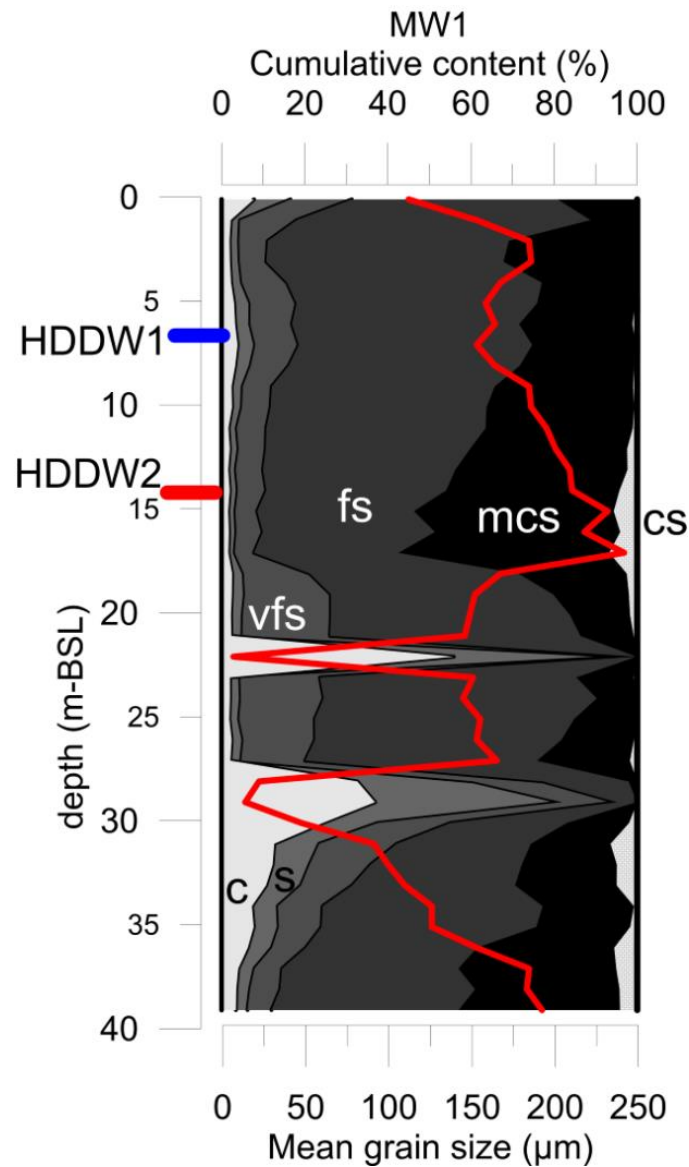


Figure 3.1: Cumulative grain size distribution in the target aquifer at MW1 (c = clay, s = silt, vfs = very fine sand, fs = fine sand, mcs = medium coarse sand, cs = coarse sand). The mean grain size is indicated in red.

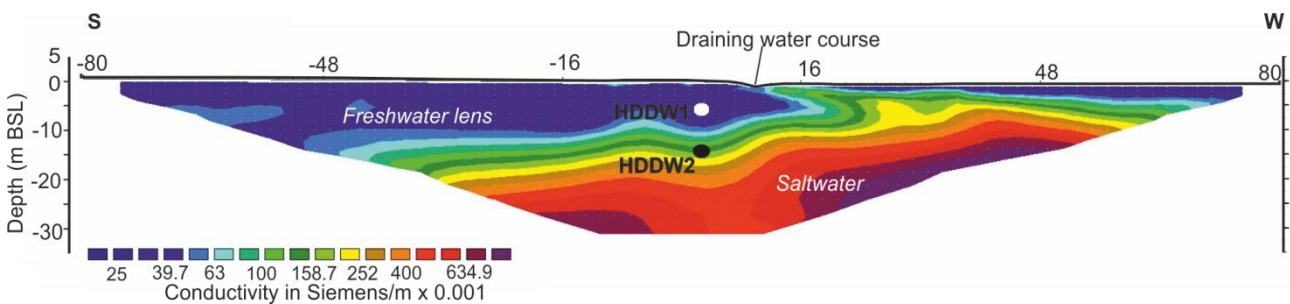


Figure 3.2: Continuous vertical electrical sounding (CVES) at the Ovezande field site, before the start of the pilot. The positions of the HDDWs are marked white (upper: HDDW1) and black (deeper: HDDW2). The higher the conductivity (red colours), the more saline the groundwater.

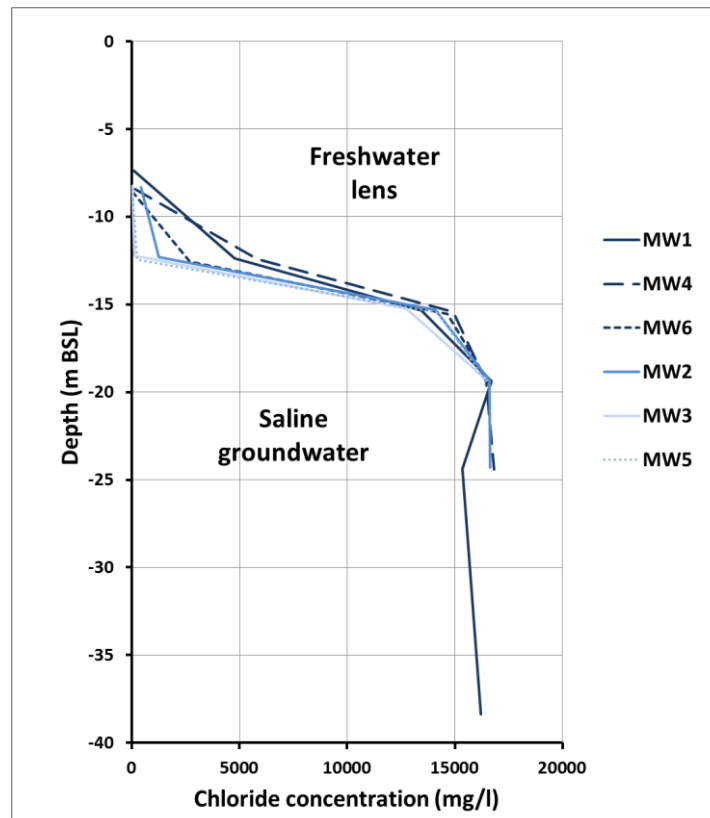


Figure 3.3: Chloride concentration profiles at each monitoring well, observed on December 12, 2012, prior to operation of the Freshmaker.

The typical hydrogeochemical groundwater compositions of the freshwater lens and the ambient brackish groundwater are given in Table 3.1. The EC, and concentrations of Na, K, Ca, Mg, Cl, and  $\text{SO}_4$  are especially useful for characterization of both water types regarding the salinity. Temperatures of both water types are comparable. Both water types are anoxic. The brackish water is marked by high Fe and Mn concentrations. The freshwater is high in As, which is common for shallow groundwater and surface water in the area. The groundwater is marked by a high alkalinity. The freshwater shows signs of freshening, indicated by the relatively low concentrations of Cl with respect to Na. This is a common phenomenon during the formation of a freshwater lens.

Table 3.1: Typical hydrogeochemical composition of freshwater in the shallow freshwater lens and of saline groundwater underneath, based on average concentrations in the monitoring wells on December 12, 2012. EC-25 Field is the electrical conductivity measured in the field with a reference temperature of 25°C. The presence of NO<sub>3</sub> in the saltwater can be a result of inaccuracy during analysis as a consequence of necessary dilution and nitrification of NH<sub>4</sub> in the lab.

Sample code	Freshwater lens (at 8.2 m BSL)	Saline groundwater (at 19.2 - 24.4 m BSL)
EC-25 Field (µS/cm)	1058	38960
Temperature (°C)	11.2	11.1
pH (Field)	8.1	7.2
Na (mg/L)	187.8	7712.9
K (mg/L)	53.1	400.8
Ca (mg/L)	24.1	622.9
Mg (mg/L)	44.4	1133.4
Fe (mg/L)	0.5	21.0
Mn (mg/L)	0.1	1.1
Cl (mg/L)	72.0	16446
SO <sub>4</sub> (mg SO <sub>4</sub> /L)	31.8	1960
HCO <sub>3</sub> (mg HCO <sub>3</sub> /L)	690.3	771
NO <sub>3</sub> (mg N/L)	0.1	1.4
PO <sub>4</sub> -t (mg P/L)	13.4	11.2
NH <sub>4</sub> (mg/L)	6.8	16.5
SiO <sub>2</sub> (mg/L)	40.1	31.5
As (µg/L)	11.9	1.1
Zn (µg/L)	2.5	24.1

## 4. Groundwater flow and transport model

### 4.1. Model set-up

Before the implementation of the Freshmaker, a 2D SEAWAT (Langevin et al., 2007) model was built to analyse the performance of the Freshmaker set-up for a typical seasonal ASR scheme. During the implementation of the Freshmaker pilot in Ovezande, this 2D SEAWAT model was calibrated on actual field measurements, by mimicking the fresh-salt interface dynamics observed in Ovezande (Van der Linde, 2015). The results of this calibration are given in Table 4.1. The aquifers are relatively homogeneous and isotropic (anisotropy = 1). Draining water courses were simulated using MODFLOW's river package (Harbaugh, 2005). Aquifer recharge (precipitation minus evapotranspiration) applied to the upper boundary of the model was assumed 0.466 mm/d throughout the year, neglecting seasonal variations in phreatic water levels. In reality, the aquifer recharge is only positive from August to March. For more information regarding the SEAWAT groundwater flow model, the reader is referred to Zuurbier et al. (2015) and Van der Linde (2015). The modelled operational period is from 18 June 2013 until 6 September 2017.

Table 4.1: Calibrated properties of the SEAWAT model constructed for the Freshmaker set-up in Ovezande. ASL is the abbreviation of above sea level.

Model property	Value
Top elevation (m ASL)	Varies between 1.5 and -0.16 m
Bottom elevation (m ASL)	-63.5
Thickness of the cross sectional model slice (m)	10
Horizontal extent (m)	1690
Hydraulic conductivity of the semi confining layer (m/d)	0.45
Hydraulic conductivity of aquifer 1 (m/d)	2.5
Resistance of the clay aquitard (d)	4000
Hydraulic conductivity of aquifer 2 (m/d)	2.5
Porosity (-)	0.3
Specific yield (-)	0.25
Longitudinal dispersivity (m)	0.33
Storativity ( $m^{-1}$ )	0.0001
Vertical anisotropy (-)	1
Conductance river bottom ( $m^2/d$ ) (river 1,2,3,4 from left to right in Figure 4.1)	1000, 2, 10, 33

A 3D SEAWAT model was subsequently constructed on the basis of the calibrated 2D model (Van der Linde, 2015). This is a semi-domain model mirrored over the X-axis. The domain of this 3D model is given in Figure 4.1. The HDDWs are situated in the Y-direction (figure coordinates:  $X = 841.;$   $-410. < Y < -445.$ ). The blue lines indicate draining water courses.

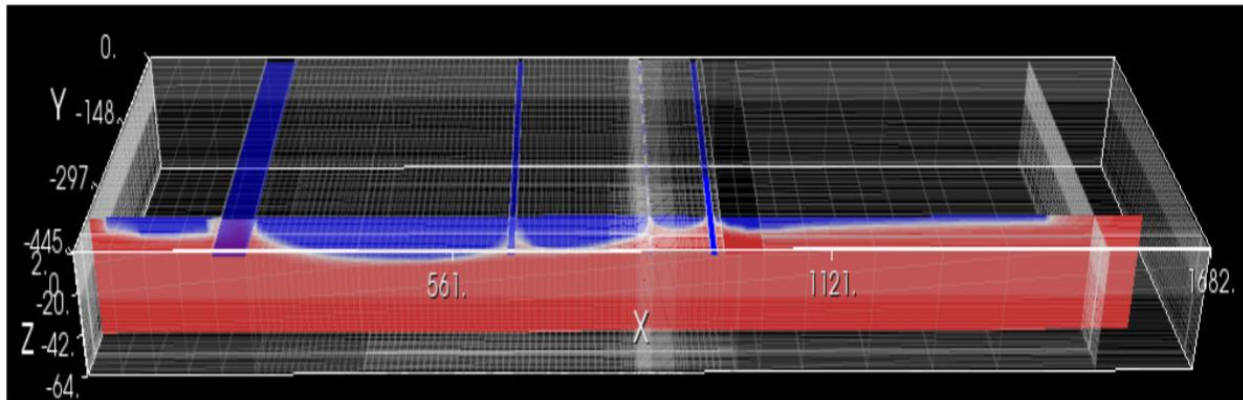


Figure 4.1: Domain and grid of the 3D SEAWAT model constructed for the Freshmaker at Ovezande, The initial chloride concentration distribution is also given (blue = low (fresh), red = high (saline)) (Van der Linde, 2015). Blue lines are draining water courses.

## 4.2. Modelling strategy

The calibrated 3D density-dependent groundwater flow model is currently used to simulate the Freshmaker implementation at the Ovezande field site. The main aim of the model is to determine whether the results of the computer model are in line with real field data; to predict future performance, and to assess the hydrological effects in the surroundings.

Starting from a reference situation, several scenarios were simulated with the 3D SEAWAT model by adjusting the operational and hydrogeological parameters. This allowed to determine the effect of the controlling parameters on the recovery efficiency, which is an important prerequisite for optimization of the Freshmaker implementation.

The results of this sensitivity analysis subsequently allowed to determine the optimal combination of pumping rates in both HDDWs and to determine the maximum freshwater storage and recovery capacity of the Freshmaker in Ovezande. This is especially valuable for prediction of its future performance, which allows to conclude on the suitability of the Freshmaker as a technique to improve freshwater management in coastal areas.

## 5. Monitoring during operation

### 5.1. Water quantity analysis

The pumped volumes were measured by Bermad (Bermad BV, The Netherlands) mechanical water meters in the infiltration line (filling the standpipe and thereby HDDW1) and the discharge lines of HDDW1 and HDDW2 (right behind the pump). Due to absence of automated logging, the cumulative water volumes were noted directly from the water meter. This was done during every site visit by KWR, by the installer (Meeuwse Goes BV), and by the fruit grower.

Between May and August, a malfunctioning water meter in the discharge line of HDDW2 caused a gap in the data collection. The meter was repaired in August 2017.

### 5.2. Water quality analysis

Water samples were frequently obtained from the infiltration water, HDDW1, HDDW2, MW1, MW2, MW4, and MW6. All samples were analysed in the field in a flow-through cell for EC (GMH 3410, Greisinger, Germany), pH, temperature (Hanna 9126, Hanna Instruments, USA), and dissolved oxygen (DO) (Odeon Optod, Neotek-Ponsel, France). The samples were filtrated using 0.45 µm cellulose acetate membranes (Whatman FP-30, UK) in the field and sent to the VU University Water Lab (2012-2015) and the WUR University Water Lab (2015-2017). Here, the macrochemical composition was analysed. At the VU University, samples were stored in two 10-ml plastic vials, of which one was acidified with 100 µl 65% HNO<sub>3</sub> (Suprapur, Merck International) for analysis of cations (Na, K, Ca, Mg, Mn, Fe, S, Si, P, and trace elements) using ICP-OES (Varian 730-ES ICP OES, Agilent Technologies, U.S.A.). The other 10 ml vial was used for analysis of F, Cl, Br, NO<sub>2</sub>, NO<sub>3</sub>, PO<sub>4</sub>, and SO<sub>4</sub> using the Dionex DX-120 IC (Thermo Fischer Scientific Inc., USA), and NH<sub>4</sub> using the LabMedics Aquakem 250 (Stockport, UK). All samples were cooled to 4°C immediately after sampling. At the WUR university, 100 ml samples with filtrated samples were used for ICP-AES (Al, Ca, Fe, K, Mg, Mn, Na, P, S, Zn, Si) and ICP-MS (As) upon Aqua-Regia extraction, Segmented Flow Analyzer (NH<sub>4</sub>, NO<sub>3</sub>+NO<sub>2</sub>, PO<sub>4</sub>), Flow Injection Analyzer (Cl), and Shimadzu analyzer (TC, IC).

### 5.3. Hydrological effects

MW1.0 (phreatic groundwater), MW1.1 and MW1.2 were equipped with CTD divers (Schlumberger Water Service, The Netherlands), measuring pressure, temperature, and electrical conductivity (EC). A CTD diver was also used to keep track of the water column in the 3 m high standpipe, which can be considered the injection pressure on HDDW1. The measurement frequency of these divers was 15 minutes. A barometer was placed in order to correct for changes in air pressure with measurements every hour. During sampling, hand measurements were done to validate the data produced by the divers. Barometer corrected values for the hydraulic head and the water column in the standpipe were used to validate hydrological effects, in combination with 3D density-dependent groundwater flow modelling.

#### **5.4. Geophysical measurements**

Continuous vertical electrical soundings (CVES) were conducted to construct profiles of the electrical resistivity of the subsurface. This was done in March 2016 and October 2016 in order to analyse the development of the freshwater lens in one ASR cycle, and in January 2013 to measure the reference situation. This was used to determine the long term development of the freshwater lens.

In addition, electrical conductivity profiles were constructed by geophysical borehole logging (EM-39) to determine the development of the fresh-salt interface during different phases of consecutive ASR cycles of the Freshmaker operation from 2013 till 2016.

## 6. Results: Monitoring

### 6.1. Water quantity analysis

The volumes of freshwater infiltrated through and recovered from HDDW1, the resulting net volume of infiltrated freshwater, and the cumulative volume of brackish groundwater intercepted by HDDW2 are given for the total period of measurement (17 June 2013 until 6 September 2017) as cumulative volumes (Figure 6.1 to Figure 6.5) and seasonal volumes (Figure 6.6 to Figure 6.9). The statistics of these figures are also tabulated in Table 6.1.

During the first year of operation (2013/2014), the Freshmaker was still in its start-up phase. In 2014, the infiltrated volume of freshwater was completely recovered for the pilot. Since then, the Freshmaker infiltrated as much freshwater as possible into the subsurface in times of surplus, and recovered the required amount of freshwater again only in times of demand. In 2017, almost all of the freshwater that was previously infiltrated was recovered for use in the dry springtime, resulting in a recovery efficiency of >100%.

On average, almost 5,000 m<sup>3</sup> is infiltrated per year and more than 4,600 m<sup>3</sup> is recovered, resulting in a recovery efficiency of the freshwater of 94%. To protect the freshwater from the underlying saltwater, an average interception of 10,600 m<sup>3</sup>/yr was required.

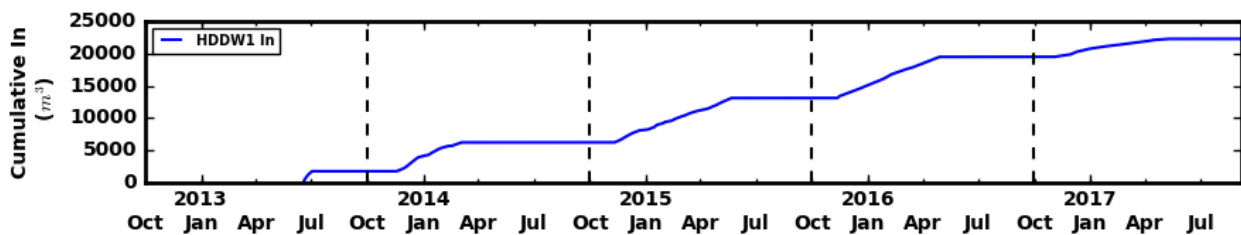


Figure 6.1: Cumulative volume (m<sup>3</sup>) of freshwater infiltrated through HDDW1 from 17 June 2013 until 6 September 2017.

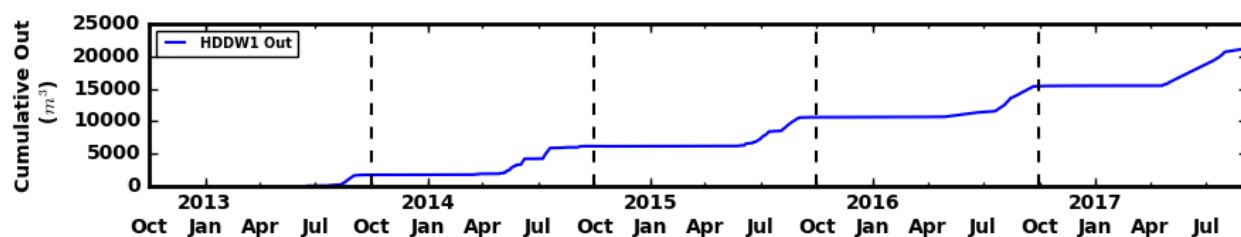


Figure 6.2: Cumulative volume (m<sup>3</sup>) of freshwater recovered from HDDW1 17 June 2013 until 6 September 2017.

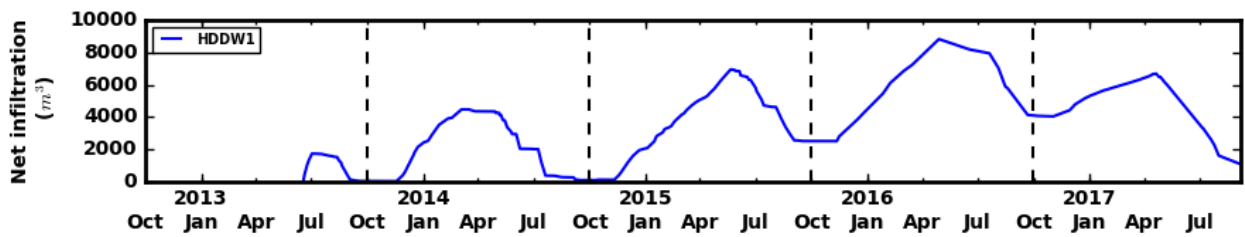


Figure 6.3: Net volume (m<sup>3</sup>) of freshwater infiltrated through HDDW1 from 17 June 2013 until 6 September 2017.

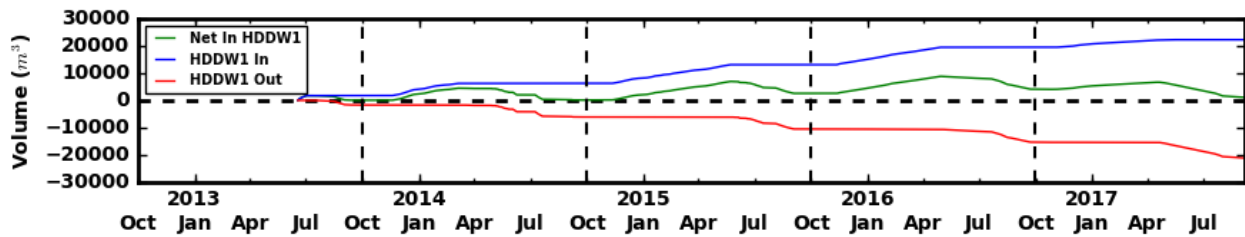


Figure 6.4: Cumulative volume (m<sup>3</sup>) of freshwater infiltrated through and recovered by HDDW1 and its resulting net volume of freshwater infiltrated from 17 June 2013 until 6 September 2017.

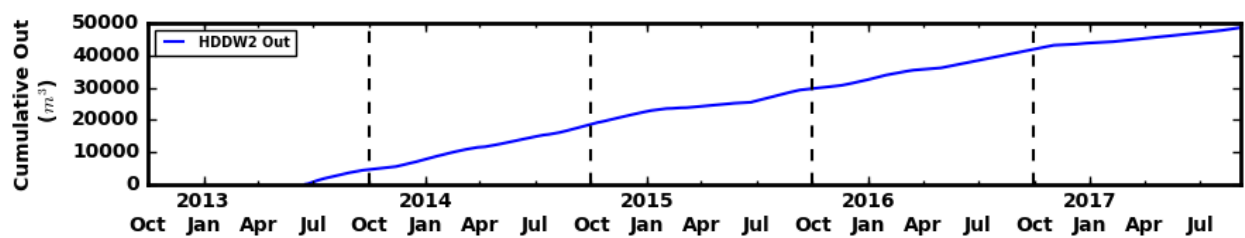


Figure 6.5: Cumulative volume (m<sup>3</sup>) of brackish water intercepted by HDDW2 from 17 June 2013 until 6 September 2017. Due to a malfunctioning water meter at HDDW2, no pumping was recorded between May and August 2017. This was corrected for by extrapolating, using the average abstraction rate between 2 February 2017 and 8 May 2017.

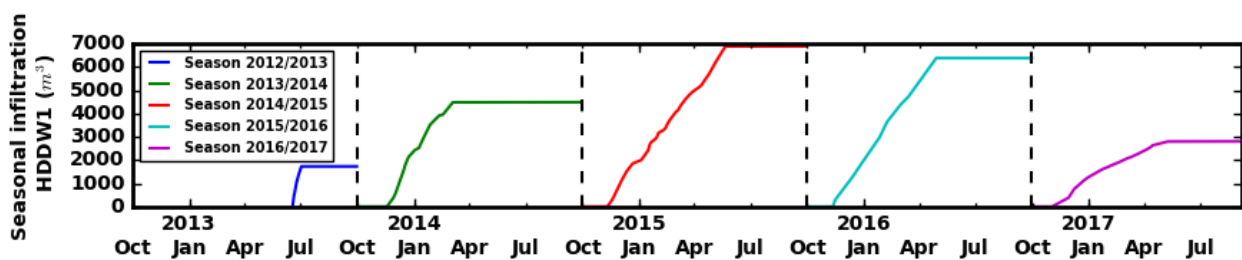


Figure 6.6: Seasonal infiltration of freshwater (m<sup>3</sup>) by HDDW1 from 17 June 2013 until 6 September 2017.

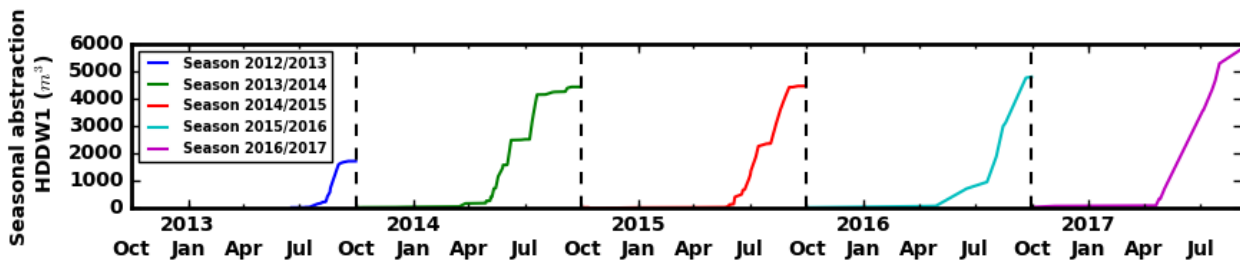


Figure 6.7: Seasonal abstraction of freshwater (m<sup>3</sup>) by HDDW1 from 17 June 2013 until 6 September 2017.

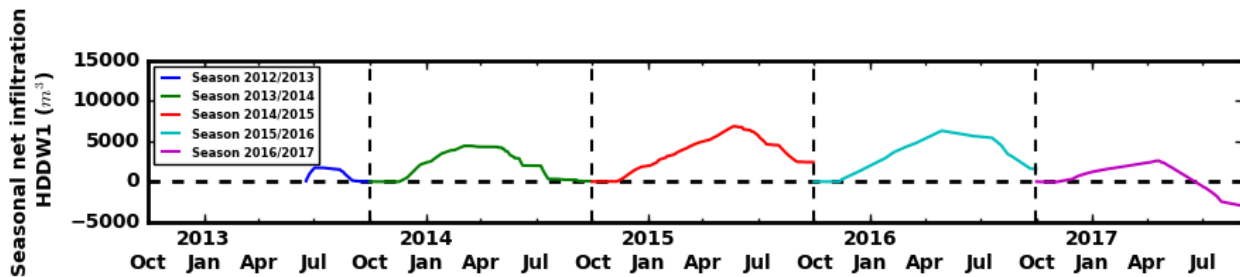


Figure 6.8: Seasonal net infiltration of freshwater (m<sup>3</sup>) by HDDW1 from 17 June 2013 until 6 September 2017.

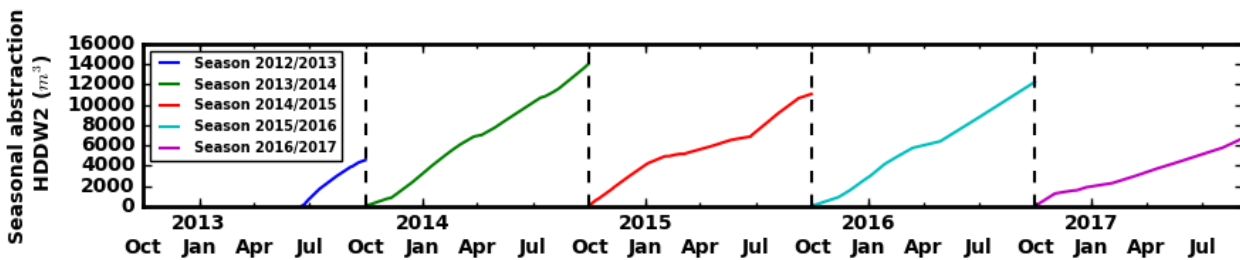


Figure 6.9: Seasonal abstraction of brackish water (m<sup>3</sup>) by HDDW2 from 17 June 2013 until 6 September 2017.

Table 6.1: Operational performance of the Freshmaker in Ovezande for every hydrological year (Oct 1 – Sep 30) from 2012 until 2017. The recovery efficiency is calculated as the percentage of infiltrated freshwater that is recovered by HDDW1.

Hydrological year	Volume of freshwater infiltrated (m <sup>3</sup> ) (HDDW1)	Volume of freshwater recovered (m <sup>3</sup> ) (HDDW1)	Net volume of freshwater infiltrated (m <sup>3</sup> ) (HDDW1)	Recovery efficiency of HDDW1	Volume of brackish groundwater intercepted (m <sup>3</sup> ) (HDDW2)
2012/2013	1728.1	1704	24.1	98.6%	4545.9
2013/2014	4482.6	4425.6	57.0	98.7%	14011.6
2014/2015	6882.6	4458.3	2424.3	64.8%	11065.4
2015/2016	6376.7	4793.4	1583.3	75.2%	12256.2
2016/2017	2801	5818	-3017	207.7%	6714
<b>Total (m<sup>3</sup>)</b>	<b>22271</b>	<b>21199.3</b>	<b>1071.7</b>	<b>95.2%</b>	<b>48593.1</b>
<b>Average (m<sup>3</sup>/year)</b>	<b>4938.7</b>	<b>4641.3</b>	<b>297.4</b>	<b>94.0%</b>	<b>10635.3</b>

## 6.2. Water quality analysis: infiltration water

The average water quality of the infiltration water was determined from 19 samples taken between 2013 and 2017 (Table 6.2). The temporal variation of the infiltration water quality was also determined for the operation of the Freshmaker (Figure 6.10 to Figure 6.12).

Although the EC is slightly higher than the EC of the freshwater lens (Table 3.1), it is still low and the water can be considered as freshwater in terms of its EC with respect to drinking and irrigation water limits. This is confirmed by the low concentrations of Na and Cl. EC and pH remain fairly constant throughout the operation of the Freshmaker, but temperature has a seasonal variation. The water infiltration water was always oxidic. Most of the concentrations of dissolved substances in the infiltrated freshwater remain fairly constant as well. Ca and HCO<sub>3</sub> vary over time due to variation in the contribution of overland flow and draining groundwater to the discharge of the water course. However, they are always fairly high with respect to, for instance, drinking water limits, which is a consequence of high Ca and HCO<sub>3</sub> concentrations in the shallow groundwater.

All average concentrations of natural substances in the infiltrated freshwater remain below the legal limits set by the Water Act of The Netherlands which is valid during operation, except for As and Zn. Zn significantly exceeded the legal limit a few times. One observation of 1061 µg/l resulted in an average infiltration concentration above the legal limits.

Arsenic is naturally present in the subsurface of this coastal area of the Netherlands with young, organic-rich marine sediments. This can also be derived from the hydrogeochemical characterization of the freshwater lens (Table 3.1). Therefore, the exceedance of the legal limit of As in infiltration water is not considered to be hazardous for the subsurface. However, crops can suffer from irrigation water with elevated As-concentrations. The recommended limit and guideline for As in reclaimed water for long-term irrigation is 100 µg/L (Ayers and Westcott, 1976; Fipps, 2003; Rowe and Abdel-Magid, 1995) and the toxicity is as low as 50 µg/L for vulnerable crops like rice. Section 6.3 will clarify that the concentration of As in recovered water remains well below these limits after infiltration with water having slightly elevated As-concentrations.

Table 6.2: Observed infiltration water quality averaged over 19 measurements between 2013 and 2017, tabulated together with the legal limits set by the Water Act of The Netherlands in 2017. EC-25 Field is the electrical conductivity measured in the field with a reference temperature of 25°C.

Sample code	Average 2013-2017	Legal limits Water Act, The Netherlands, 2017
EC-25 Field (µS/cm)	1097	-
Temperature (°C)	10.4	-
pH (Field)	8.0	-
DO (mg/L)	7.24	-
Na (mg/L)	88.2	120
K (mg/L)	23.3	-
Ca (mg/L)	128.6	-
Mg (mg/L)	26.4	-
Fe (mg/L)	0.1	-
Mn (mg/L)	0.1	-
NH <sub>4</sub> (mg NH <sub>4</sub> /L)	0.3	3.2
Cl (mg/L)	108.7	200
SO <sub>4</sub> (mg SO <sub>4</sub> /L)	80.0	150
HCO <sub>3</sub> (mg HCO <sub>3</sub> /L)	470.2	-
NO <sub>3</sub> (mg N/L)	6.8	24.8
PO <sub>4</sub> -t (mg P/L)	0.7	1.25
As (µg/L)	13.1	10
Zn (µg/L)	73.7	65

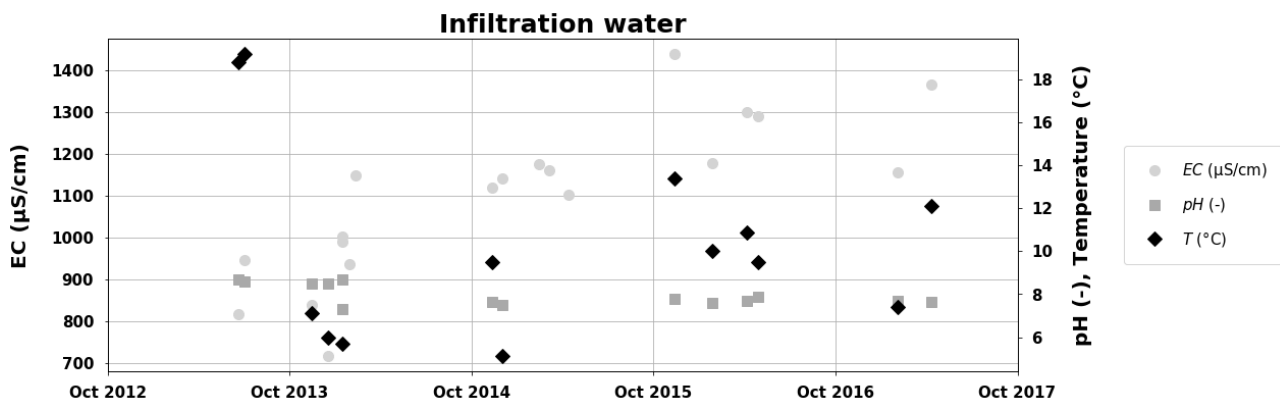


Figure 6.10: Electrical conductivity (EC in µS/cm), pH (-), and temperature (Temp in °C) of the freshwater infiltrated into the fresh groundwater lens through HDDW1.

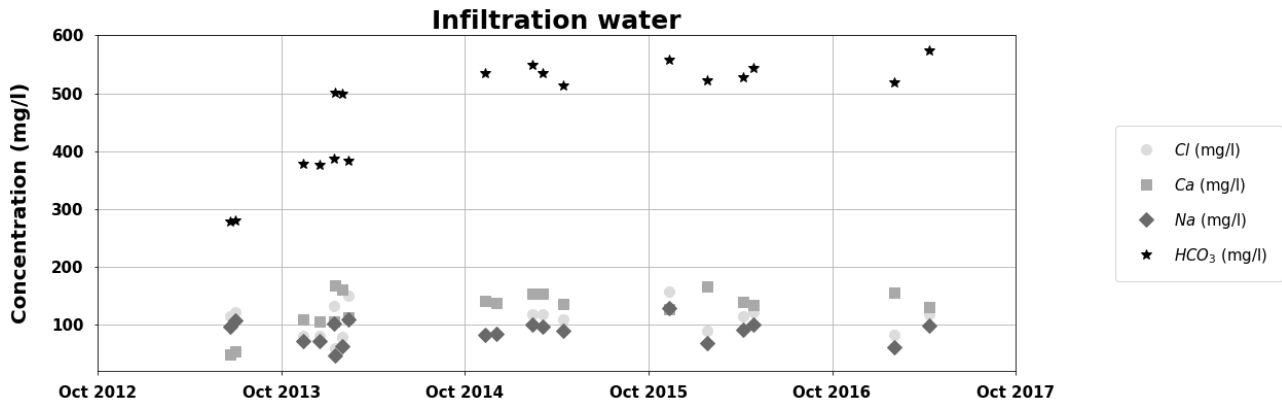


Figure 6.11: Concentrations of Cl, Ca, Na, and HCO<sub>3</sub> in the freshwater infiltrated into the fresh groundwater lens through HDDW1.

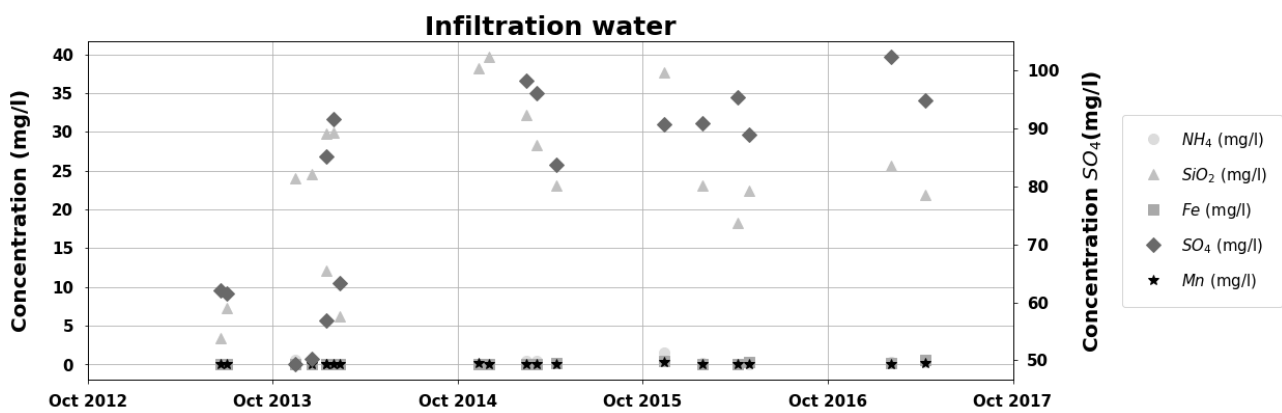


Figure 6.12: Concentrations of NH<sub>4</sub>, SiO<sub>2</sub>, Fe, SO<sub>4</sub>, and Mn in the freshwater infiltrated into the fresh groundwater lens through HDDW1. Be aware that the concentrations of SO<sub>4</sub> are plotted on the secondary (right) y-axis.

The infiltration water at the Freshmaker site could be contaminated with pesticides, which are frequently used in agricultural areas and may find their way to the surface water. Therefore, specific samples were taken by the Eurofins lab and analysed on the presence of pesticides (2013-2017) and other anthropogenic pollutants (2013-2014). The results are listed in Table 6.3. In April 2016, an exceedance of even the sum of pesticides was observed. This may be related to the start of the growing season and the increased use of pesticides therein. The pesticides were not found in the recovered water later on, indicating that the contamination might have been temporary. However, these pesticides might also have been immobilised, diluted, or degraded in the aquifer upon degradation. The concentrations found during infiltration were never high enough to result in negative impacts on the orchard trees, as the concentrations were significantly lower than the concentrations attained up during usage for pest-control following the description of the suppliers of the specific pesticides.

Based on these results, it was proposed to the Water Authority (Scheldestromen) to limit the infiltration season from November 15 to April 15, when limited pesticides are used in the area.

Table 6.3: Concentrations of pesticides observed in infiltration water. The sum of pesticides should not exceed the legal limit of 0.5 µg/l, while individual pesticides should not exceed 0.1 µg/l, according to the Dutch Water Act and the EU Water Framework Directive.

<i>Date</i>	<i>Type</i>	<i>Source</i>	<i>Sum of pesticides (µg/l)</i>	<i>Exceedance</i>
01/06/2013	Infiltration water	Large watercourse	0.06	As, phenanthrene
01/12/2013	Infiltration water	Large watercourse	0.18	Bentazon
01/12/2014	Infiltration water	Small watercourse	0.38	None
19/03/2015	Infiltration water	Small watercourse	0.18	None
25/02/2016	Infiltration water	Small watercourse	0.19	None
21/04/2016	Infiltration water	Small watercourse	1.22	Fluopyram, Glyphosate, AMPA, Pyrimethanil, Sum
29/06/2016	Stored water	Small watercourse	0.04	None
22/12/2016	Infiltration water	Small watercourse	0.22	None

### 6.3. Water quality analysis: recovered freshwater (HDDW1)

To assess the quality of the freshwater recovered with HDDW1, the hydrogeochemical composition of this water was monitored over time (Figure 6.13 to Figure 6.16). Besides the seasonal variation of temperature, a seasonal variation is also obvious from the EC and the concentrations of dissolved substances. This can be attributed to the seasonality in the operation of the Freshmaker. Especially in the first years of operation, the EC and the concentrations of Cl, Na, HCO<sub>3</sub>, and SO<sub>4</sub>, i.e. of species that characterize saltwater, increase during the recovery phase of one ASR cycle. As a result of the recovery, the freshwater lens attains its minimal extent and more brackish water is being recovered, thereby increasing the concentrations of the abovementioned species. During upconing, cation exchange processes result in a retarded arrival of Na with respect to Cl. After infiltration of freshwater, the concentrations of these dissolved species again attain lower levels.

Although the injected water was always oxic, there was no recovery of oxygen containing water, indicating oxygen-consumption during aquifer storage. To a large extent, this was a result of pyrite oxidation, as marked by an approximately 10 mg/l increase in SO<sub>4</sub>. In this process, Fe-hydroxides are formed close to the infiltration water. Fe is immobilised in that state. However, at the start of each cycle, elevated Fe-concentrations were observed in the

first ~100 m<sup>3</sup> of recovered freshwater (up to > 2 mg/l). This was followed by freshwater with concentration in the range of 0.5-1.0 mg/l (2013-2015). An explanation may be the biomass mineralization around the well during the storage phase, creating deeply anoxic conditions. During the last two cycles, Fe was not sampled at the very start of recovery and later concentrations remained lower (around 0.2 mg/l).

As-concentrations increase during recovery from 5-10 µg/L up to 26 µg/L in the first ASR-cycles (Figure 6.16). During the last two recovery phases in 2016 and 2017, As-concentrations remained below 15 µg/L. The recommended limit and guideline for arsenic in reclaimed water for long-term irrigation is 100 µg/L (Ayers and Westcot, 1976; Fipps, 2003; Rowe and Abdel-Magid, 1995) and the toxicity is as low as 50 µg/L for vulnerable crops like rice. Hence, the recovered irrigation water in Ovezande does not exceed the general toxicity limit for crops, thereby confirming the limited risk of the slightly elevated As-concentrations in the infiltration water for crop health. The higher As-concentrations are often found during the first ASR-cycles and are related to oxidation of As-bearing pyrite. Pyrite oxidation was identified based on the increase in SO<sub>4</sub>. Under oxidizing conditions caused by the injection of oxygen-containing water, the As-mobility reducing over time (Wallis et al., 2011).

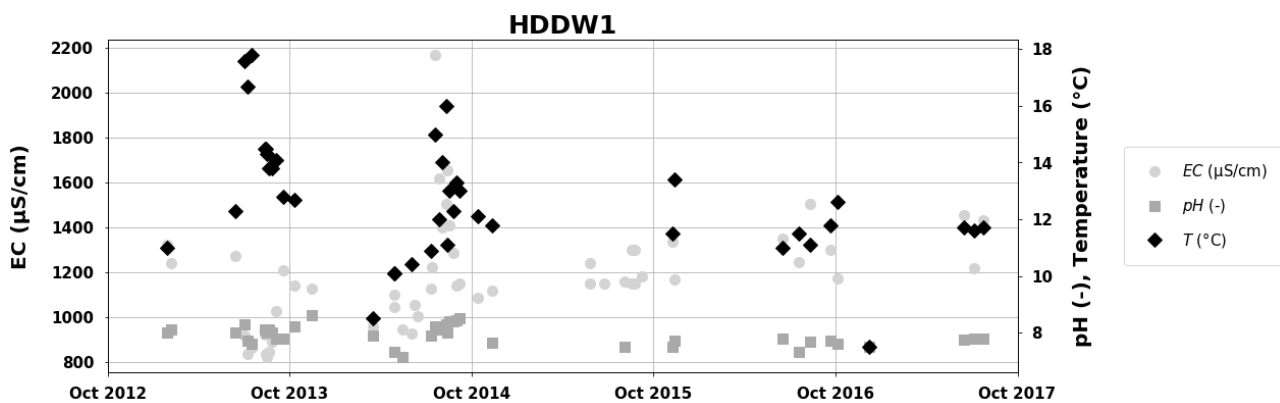


Figure 6.13: Electrical conductivity (EC in µS/cm), pH (-), and temperature (Temp in °C) of the freshwater recovered through HDDW1.

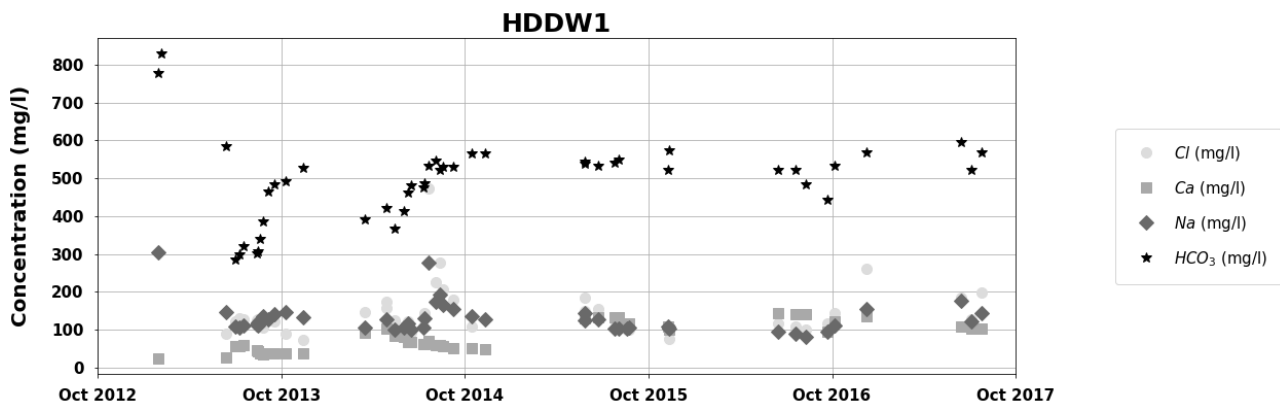


Figure 6.14: Concentrations of Cl, Ca, Na, and HCO<sub>3</sub> in the freshwater recovered through HDDW1.

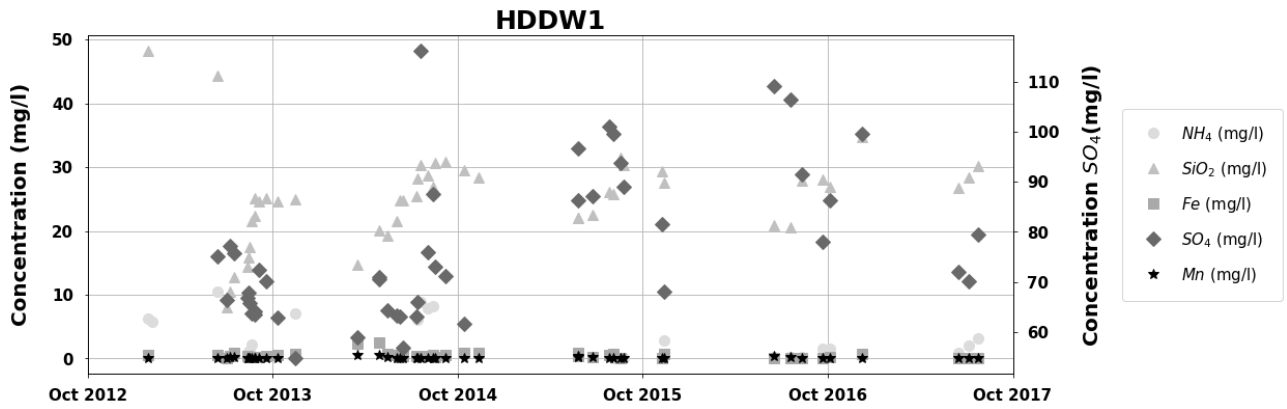


Figure 6.15: Concentrations of  $NH_4$ ,  $SiO_2$ , Fe,  $SO_4$ , and Mn in the freshwater recovered through HDDW1. Be aware that the concentrations of  $SO_4$  are plotted on the secondary (right) y-axis.

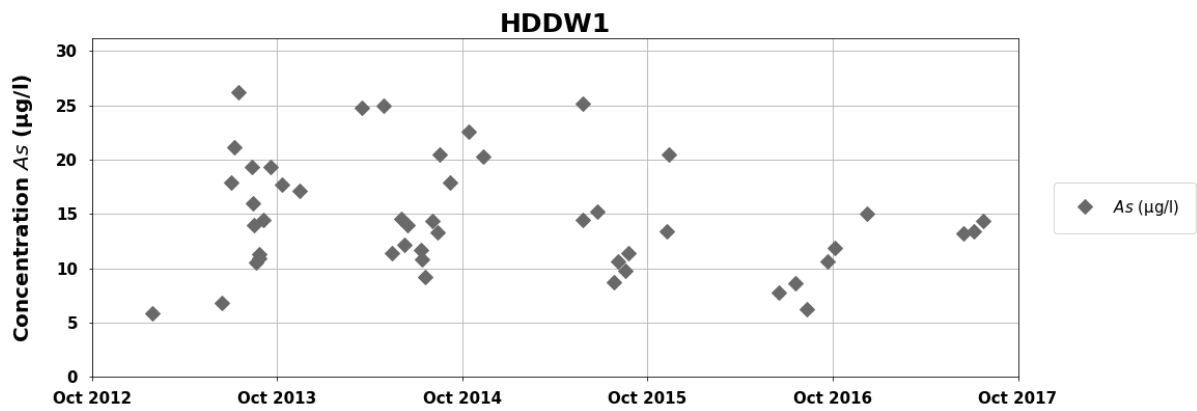


Figure 6.16: Concentrations of As in the freshwater recovered through HDDW1.

## 6.4. Water quality analysis: intercepted brackish groundwater (HDDW2)

The hydrogeochemical composition of saline groundwater intercepted by HDDW2 and subsequently disposed to the surface water was also monitored over time (Figure 6.17 to Figure 6.19). The seasonal pattern of the operation of the Freshmaker is especially obvious from the variation of EC, Cl, Na, Ca, and SO<sub>4</sub>, i.e. species that are dominant in saltwater. These concentrations decrease in winters, when HDDW1 infiltrates freshwater and causes the freshwater lens to attain its maximal extent. As a result, HDDW2 intercepts some of the infiltrated freshwater, which dilutes the intercepted brackish water. In summer, these concentrations are high because HDDW1 recovers freshwater and causes the freshwater lens to attain its minimal extent. HDDW2 therefore mainly intercepts the more brackish water below the freshwater lens. The intercepted water contained Fe (average: 4.0 mg/l), NH<sub>4</sub> (9.9 mg/l), and PO<sub>4</sub> (9.3 mg/l), which is higher than observed in the receiving surface water. There is a decreasing trend for SiO<sub>2</sub>, and an increasing trend for Fe.

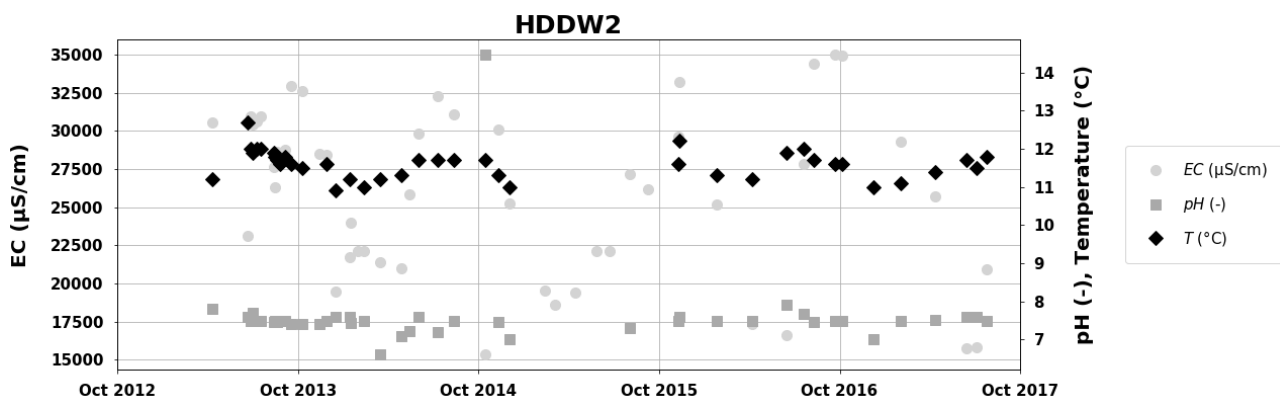


Figure 6.17: Electrical conductivity (EC in  $\mu\text{S}/\text{cm}$ ), pH (-), and temperature (Temp in  $^{\circ}\text{C}$ ) of the brackish groundwater intercepted by HDDW2.

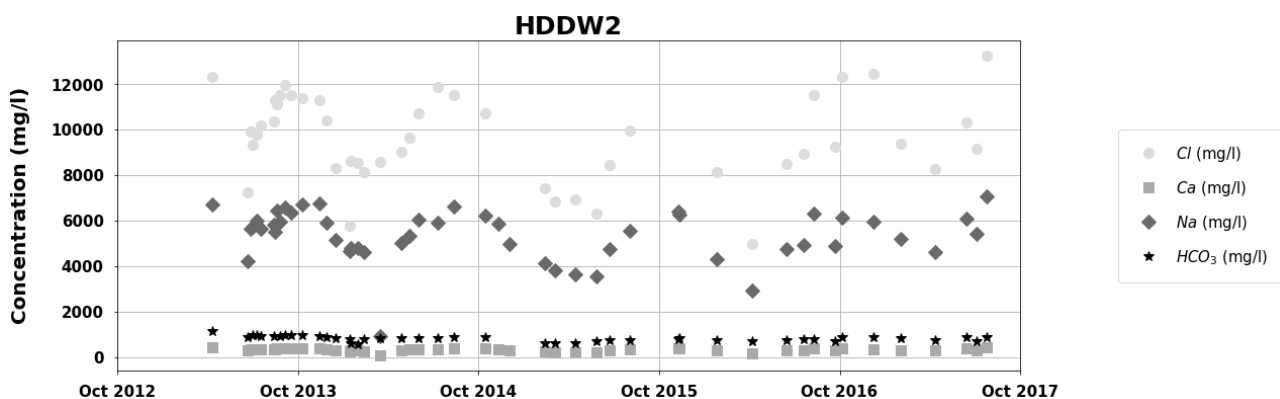


Figure 6.18: Concentrations of Cl, Ca, Na, and HCO<sub>3</sub> in the brackish groundwater intercepted by HDDW2.

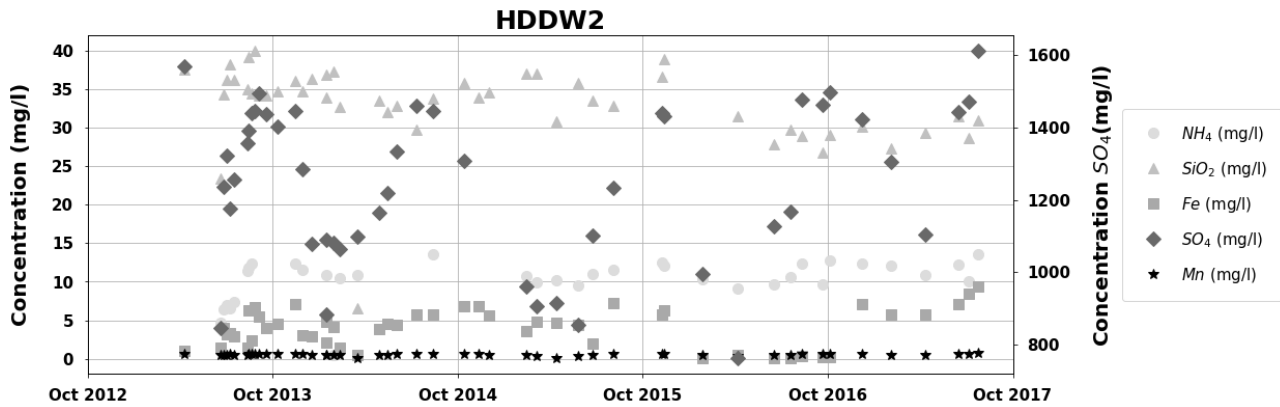


Figure 6.19: Concentrations of NH<sub>4</sub>, SiO<sub>2</sub>, Fe, SO<sub>4</sub>, and Mn in the brackish groundwater intercepted by HDDW2. Be aware that the concentrations of SO<sub>4</sub> are plotted on the secondary (right) y-axis.

In 2013, the impact of the disposal of saline water from HDDW2 on the surface water was evaluated. Based on the limited disposal rate (generally <40 m<sup>3</sup>/d) versus the sometimes high discharge of the water course (up to 2000 m<sup>3</sup>/u), a minor impact was expected. In Figure 6.20, it is shown concentrations in the water course remain well below the concentrations of HDDW2, indicating that a built-up of saltwater is not occurring. Furthermore, concentrations in the water course were in line with was normally observed during summers. Therefore, it was decided by the Water Authorities to accept the disposal of the HDDW2 water.

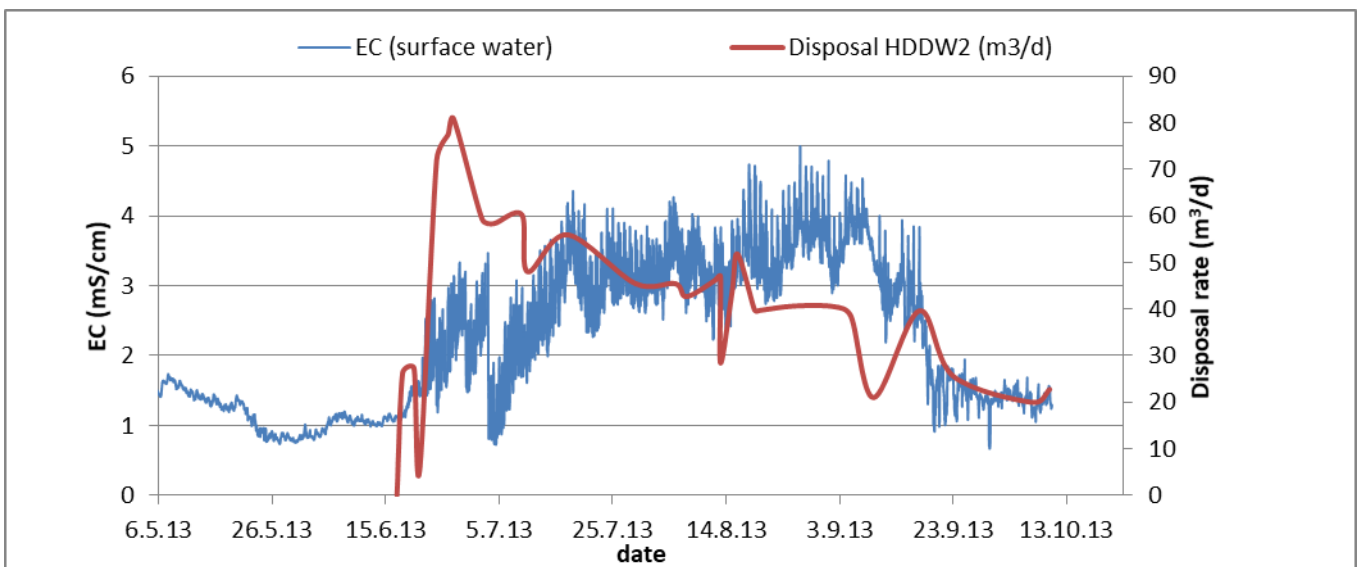


Figure 6.20: EC versus disposal rate in the water course where intercepted brackish water from HDDW2 (EC: 20 – 35 mS/cm) was disposed.

## 6.5. Hydrological effects

Pressure transducers were used to monitor the influence of the operational HDDWs on both the phreatic water level (MW1.0) and the hydraulic head in the shallow aquifer (MW1.1: -7.36 m above sea level (m ASL) ; MW1.2: -12.36 m ASL), but also to monitor the water column in the 3 m high standpipe; see Figure 6.21 to Figure 6.24 (period: 10 April 2013 until 25 July 2017; and ongoing). A relatively low infiltration rate of the HDDW in combination with a relatively high water column in the standpipe is an indicator for potential clogging.

Aside from monitoring of the hydrological effects of the Ovezande Freshmaker in the field, a calibrated 3D density-dependent groundwater model was used to construct map views of the maximum increase and decrease in both the phreatic water level and the hydraulic head in the shallow aquifer in times of high infiltration rate of HDDW1 (Date: 13 July 2014; Figure 6.25) and of high abstraction rate of HDDW1 (Date: 19 January 2015; Figure 6.26), respectively. The reference date is 18 June 2013 (before operation).

Hydrological effects of (maximum) infiltration are limited to a 90 m radius (i.e., > 0.05 m increase of hydraulic heads) in both the phreatic layer and the shallow aquifer. The marginal hydrological effects during infiltration are explained by the simultaneous abstraction of brackish water by HDDW2 in times of infiltration of freshwater through HDDW1. During periods of maximum abstraction the change in phreatic water level and hydraulic head can be more significant as both HDDWs abstract groundwater simultaneously. The region of influence (> 0.05 m decrease of hydraulic heads) covers 170 m northwards and 250 m southwards. This asymmetry is caused by the draining ditches in the North, dampening the effects in this direction.

In the Ovezande case the regional impact on the phreatic water level and the hydraulic head is very small, especially during periods of infiltration. The region of influence as marked by the area where a change of groundwater head of more than 5 cm is observed mostly fell within the borders of the user's terrain and therefore the Freshmaker did not affect other groundwater users. Regionally, groundwater flows were not affected based on the monitoring and modelling data, but changes were observed locally: the brackish water seepage to the draining ditch decreased and thickening of the freshwater lens were the result.

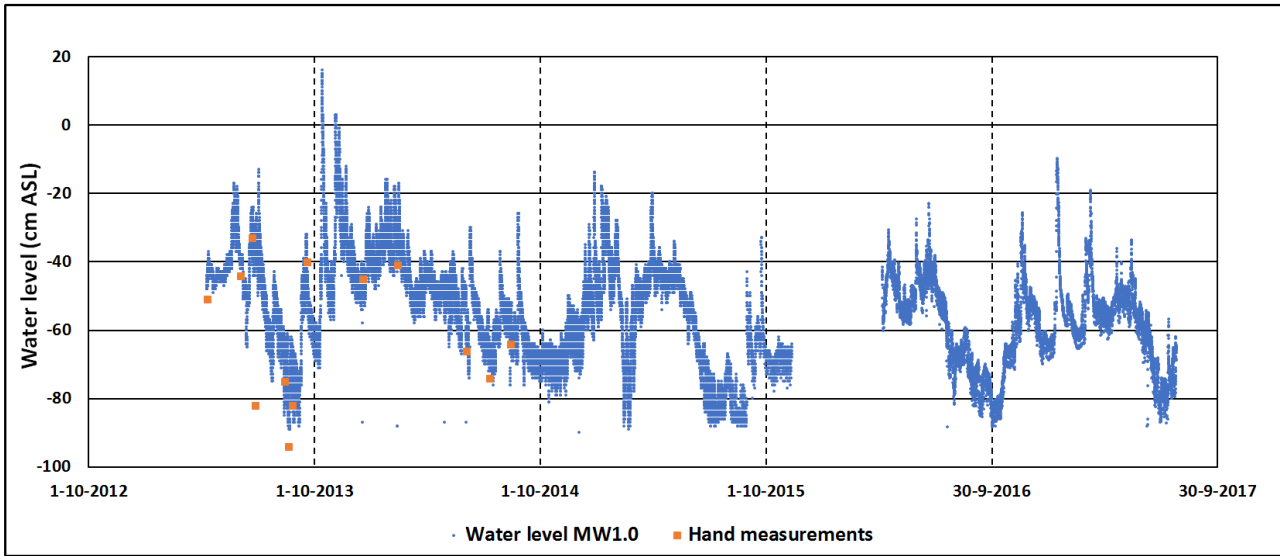


Figure 6.21: Phreatic water level (in cm ASL) monitored with a pressure transducer at MW1.0 and validated by using hand measurements.

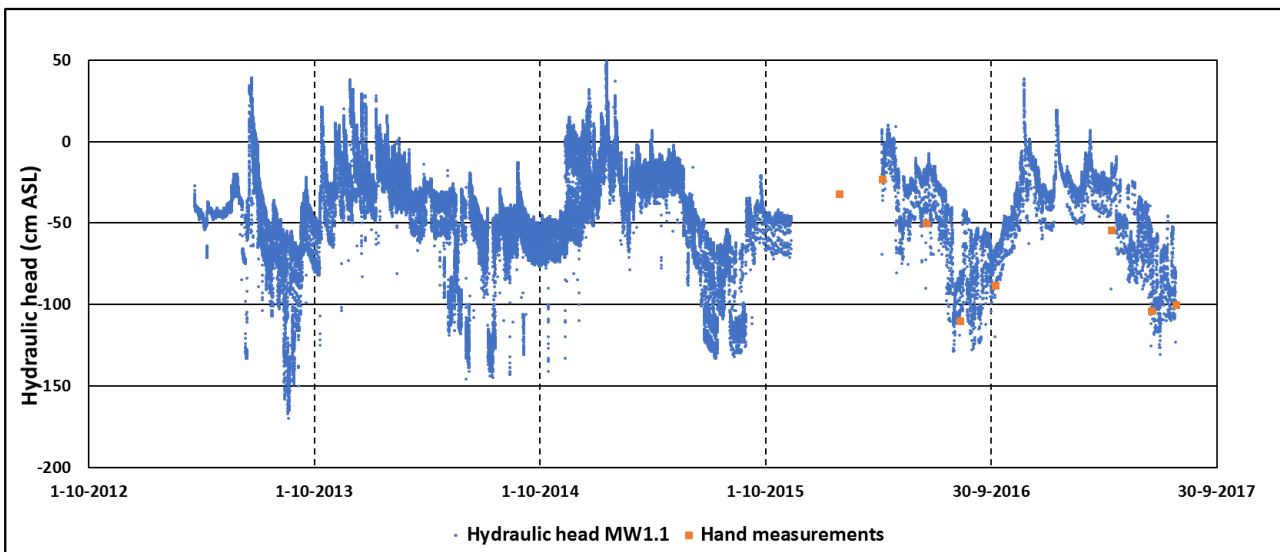


Figure 6.22: Hydraulic head in the shallow aquifer (in cm ASL) monitored with a pressure transducer at MW1.1 and validated by using hand measurements.

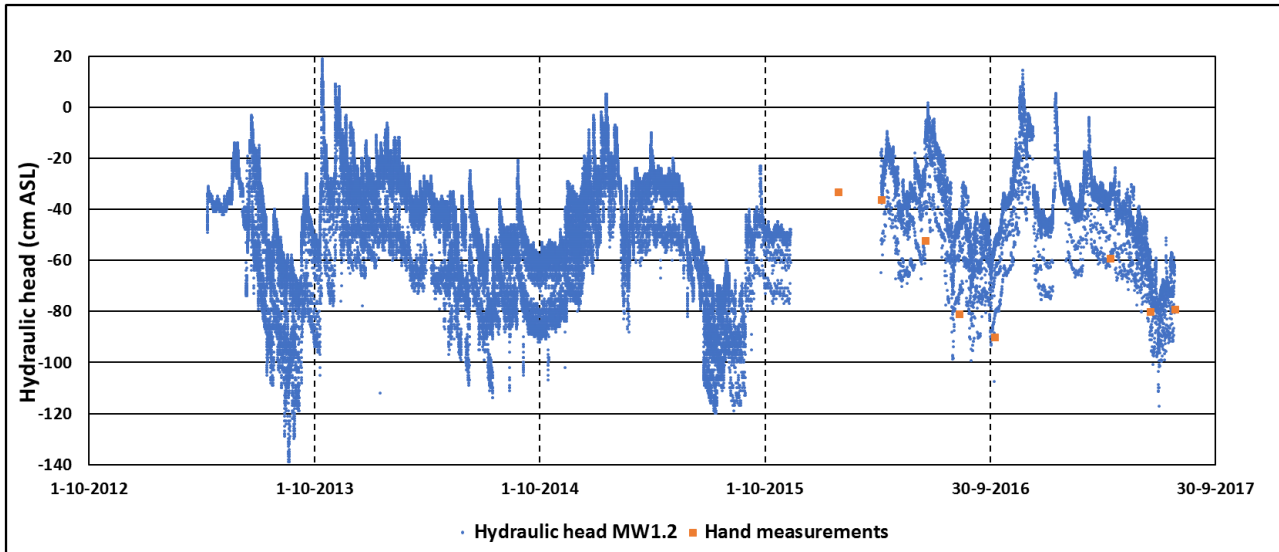


Figure 6.23: Hydraulic head in the shallow aquifer (in cm ASL) monitored with a pressure transducer at MW1.2 and validated by using hand measurements. Lowest measurements indicate head during interception of brackish water (2 to 8 times per day).

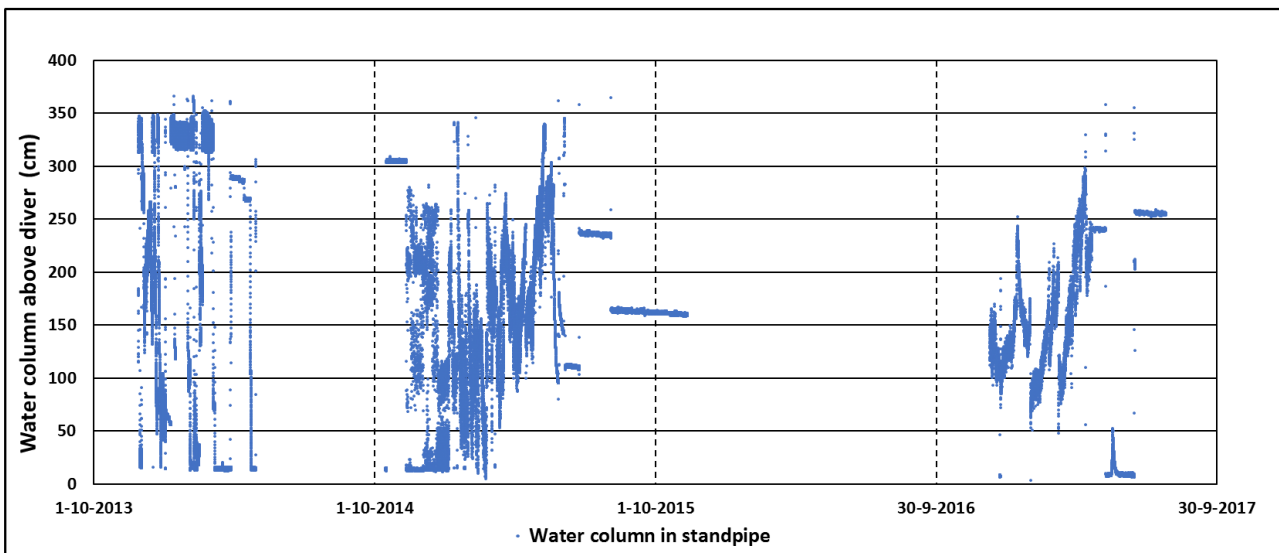
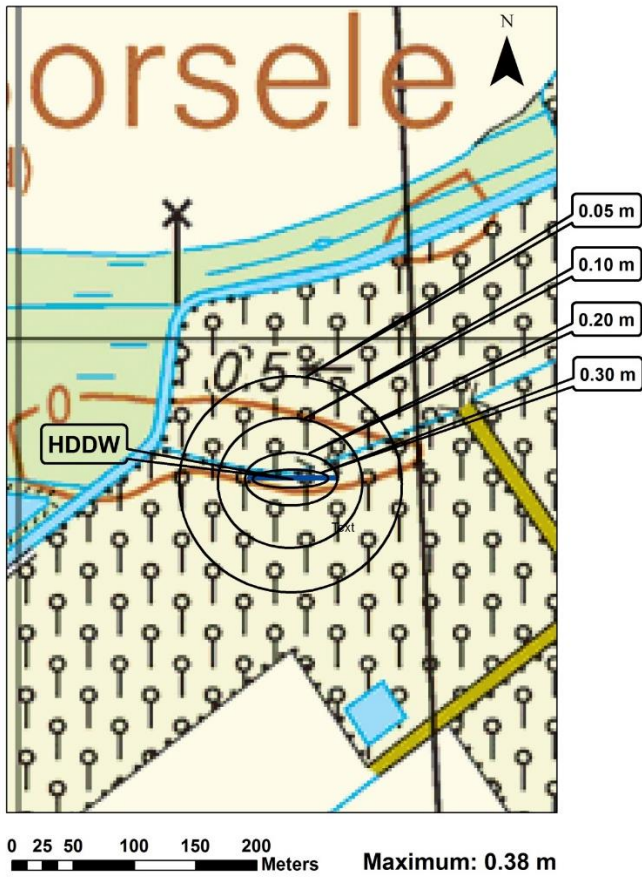


Figure 6.24: Water column above the pressure transducer ("diver") in the standpipe.

Maximum phreatic head increase  
Ovezande Freshmaker



Maximum hydraulic head increase: aquifer  
Ovezande Freshmaker

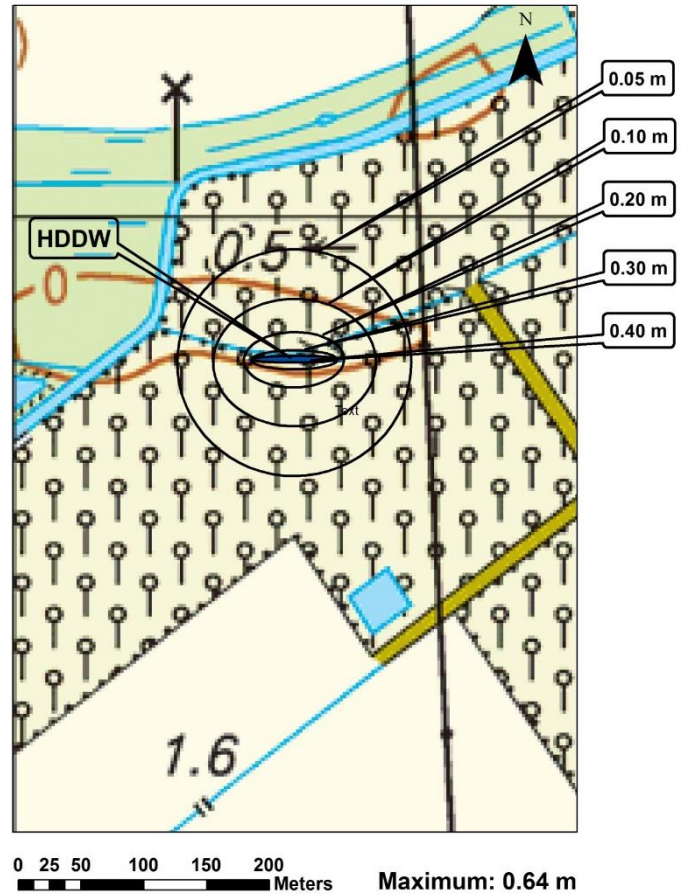
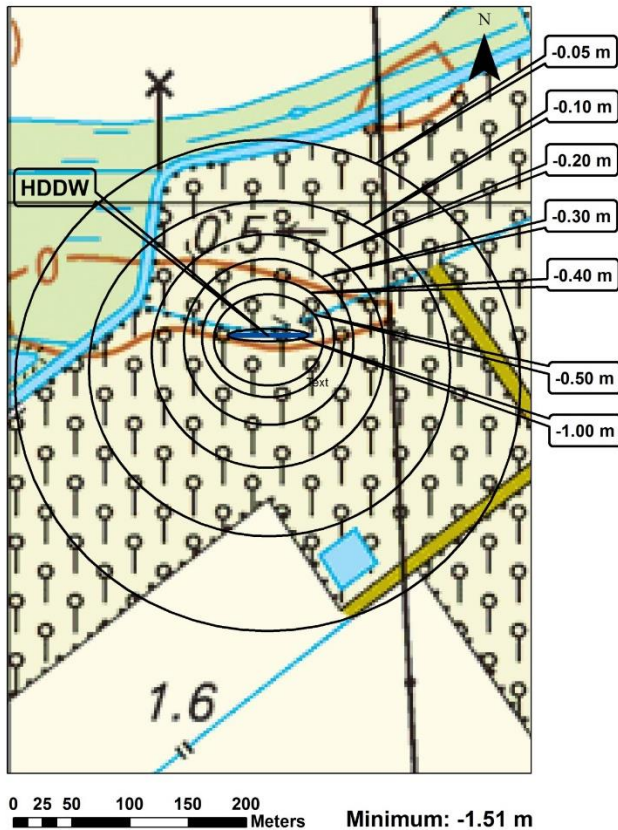


Figure 6.25: Increase of the hydraulic head in the target aquifer (left) and of the phreatic groundwater level (right) at a high infiltration rate of HDDW1 (Date: 13-7-14).

**Maximum hydraulic head decrease: aquifer  
Ovezande Freshmaker**



**Maximum phreatic head decrease  
Ovezande Freshmaker**

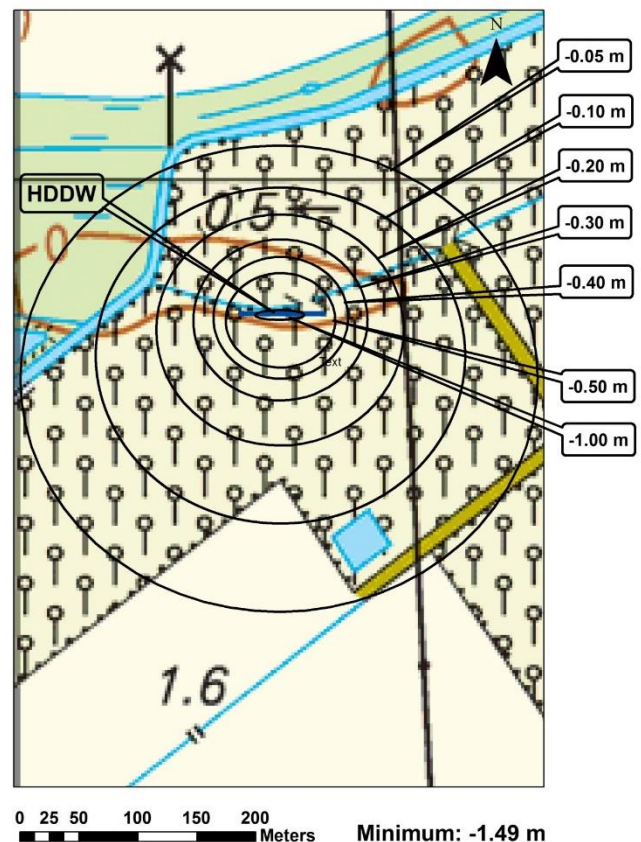


Figure 6.26: Decrease of the hydraulic head in the target aquifer (left) and of the phreatic groundwater level (right) at a high abstraction rate of HDDW1 (Date: 19-1-15).

## 6.6. Geophysical measurements: CVES

### 6.6.1. CVES-1: along the HDDWs (within Cycle 2016)

During infiltration, the maximum extent of the Freshwater lens is attained. This moment was caught in March 2016 using CVES (Figure 6.27). It shows that electrical resistivity (the reciprocal of the electrical conductivity) is relatively high around HDDW1 (40-50 Ohm m: indicating freshwater in a fine sand aquifer) and that there is a steep transition to the deeper saltwater (<5 Ohm m: saltwater in fine sand). At the end of the recovery phase (October 16, the biggest changes are observed in the zone around HDDW1 and between both HDDWs, where resistivity decreases by 5 – 20 ohm m, indicating slight salinization as a consequence of freshwater recovery. Remarkably, most changes are observed at the western 2/3 of the HDDW, which is the suction side of the HDDWs. This might indicate an unequal distribution of abstraction along the HDDWs, with dominant abstraction on the suction side. An alternative explanation is that the western side is close to a large draining water course, which attracts brackish water.

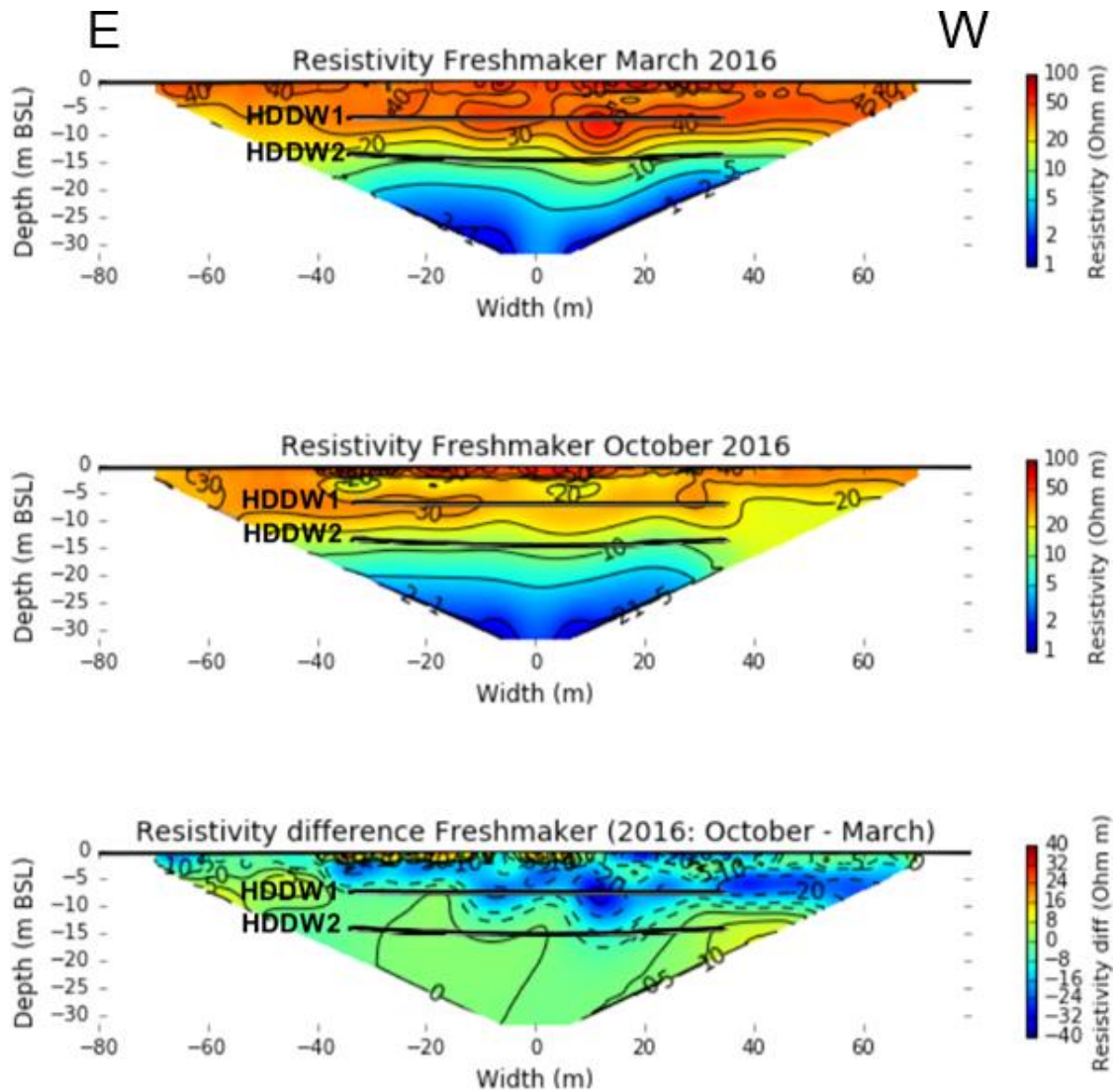


Figure 6.27: Continuous vertical electrical sounding (CVES) at the Ovezande field site for a profile along the HDDWs. The positions of the HDDWs are marked by black solid lines. The resistivity measured in March 2016 and October 2016 is indicated in the upper and middle graphs, respectively. In the lower graph, the difference in resistivity between March 2016 and October 2016 is indicated.

### 6.6.2. CVES-2: perpendicular to the HDDWs (Cycle 2016)

The perpendicular CVES results (Figure 6.28) indicate that a virtually horizontal stratification is present at the end of the infiltration stage (fresh on top of saltwater) around the HDDWs. In the northern direction, the effect of a draining ditch is clear: saltwater is attracted and the formation of a thick freshwater lens is hampered in that area. During recovery, it appears that a part of the saltwater moving from the area of the ditch is attracted by HDDW1 in shallow zones of the aquifer, which is marked by decreasing resistivity in that area (approximately 30 ohm m). Potentially, the ditch (which salinizes during summer and has a fixed water level of 0.7 m BSL, is feeding the aquifer with brackish water. The deeper aquifer just south of the HDDWs also shows some salinization upon recovery, while north of this HDDW, no major changes were observed.

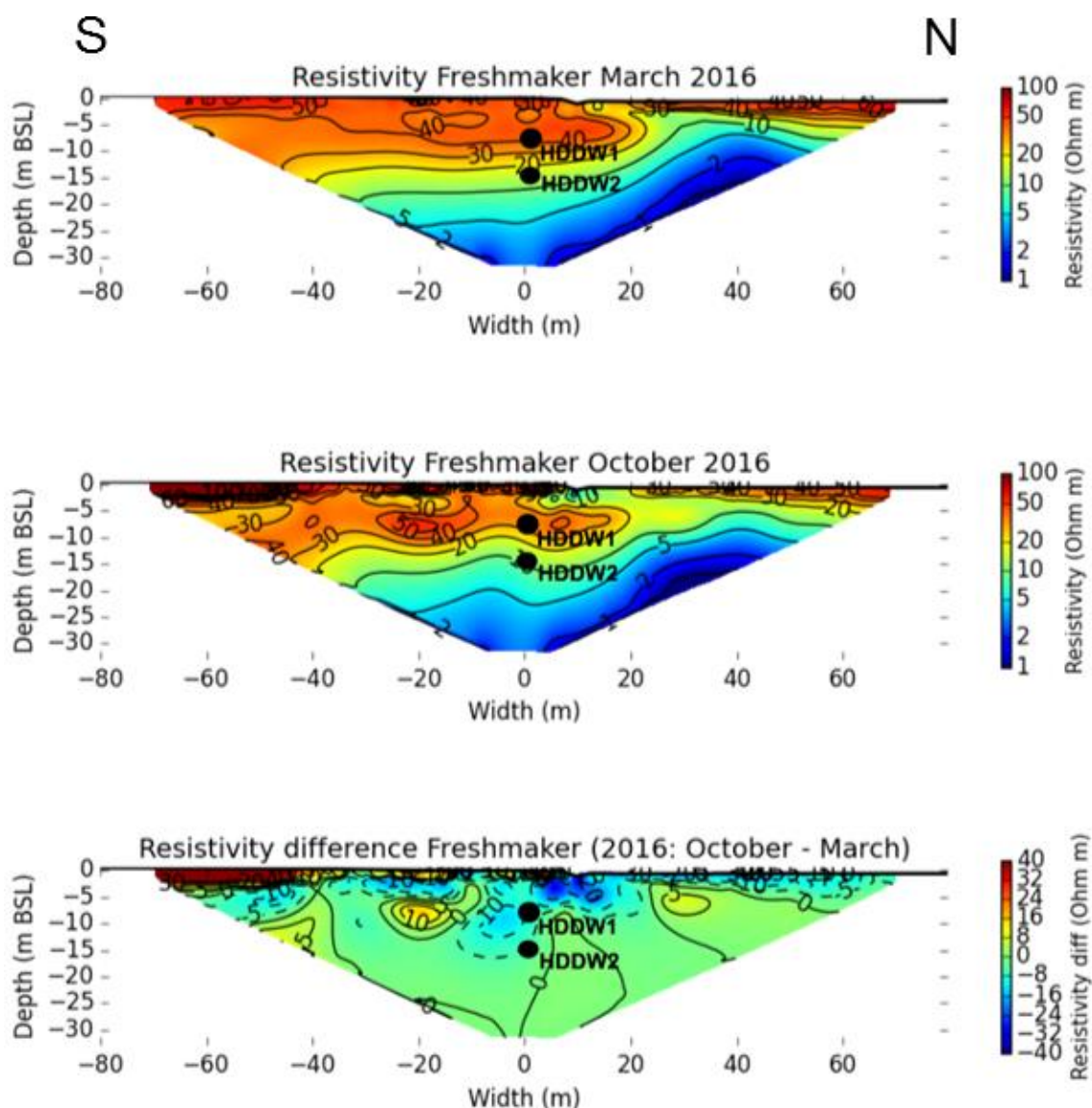


Figure 6.28: Continuous vertical electrical sounding (CVES) at the Ovezande field site for a profile perpendicular to the HDDWs. The positions of the HDDWs are marked black. The resistivity measured in March 2016 and October 2016 is indicated in the upper and middle graphs, respectively. In the lower graph, the difference in resistivity between March 2016 and October 2016 is indicated.

### 6.6.3. CVES-1: along the HDDWs (long-term effects: 2013-2016)

When the effects after 3.5 years of operation (at the end of a recovery stage) are evaluated, three zones can be distinguished in CVES-1 (Figure 6.29):

1. The deeper aquifer: no changes, saltwater remains saltwater;
2. Mixing zone between HDDW1 and 2: slight freshening
3. The freshwater lens around/above HDDW1: slight salinization, but still fresh. This can be a result of injection water left in the aquifer, which has a slightly higher EC (200 – 300  $\mu\text{S}/\text{cm}$ ) than the pristine freshwater (Table 3.1 and Table 6.2).

Again, effects on the western side seem to be dominant and have a larger extent away from the HDDWs.

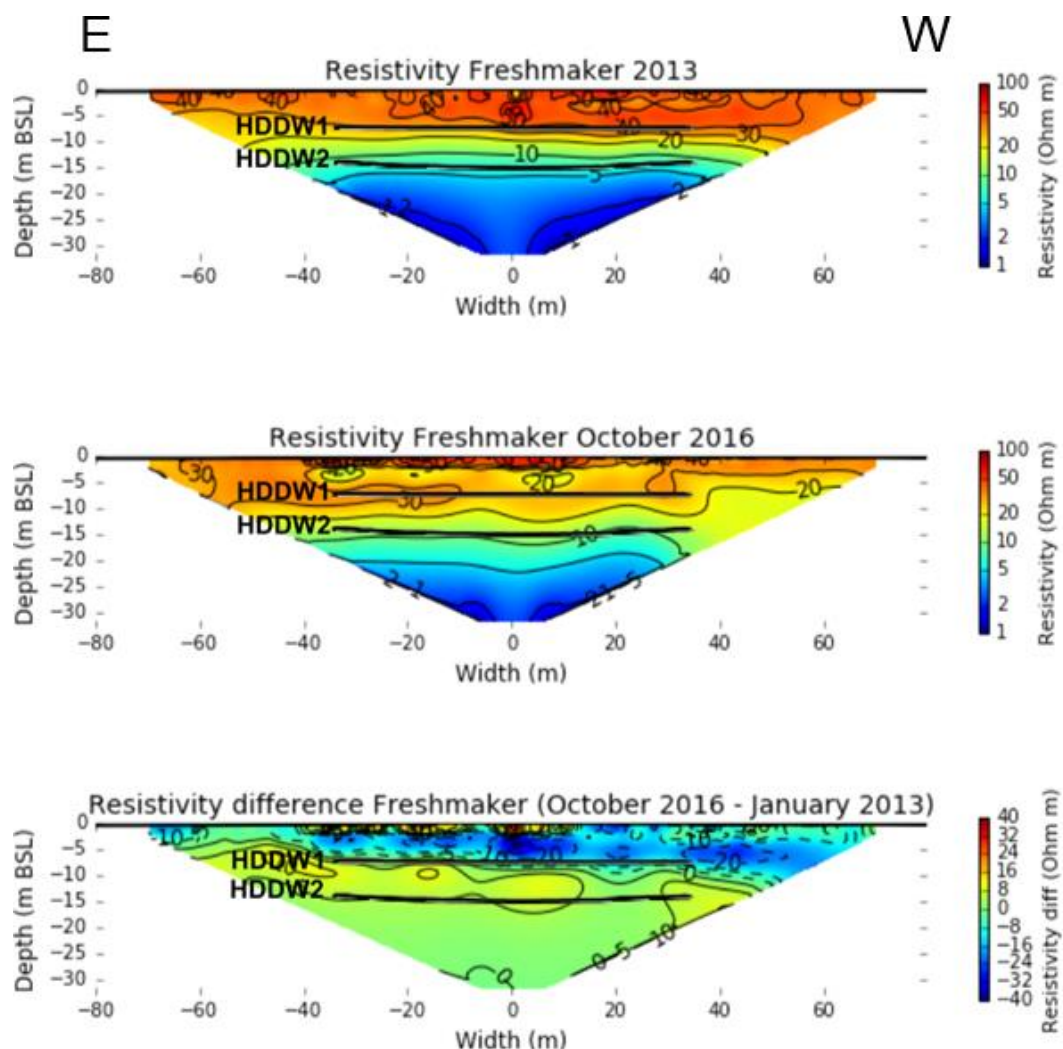


Figure 6.29: Continuous vertical electrical sounding (CVES) at the Ovezande field site for a profile along the HDDWs. The positions of the HDDWs are marked by black solid lines. The resistivity measured in January 2013 and October 2016 is indicated in the upper and middle graphs, respectively. In the lower graph, the difference in resistivity between January 2013 and October 2016 is indicated.

#### 6.6.4. CVES-2: perpendicular to the HDDWs (long-term effects: 2013-2016)

At CVES-2 (Figure 6.30), it was found that between 2013 and 2016, the deeper parts of the aquifer below the ditch freshened (increase around 10 ohm), while the shallow part between the ditch and HDDW1 salinized (decrease around 30 ohm m). The freshening in deeper parts can be attributed to the interception by HDDW2, which attracts saltwater that would otherwise flow towards the draining ditch. The shallow salinization is most likely caused by infiltration of brackish water from the ditch in the summer, during times when the hydraulic heads in the aquifer are below the fixed level of the ditch (0.7 m BSL).

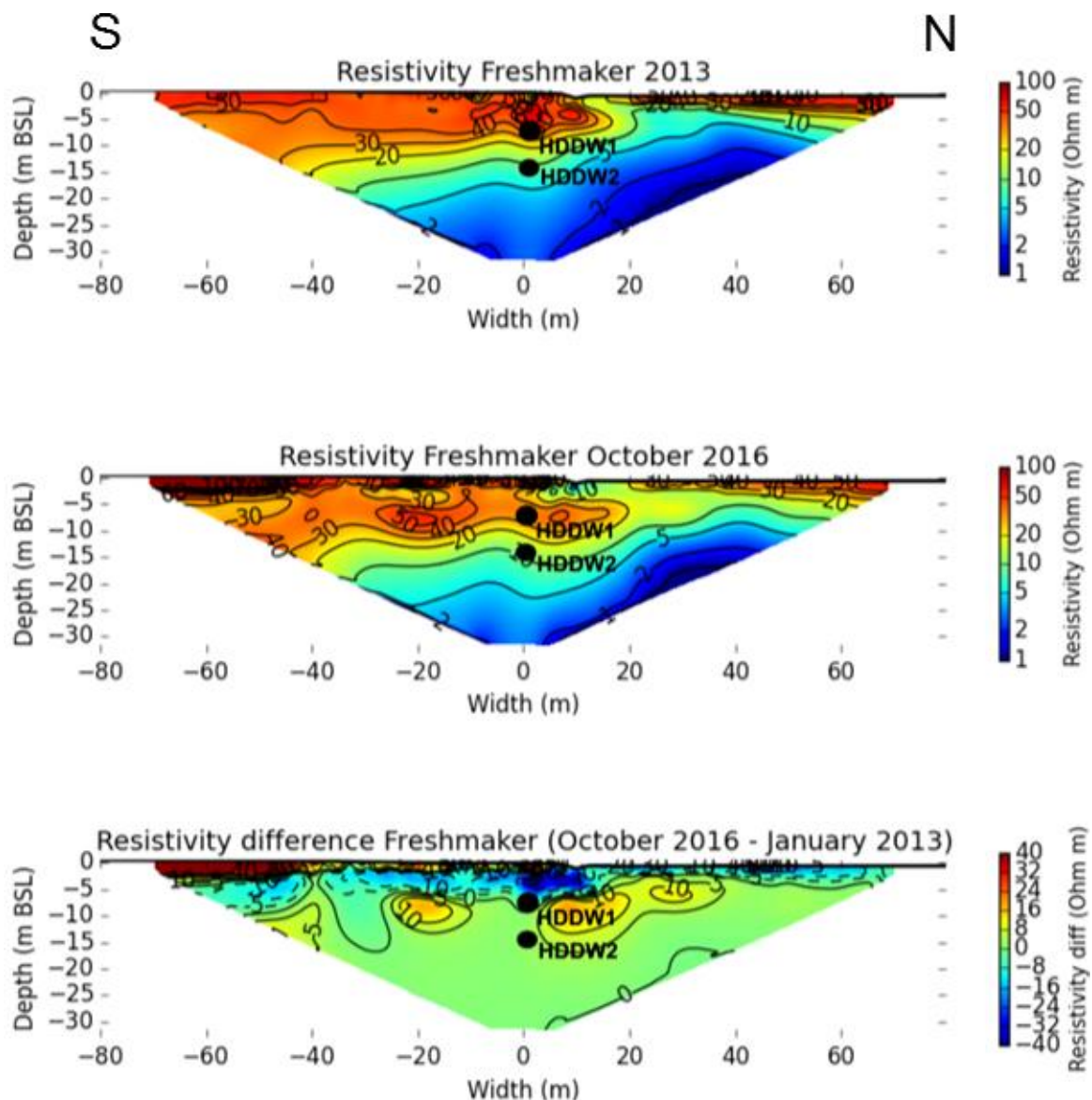


Figure 6.30: Continuous vertical electrical sounding (CVES) at the Ovezande field site for a profile perpendicular to the HDDWs. The positions of the HDDWs are marked black. The resistivity measured in January 2013 and October 2016 is indicated by the upper and middle frames, respectively. In the lower frame, the difference in resistivity between January 2013 and October 2016 is indicated.

### 6.7. Geophysical measurements: EM-39

With the CVES measurements, spatial trends in the surroundings of the HDDWs could be derived, but unfortunately they have a low resolution and are not able to capture sharp transitions between fresh and saltwater. EM-39 logging provided more detail about the local (MW1, MW2, MW4) changes at the interface of fresh and saltwater (Figure 6.31 and Figure 6.32). Based on the results, it can be concluded that:

1. A sharper transition between fresh and saltwater is created during injection: the mixing zone becomes as thin as 1 m, whereas it was around 4 m before operation started.
2. The transition is lowered at the centre of the HDDWs (MW1: ~ 2 m), at 10 m perpendicular from the centre of the HDDWs (MW2: ~1.5 m), and at the edge of the HDDWs (MW4: ~1 m).
3. During recovery: the transition between freshwater and saltwater does not move back to its original position, but remains 0.5 – 1 m below its original position. No saltwater appears to be upconing to the shallow well (on the moment of logging).

The EM-39 measurements underline the freshening observed by CVES in the zone between HDDW1 and HDDW2. The potential salinization in the freshwater lens was not observed by the EM-39. This can be a result of the presumably minor changes in EC of the water types in the freshwater lens, which can however lead to significant changes in the resistivity at low ECs.

The results also indicate that edge effects can be relevant: the observations at MW4 show significantly less dynamics compared to MW1. This can be a result of the flow-field at and around the HDDWs, which is quasi-2D in the centre of the HDDWs, but 3-D at the edges. As a result: infiltration of the same volume in the last meter of HDDW1 will result in less thickening than in the central meter of HDDW1.

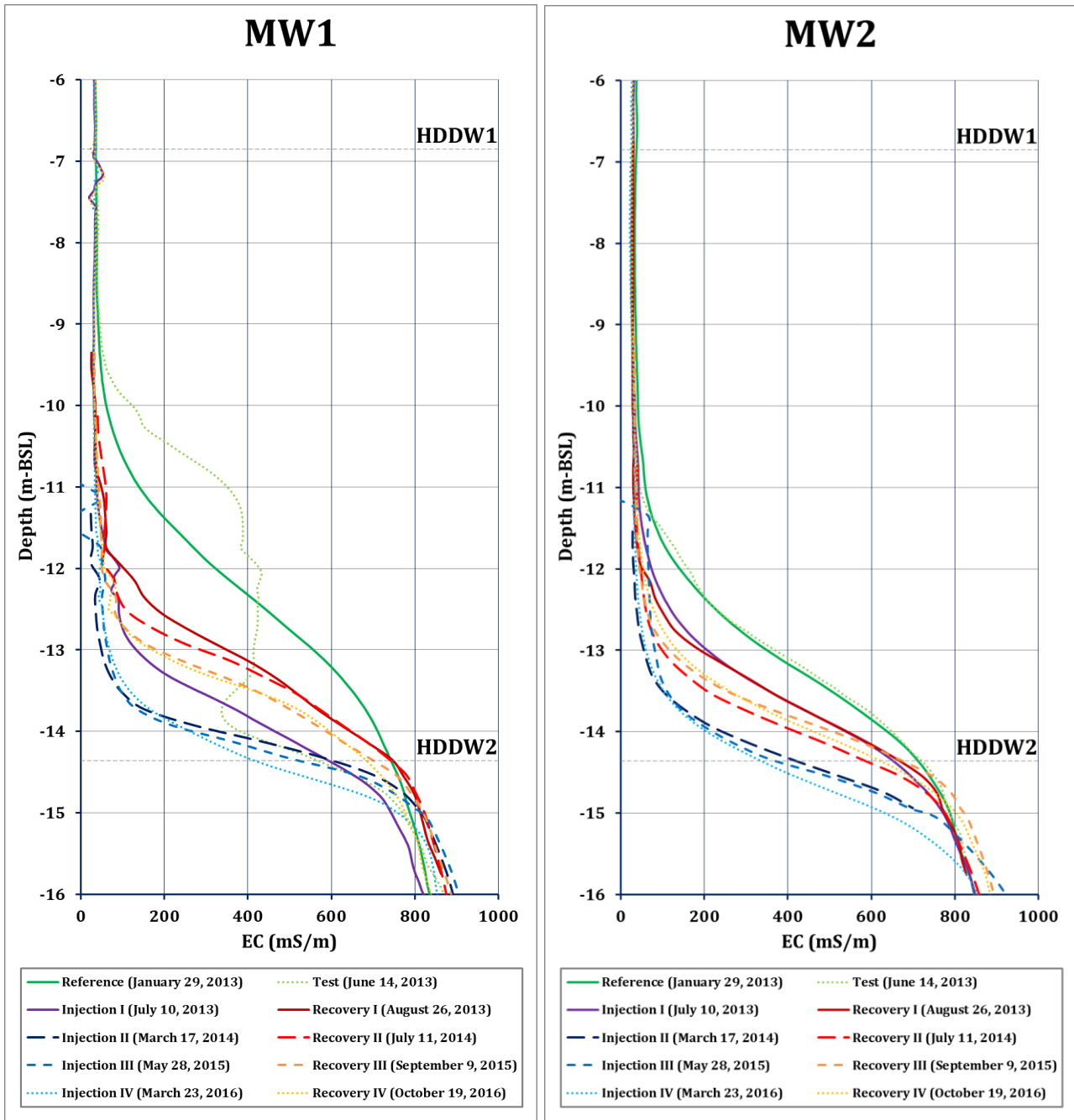


Figure 6.31: Conductivity profile (EC [mS/m] vs. Depth [m BSL]) measured in MW1 (left) and MW2 (right) during different phases of the Freshmaker operation in Ovezande.

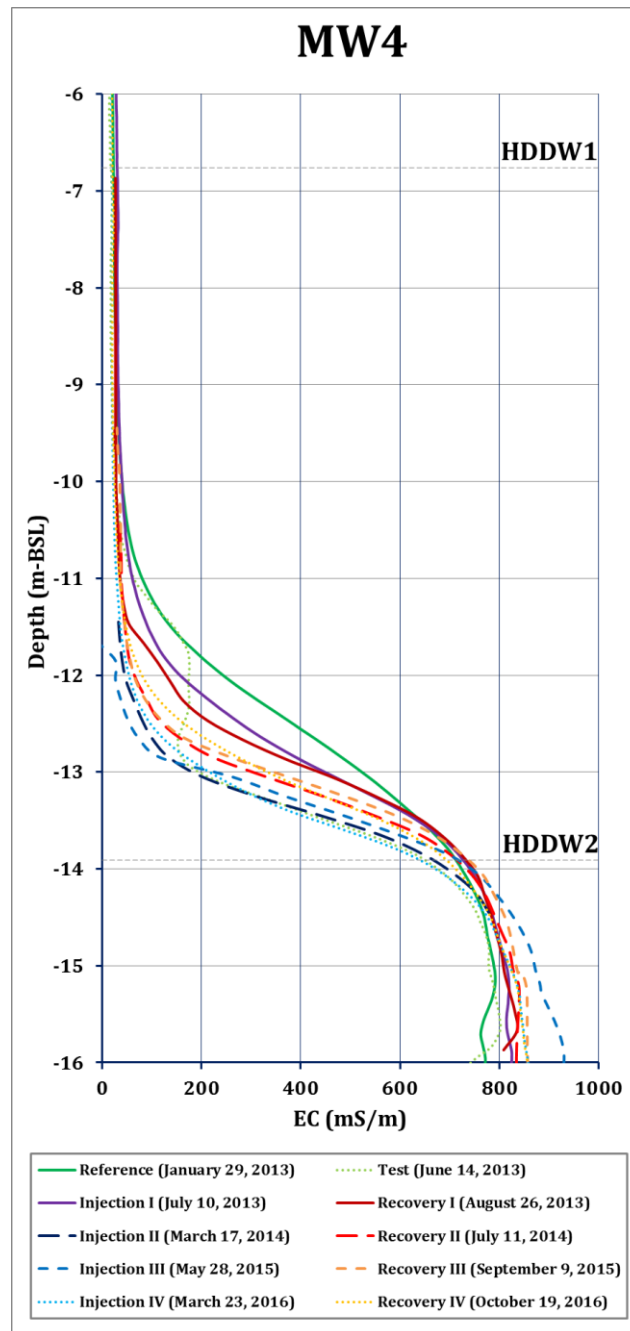


Figure 6.32: Conductivity profile (EC [mS/m] vs. Depth [m BSL]) measured in MW4 during different phases of the Freshmaker operation in Ovezande.



## 7. Results: Modelling

### 7.1. Comparison field data and groundwater modelling

A calibrated 3D density-dependent groundwater flow model was used to simulate the Freshmaker implementation at the Ovezande field site over the period of 18 June 2013 until 6 September 2017. The model uses regular hand-measurements (average frequency: near-weekly) of the cumulative infiltrated volume of HDDW1, and of the cumulative abstracted volumes of HDDW1 and HDDW2 as input for well rates.

Model results are compared with real field data to validate its capability to predict future performance. Therefore, measured chloride concentrations at measuring wells 1, 2, 4 and 6, and at HDDW1 and 2 were plotted together with modelled values (Figure 7.1 to Figure 7.5).

The comparison between the model results and the water quality observation indicates that the model is able to reproduce the trends near HDDW1 and HDDW2, but that concentrations are generally overestimated in the shallow regions at the fringes of the injected freshwater body (MW4 and MW6) and underestimated at greater depth parallel to the HDDWs (MW2.3). Especially in the last years of operation, the model produces higher salinities than observed.

This can be caused by an overestimation of the numerical dispersion in the model relative to the field case. In the field situation, a steep thin mixing zone is observed (ca. 3 m), whereas cross-sections of the modelled chloride distribution in the aquifer indicates a wider mixing zone further away from the HDDWs (Figure 7.6: Initial situation, Figure 7.7, Figure 7.8 and Figure 7.9: Current situation). Over time, a very sharp transition from freshwater to saltwater is formed by the Freshmaker's operation (as indicated by the EM borehole loggings), which is hard to simulate in a SEAWAT model.

Aside from the relatively large mixing zone, the model predicts that despite the simultaneous abstraction of brackish water by HDDW2, brackish water can reach HDDW1 after a prolonged period of freshwater abstraction. A relatively large amount of brackish water reached HDDW1 during the summer of 2017 (according to the model, compared to other summers). This can be caused by the large volume of seasonal freshwater abstraction combined with the relatively low seasonal volume of brackish water abstraction and indicates there are operational constraints the safeguard freshwater recovery.

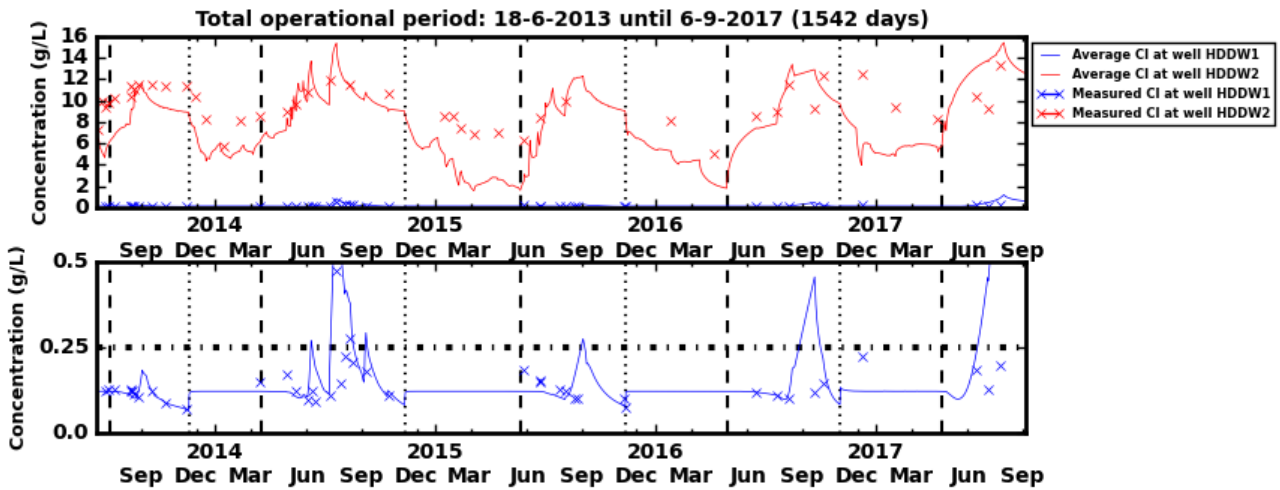


Figure 7.1: Measured (crosses) and modelled (solid lines) chloride concentration in water in HDDW1 and HDDW2 from 2013 until 2017. The black dotted and dashed vertical lines indicate the start of infiltration and recovery of freshwater through HDDW1, respectively. The horizontal dashed line in the bottom graph represents the maximum allowable concentration limit of chloride upon abstraction.

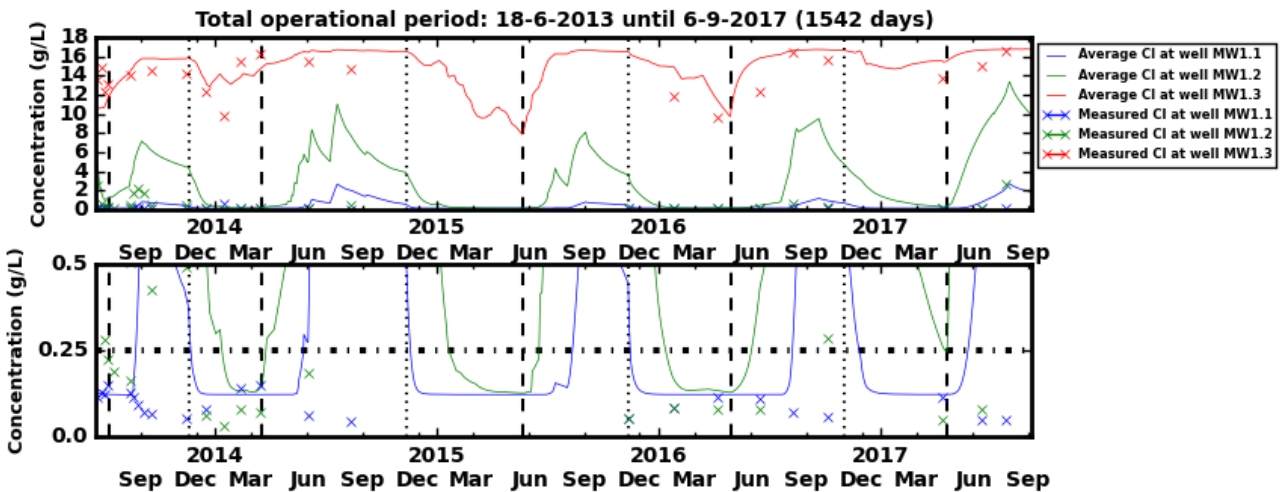


Figure 7.2: Measured (crosses) and modelled (solid lines) chloride concentration in water at the well screens of MW1 from 2013 until 2017. The black dotted and dashed vertical lines indicate the start of infiltration and recovery of freshwater through HDDW1, respectively. The horizontal dashed line in the bottom graph represents the maximum allowable concentration limit of chloride upon abstraction.

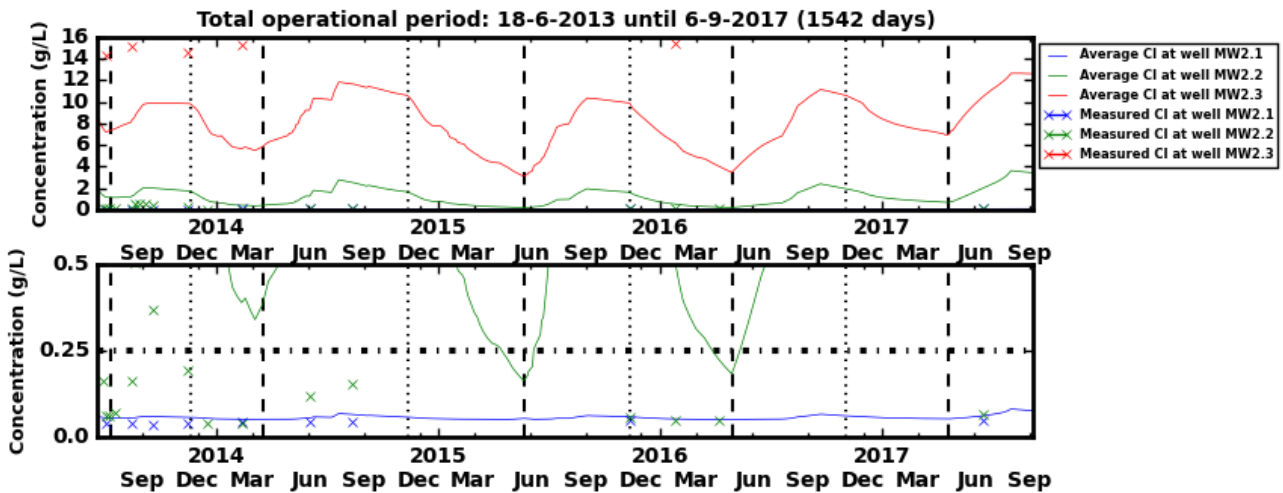


Figure 7.3: Measured (crosses) and modelled (solid lines) chloride concentration in water at the well screens of MW2 from 2013 until 2017. The black dotted and dashed vertical lines indicate the start of infiltration and recovery of freshwater through HDDW1, respectively. The horizontal dashed line in the bottom graph represents the maximum allowable concentration limit of chloride upon abstraction.

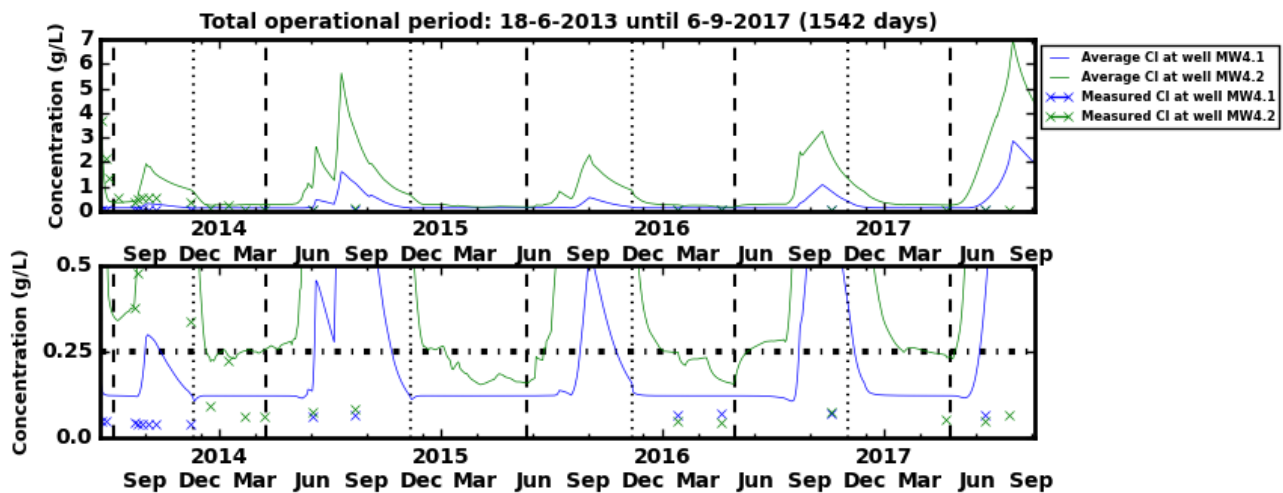


Figure 7.4: Measured (crosses) and modelled (solid lines) chloride concentration in water at the well screens of MW4 from 2013 until 2017. The black dotted and dashed vertical lines indicate the start of infiltration and recovery of freshwater through HDDW1, respectively. The horizontal dashed line in the bottom graph represents the maximum allowable concentration limit of chloride upon abstraction.

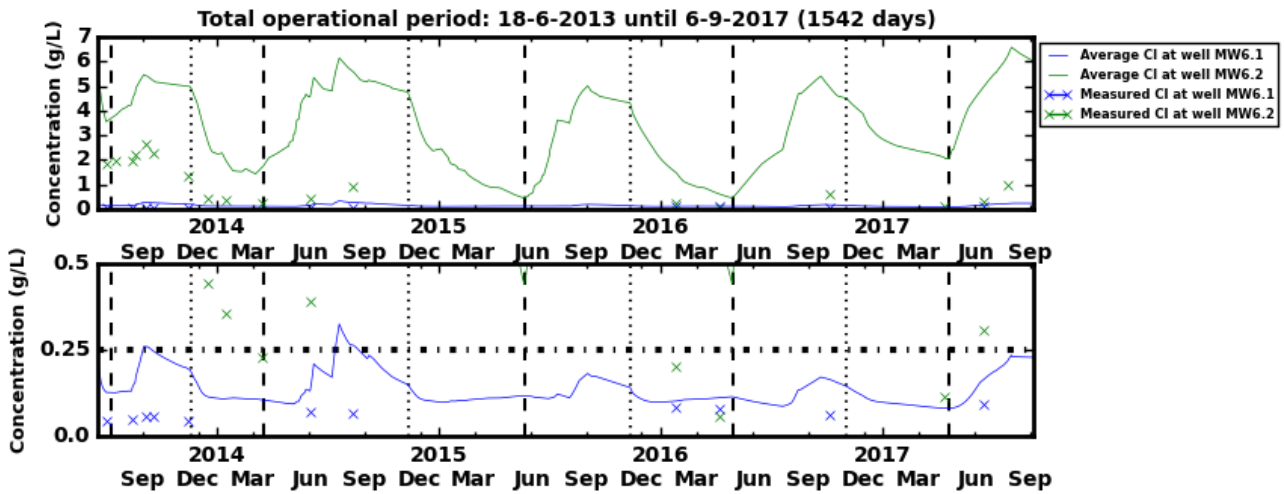


Figure 7.5: Measured (crosses) and modelled (solid lines) chloride concentration in water at the well screens of MW6 from 2013 until 2017. The black dotted and dashed vertical lines indicate the start of infiltration and recovery of freshwater through HDDW1, respectively. The horizontal dashed line in the bottom graph represents the maximum allowable concentration limit of chloride upon abstraction.

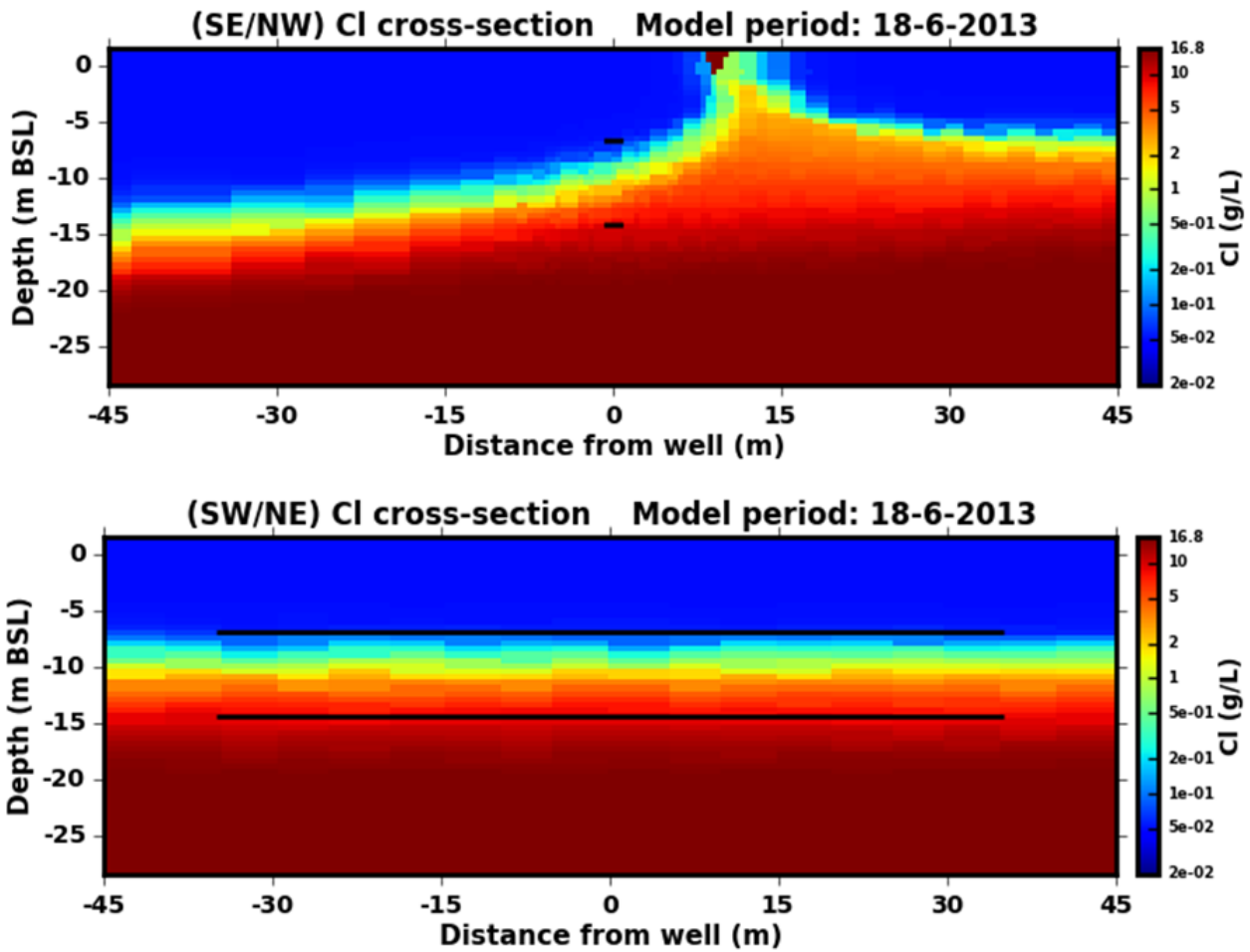


Figure 7.6: Initial modelled chloride concentrations (18 June 2013) for a cross-section of the subsurface perpendicular to the centre of the HDDWs (SE (left) / NW (right): top) and along the HDDWs (SW (left) / NE (right): bottom).

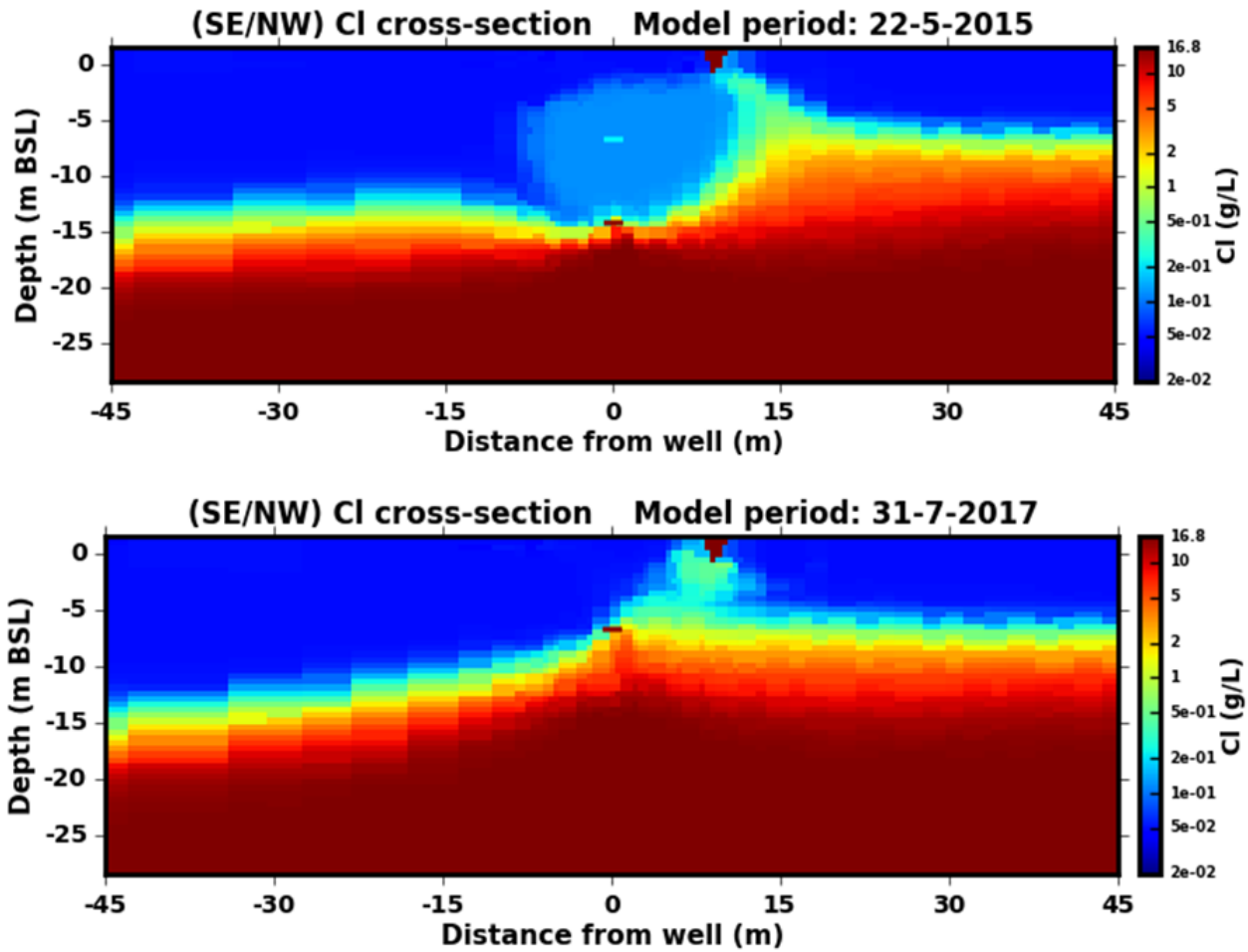


Figure 7.7: Modelled chloride concentrations for a cross-section of the subsurface perpendicular to the centre of the HDDWs (SE/NW) after infiltration of freshwater through the upper HDDW in May 2015 (top) and after maximal recovery in September 2015 (bottom).

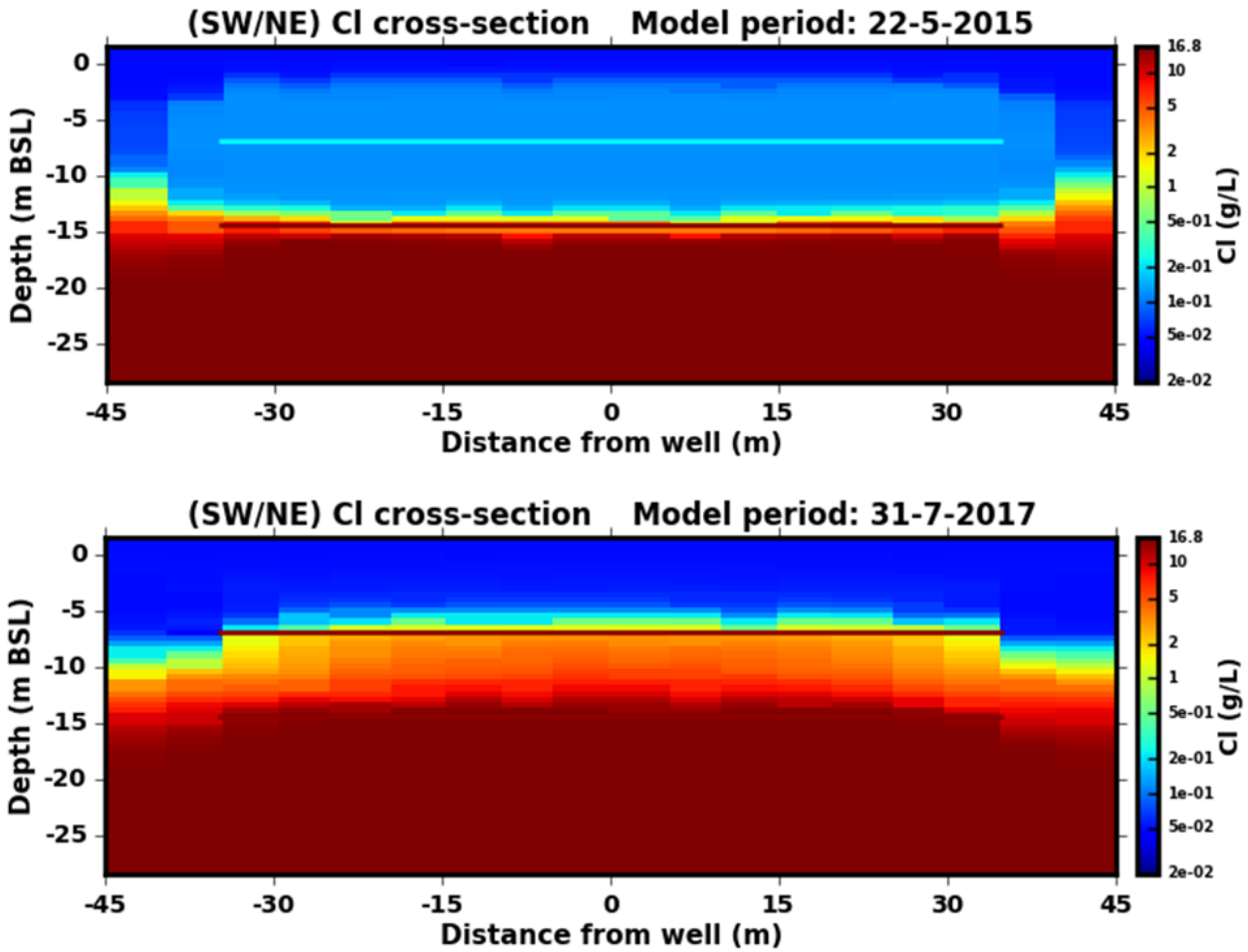


Figure 7.8: Modelled chloride concentrations for a cross-section of the subsurface along the HDDWs (SW/NE) after infiltration of freshwater through the upper HDDW in May 2015 (top) and after maximal recovery in July 2017 (bottom).

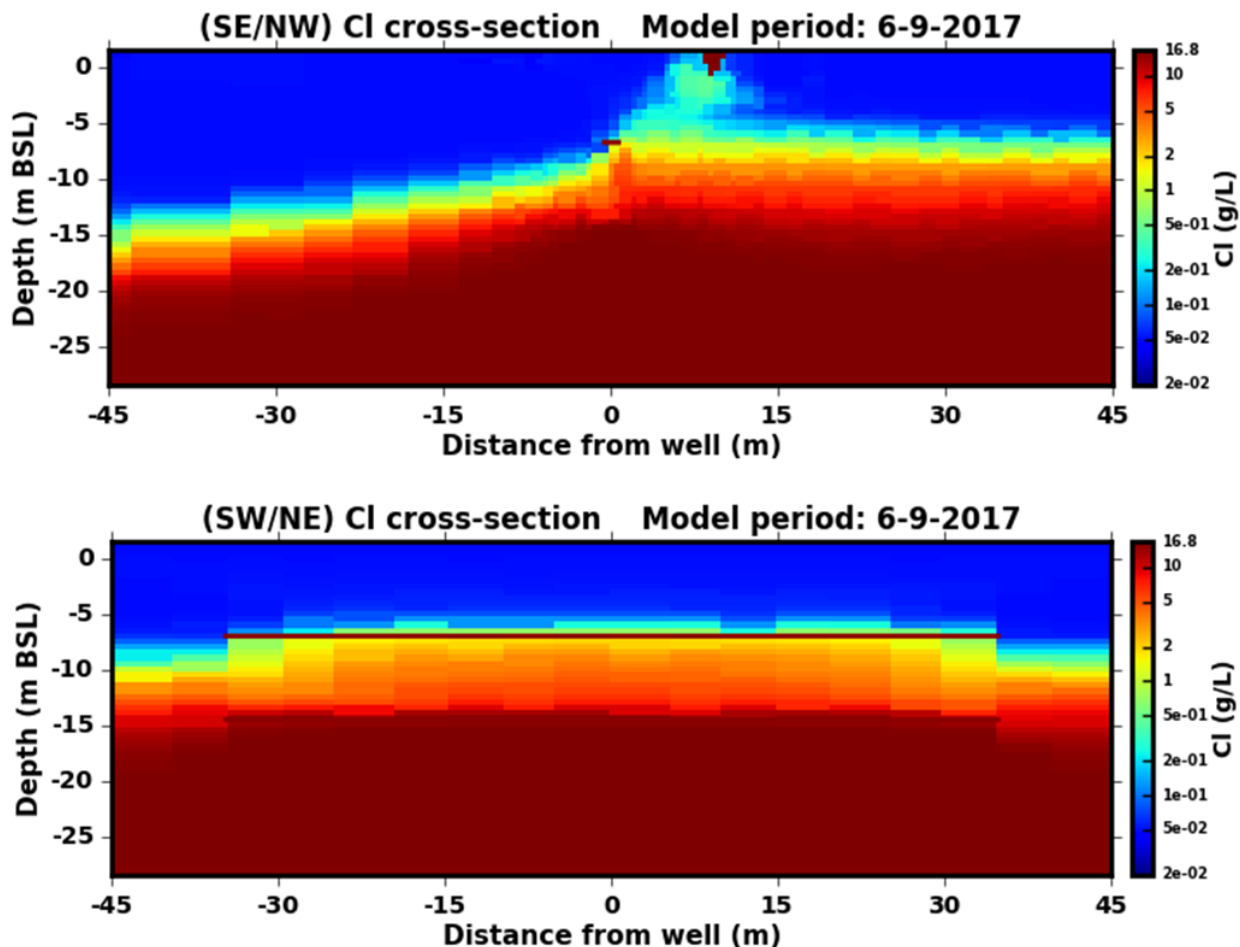


Figure 7.9: Final modelled chloride concentrations (6 September 2017) for a cross-section of the subsurface perpendicular to the centre of the HDDWs (SE/NW: top) and along the HDDWs (SW/NE: bottom).

## 7.2. Automated control unit

### Modelling of the automated control unit

The aim of the automated control unit is to optimize the abstraction by the deeper HDDW2, while maintaining a high recovery (efficiency) of infiltrated freshwater by HDDW1 (Chloride concentration below 250 mg/L).

To test a predefined optimal performance of the Freshmaker system, it was decided to model the HDDW2 at the rates indicated in Figure 7.10. A limiting EC of 10 mS/cm (corresponding to 4 g Cl/L) was chosen to (automatically) detect a breakthrough of saline water from below. Otherwise, the HDDW2 will be turned off (0.001 m<sup>3</sup>/d to keep measuring the EC). To model the HDDW2 abstraction during Storage or Idle phases, a HDDW2 abstraction rate of 22.2 m<sup>3</sup>/day was used during periods without HDDW1 operation. This corresponds to the current average abstraction rate of HDDW2 ( $Q_{\text{HDDW2}}$ ) during the idle HDDW1 periods. The model period was from 18 June 2013 until 12 April 2017.

The infiltrated volume of freshwater during this period was 21843.8 m<sup>3</sup>, the abstracted volume of freshwater was 15334.3 m<sup>3</sup>, and the abstracted volume of brackish or saline water by HDDW2 was 45454.9 m<sup>3</sup>. The resulting recovery efficiency of freshwater was 70.2 % until 12 April 2017.

A comparison between the current operational performance and the alternative operational performance estimate is given in Table 7.1. With the current model it was possible to recover 54.8 % of the infiltrated freshwater with a chloride concentration below 250 mg/L. The total chloride mass abstracted by HDDW2 during this period was 351 tonnes. With the alternative operational design a recovery efficiency of 54.0 % was obtained, abstracting slightly less freshwater through HDDW2 and releasing 346.6 tonnes of chloride to the surface waters. This alternative operational design thus only slightly reduces the salt load to the surface water system (by 1.3 %), indicating that the manual adjustments made to the pumping rate based on a priori models was adequate. However, automation of the saltwater interception makes the Freshmaker at least more robust by limiting the requirement of manual modifications.

Table 7.1: Comparison between the current operational field performance, the related 3D model, and the alternative model scenario of the automated control unit.

Scenario	Volume of freshwater infiltrated (m <sup>3</sup> ) (HDDW1)	Volume of freshwater recovered (m <sup>3</sup> ) (HDDW1)	Volume of brackish groundwater intercepted (m <sup>3</sup> ) (HDDW2)	Recovery efficiency of HDDW1 (Cl < 250 mg/L) (%)	Average chloride concentration at HDDW2	Total chloride mass abstracted (x 1000 kg) (HDDW2)
Field case	21843.8	15334.3	45454.9	70.2	-	-
Modelled (reference)	21843.8	11970.4	45454.9	54.8	7.722	351.0
Automated model	21843.8	11808.9	45086.5	54.0	7.687	346.6

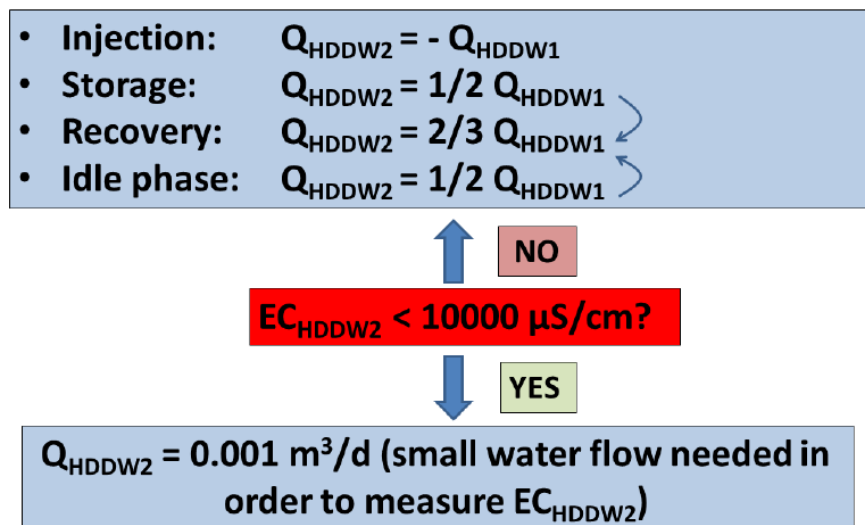


Figure 7.10: Modelled HDDW2 operational scheme, based on a limiting EC at HDDW2 of 10 mS/cm, corresponding to a chloride concentration of 4 g/L. To automate the HDDW2 abstraction based on operational HDDW1 well rates, a HDDW2 abstraction rate of 22.2 m<sup>3</sup>/day was used during periods without HDDW1 operation (Idle phase). This corresponds to half the recovery rate of HDDW1 ( $Q_{\text{HDDW1}}$ ) during the recovery phase. Because HDDW2 operates during infiltration, storage, and recovery, its total discharge will be much higher than the discharge of HDDW1.

### Practical implementation of the automated control unit in 2017

In 2017, the current set-up of the Freshmaker at Ovezande (Figure 7.11) was modified (Figure 7.12) in order to automate:

- A periodic backflush during infiltration, in order to reduce clogging of the infiltration well (HDDW1). This required an additional pump, automatic valves, and a timer.
- Interception of saltwater by HDDW2, based on abstracted EC.

CURRENT

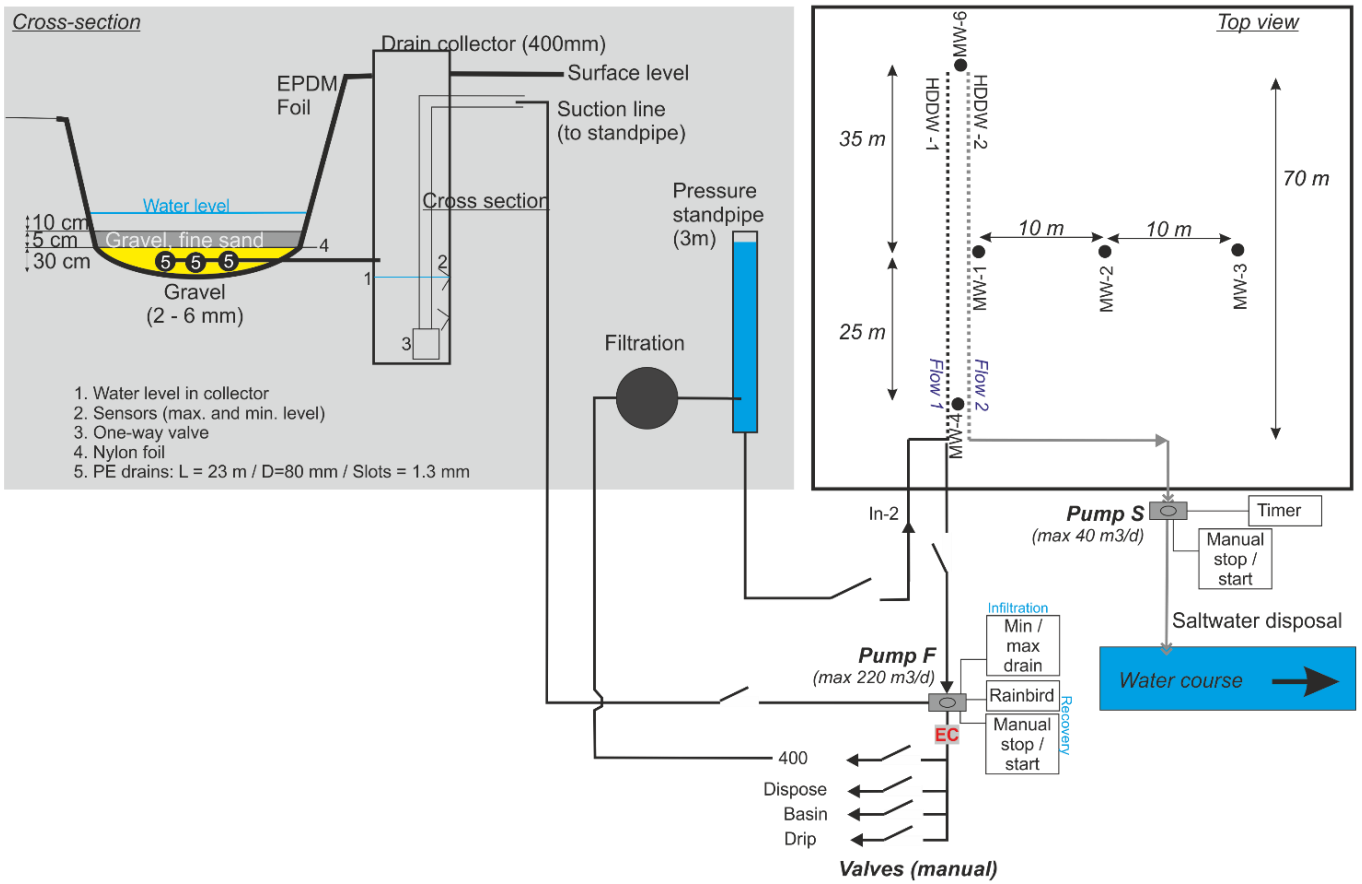


Figure 7.11: Current set-up of the Freshmaker, manually controlled. '400' = piping towards the 400 mm standpipe to provide infiltration pressure.

## FUTURE

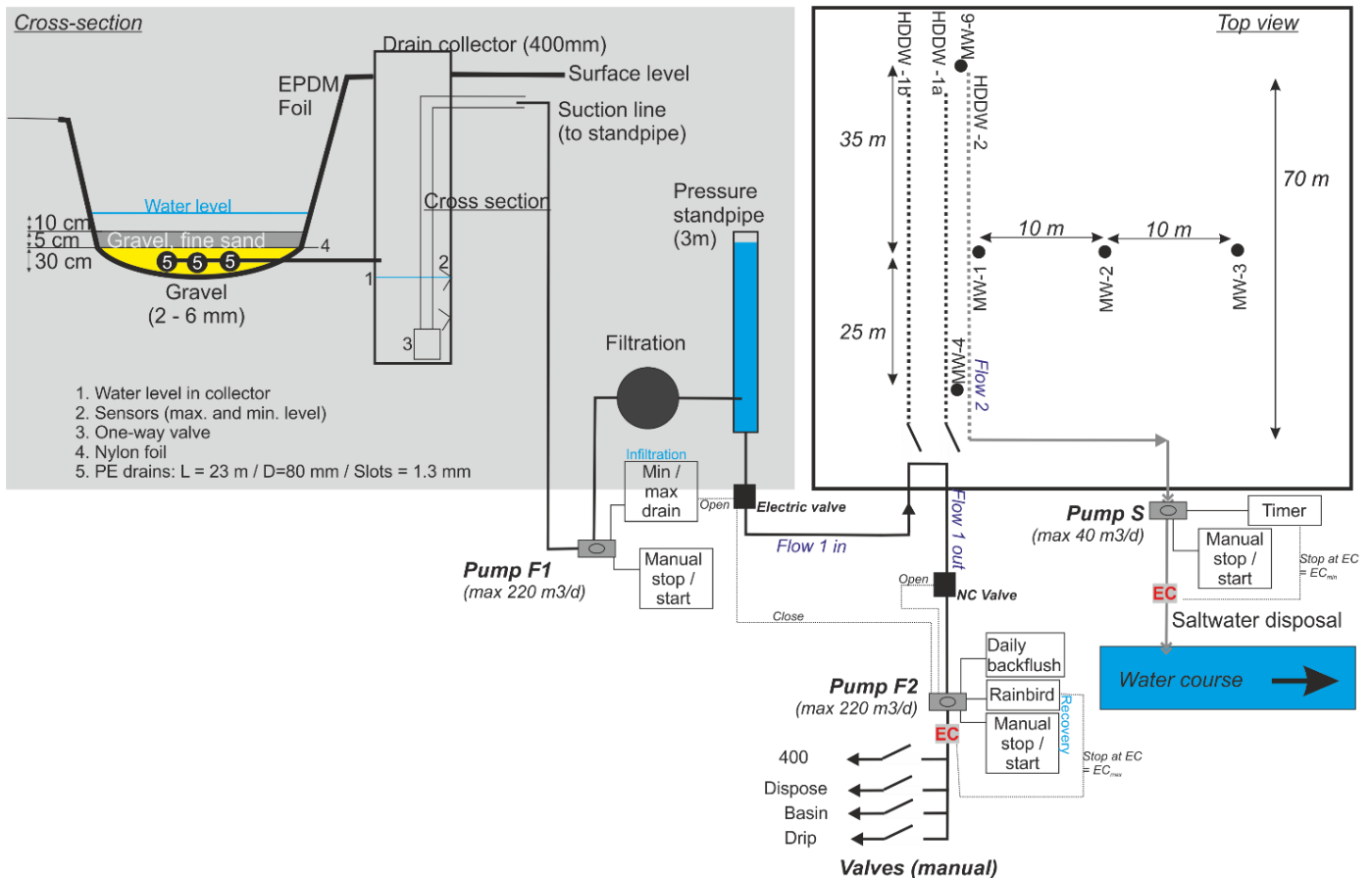


Figure 7.12: Future set-up of the Freshmaker, automatically controlled. '400' = piping towards the 400 mm standpipe to provide infiltration pressure.

### 7.3. Maximum storage capacity at Ovezande

The 3D SEAWAT model was also used to simulate several scenarios with variable target volumes and variable HDDW2 pumping rates to analyse the maximum storage capacity (here: equivalent to the recoverable volume) at Ovezande (Figure 7.13). The Freshmaker appeared to have an optimum storage capacity of 6000 m<sup>3</sup> that could achieve a recovery efficiency of 100% after multiple ASR cycles. The recovery efficiency significantly decreased when larger target volumes were simulated. The optimum capacity of 6000 m<sup>3</sup> could only be achieved with a HDDW2 pumping rate of 44 m<sup>3</sup>/d, or a pumping ratio ( $Q_{HDDW1} / Q_{HDDW2}$ ) of 1.5. Decreasing the pumping rate of HDDW2 resulted in a lower maximum target volume according to the model, which might overestimate the encroachment of saltwater when compared to the field observations.

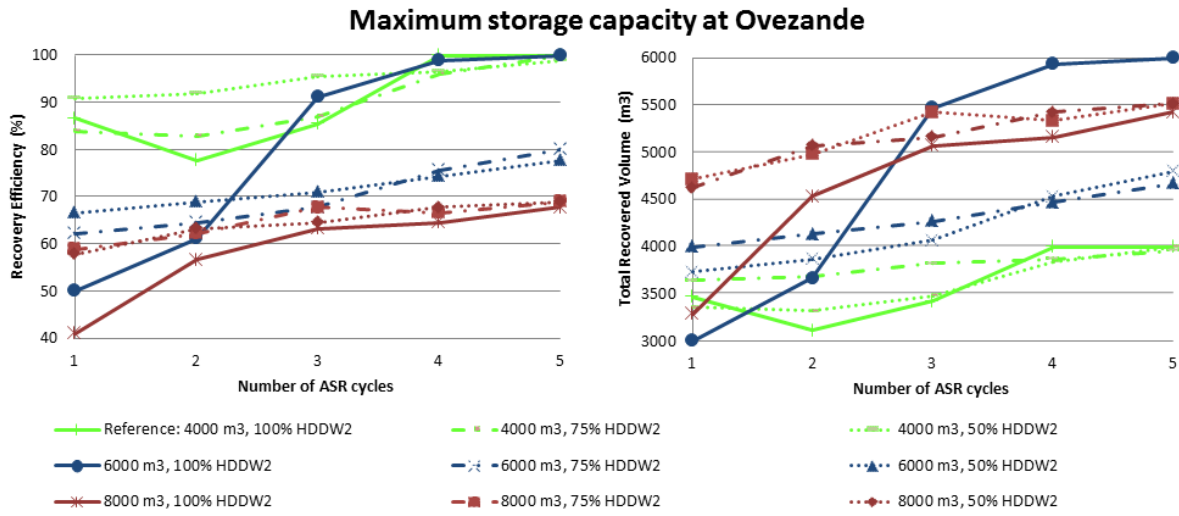


Figure 7.13: Maximum storage capacity at Ovezande. Left: the effect of different target volumes and HDDW2 pumping rates on the RE, right: the effect on the total recovered volume.



## 8. Pre-treatment using river-bed filtration

In order to better pre-treat the surface water used for infiltration by removal of suspended solids, a river-bed filtration system was designed and implemented at the Ovezande field site (see Chapter 2.5). Despite the elegant integration in the existing water course and low energy consumption (only a small pump was required to feed HDDW1, but not for pre-treatment), the results up to now were not fully satisfying:

- Clogging of the top layer and the nylon resulted in a low capacity and required regular cleaning (brushing) of the sand filter to maintain capacity. In the winter 2016/2017, the capacity was further reduced (Figure 8.1) due to a very low water level in the water course (less than 5 cm of water left on the filter), which was a consequence of a relatively dry winter;
- The modified fouling indexes (MFIs) of the pre-treated water were still relatively high (Table 8.1), especially at the start of pre-treatment. Desirable is <4 for infiltration via wells.

In 2017, a couple of improvements will be realized to improve the filtration and the sustainable capacity of the pre-treatment:

- The gravel was cleaned and a layer of sand (1 – 2 mm) was placed on top of the gravel to capture the fines and prevent deep penetration of fines into the gravel towards the drains;
- A small and adjustable dam will be installed in order to keep the water level in the water course much higher and increase the pressure on the filter bed and thereby the flow to the drains.
- Cleaning the filter using the flotation principle (by injection air in the gravel bed via tubes) was tested shortly in 2016 and will be used at a higher frequency in 2017.

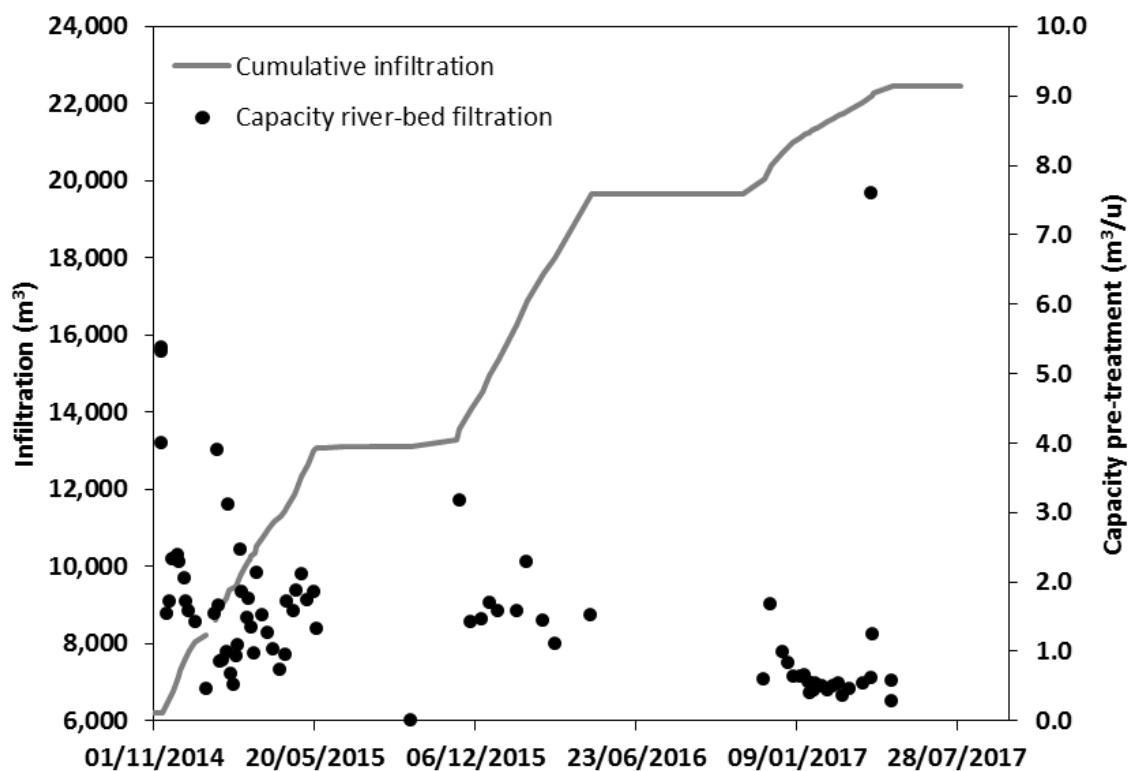


Figure 8.1: Cumulative infiltration and pre-treatment capacity of the river-bed filtration

Table 8.1: Measurements of the modified fouling index (MFI) upon infiltration by HDDW1.

Date	MFI (s <sup>2</sup> /l)
13/02/2015	37.5
06/03/2015	37.5
15/04/2015	36.0
27/01/2016	11.0
28/04/2016	6.9
Average	25.8

## 9. Low-cost HDDW: experiences with maintenance and replication

The development of robust, cost-effective, and long-lasting horizontal directional drilled wells (HDDWs) is vital for further application of the Freshmaker. At the Freshmaker reference site, two 75 mm perforated HDPE pipes wrapped in geo-textile were used for construction of the well screens. Two strategies were applied to further develop the use of this relatively simple HDDW type:

1. Analysis of clogging and mechanical and chemical well regeneration to mitigate clogging at the Freshmaker reference site in Ovezande
2. Installation of two HDDWs at the 'Groede' site (Figure 9.1):
  - a. HDDW with a well screen similar to the Ovezande site (Figure 9.2);
  - b. HDDW with a PVC wire-wrapped well screen instead of the HDPE wrapped in geotextile.



Figure 9.1: Locations of the Groede and the Ovezande sites.



Figure 9.2: Left: well type used at the Ovezande reference site: HDPE wrapped in Geotextile (75 mm). The deeper HDDW2 was protected by a 125 mm perforated HDPE pipe (right)

## Mechanical and chemical well regeneration Freshmaker

### Observations with respect to well clogging

During the first years of operation of the Freshmaker, it was observed that:

- The recovery capacity of the freshwater HDDW1 (at a vacuum of 0.6 bar) decreased from approximately 7 m<sup>3</sup>/h (in 2013) to a minimum of 0.5 m<sup>3</sup>/h (2014) in the infiltration seasons (Figure 9.3). Consequently, insufficient capacity is at hand to feed the drip irrigation.
- During the last cycles, a maximum capacity upon regeneration of 4.5 m<sup>3</sup>/h is attained.
- Upon the realisation of the sand filter for pre-treatment, the reduction in infiltration capacity during infiltration stages was reduced.
- The HDDW2 (placed in the saline groundwater) showed no loss of capacity.

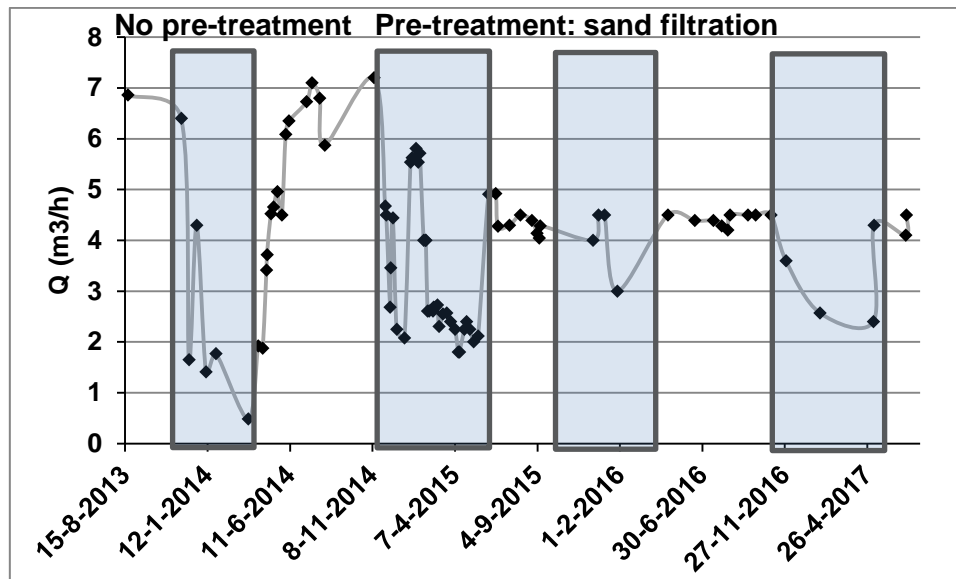


Figure 9.3: Maximum capacity of HDDW1 observed during the Ovezande Freshmaker pilot. Infiltration stages are marked in blue.

### Camera inspections (January 27, 2016)

With a Pearpoint Flexiprobe P342 camera, HDDW1 and HDDW2 were inspected (Figure 9.4 and Figure 9.5). It was shown that HDDW2 is still relatively clean after 3.5 years of operation (besides some sand on the bottom). In HDDW1, however, significant biogrowth in the well was observed. Sand at the bottom was also observed at the centre of HDDW1. It was obvious that infiltration of the nutrient rich surface water with a relatively high concentration of assimilable organic carbon (AOC) (total: 29 µg/l measured on February 2, 2015) in combination with a relatively high concentration of total suspended solids (TDS) (460 mg/l, of which 240 mg/l organic matter) induced biological growth in the well.

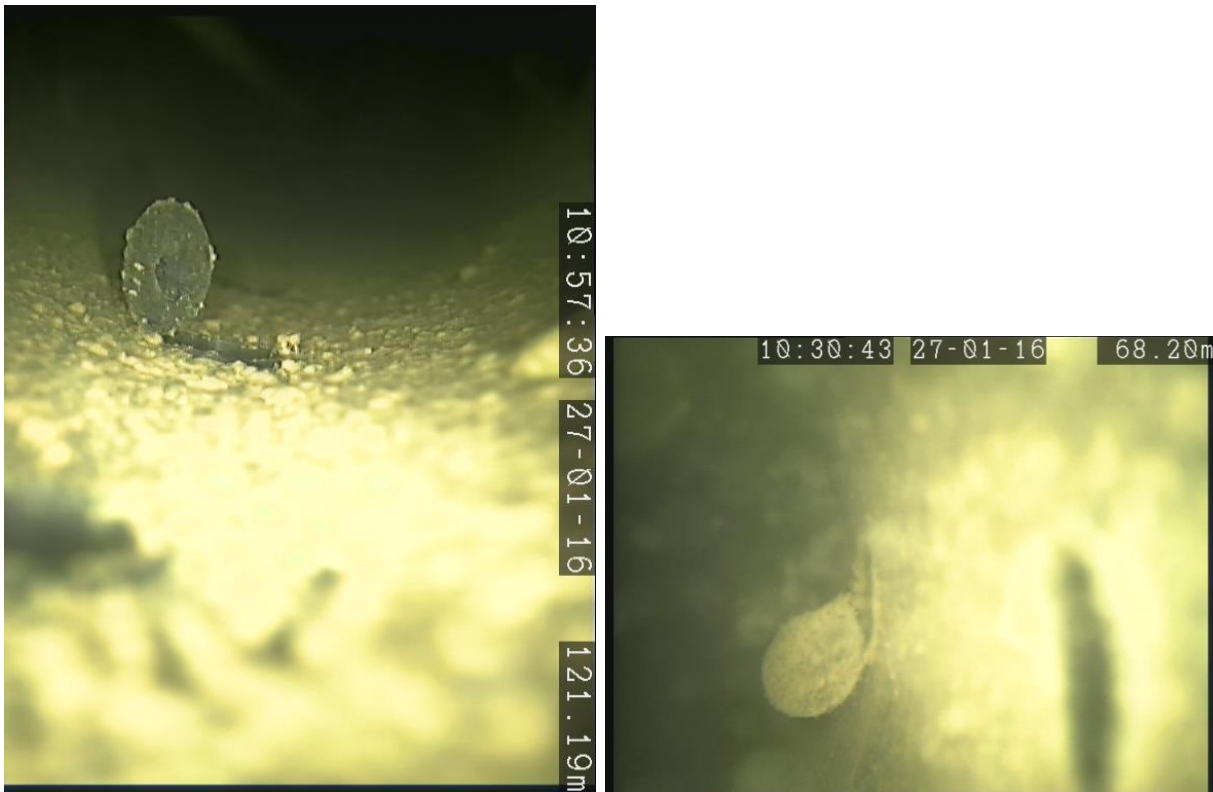


Figure 9.4: Biological growth inside HDDW1.



Figure 9.5: A relatively clean HDDW2, despite some sand on the bottom.

## Applied well regenerations, results

Over the years, several attempts were made to restore the well capacity at the end of the infiltration stages (Table 9.1). It was found that the HDDW improved both visually and in its capacity by chemical treatment (Figure 9.6 to Figure 9.9). Based on the hydrochemical observations in 2016 (Table 9.2), most of the oxidation during treatment was with organic matter in / around the HDDW, as indicated by the relation between  $\text{HCO}_3$ , TOC, and Cl (Figure 9.10 and Table 9.2).

Table 9.1: Capacities and regenerations 2013-2017

Date	Infiltration that season (m <sup>3</sup> )	Initial capacity	Treatment	Upon regeneration
<b>2013</b>	1,729	~7 m <sup>3</sup> /h	None	6.9 m <sup>3</sup> /h
<b>28-3-2014</b>	4,483	0.5 m <sup>3</sup> /h	30 L <b>Na-hypochlorite</b> (13.8%) in 1.5 m <sup>3</sup> water	6.0 m <sup>3</sup> /h direct 6.7 m <sup>3</sup> /h after 2 months
<b>5-6-2015</b>	6,884	2.4 m <sup>3</sup> /h	17 L <b>H<sub>2</sub>O<sub>2</sub></b> (35%) in 1.5 m <sup>3</sup> water	6.0 m <sup>3</sup> /h direct. Back to 4.5 m <sup>3</sup> /h after 2 months
<b>28-4-2016</b>	6,373	3.0 m <sup>3</sup> /h	Jetting Chemical cleaning (40 L <b>Na-hypochlorite</b> (13.8%) in 1.5 m <sup>3</sup> water)	6.0 m <sup>3</sup> /h upon regeneration Back to 4.5 m <sup>3</sup> /h after 2 months
<b>8-5-2017</b>	2,800.7	2.5 m <sup>3</sup> /h	Chemical cleaning ( <b>Na-hypochlorite</b> (13.8%) in 1.5 m <sup>3</sup> water)	4.3 m <sup>3</sup> /h (potentially air entrapped in suction line)
<b>14-6-2017</b>	2,800.7	4.3 m <sup>3</sup> /h	Chemical cleaning (40 L <b>Na-hypochlorite</b> (13.8%) in 1.5 m <sup>3</sup> water)	4.5 m <sup>3</sup> /h (potentially air entrapped in suction line)

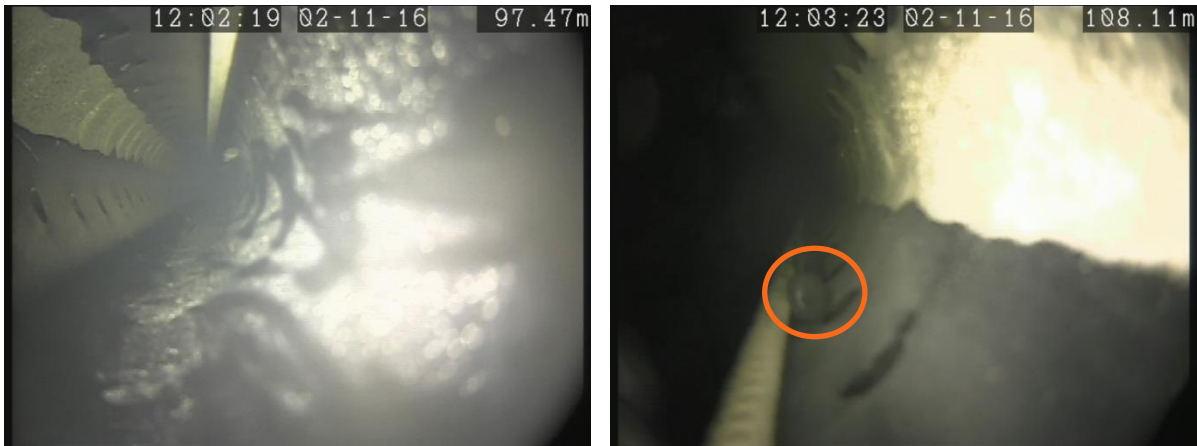


Figure 9.6: Condition of HDDW1 at the end of the recovery stage in 2016. Opening with remaining HDPE from drilling the holes indicated in the right figure.

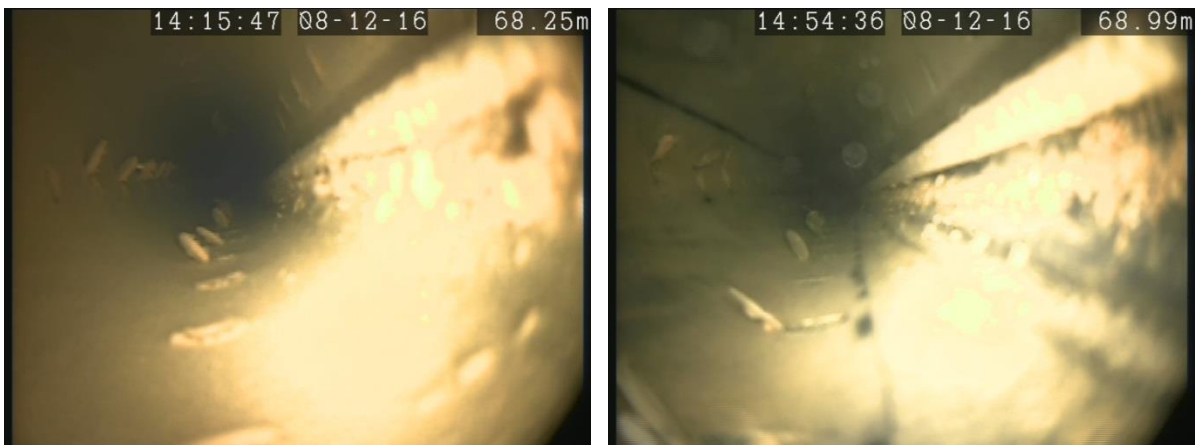


Figure 9.7: Condition of HDDW1 after one month of infiltration at the end of 2016 (before and after backflushing of the well).

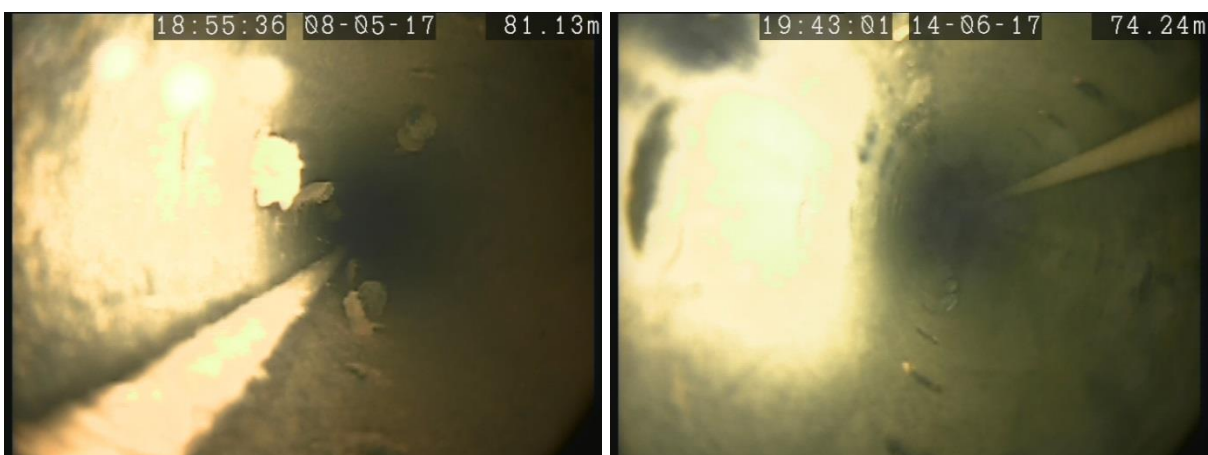


Figure 9.8: Condition of HDDW1 at the end of the infiltration stage in 2017 and after chemical cleaning with Na-hypochlorite (once).



Figure 9.9: Condition of HDDW1 in 2017 after chemical cleaning with Na-hypochlorite (second time, June, 2017).

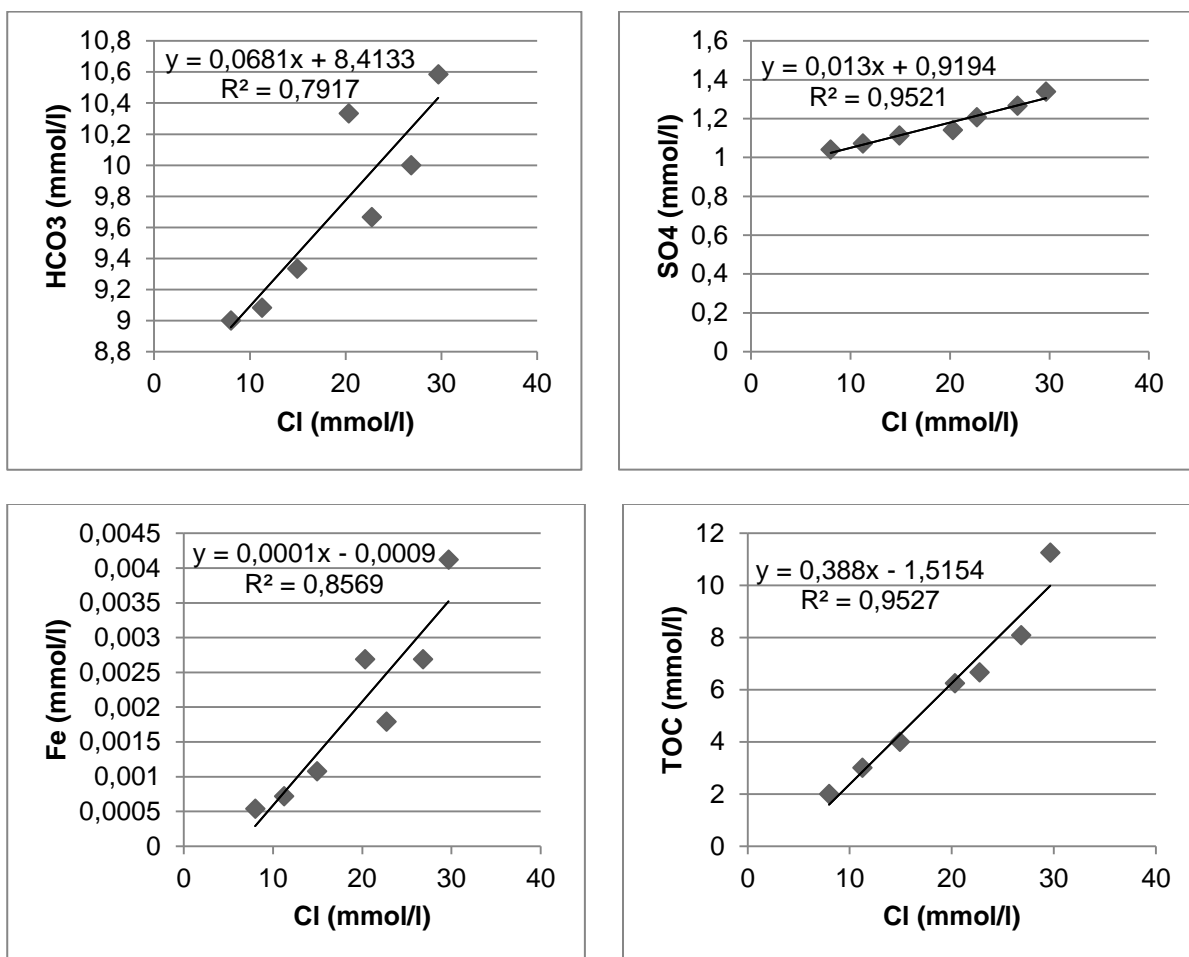


Figure 9.10: Hydrochemical observations during cleanpumping upon treatment with Na-hypochlorite.

Table 9.2: Estimated consumption of Na-hypochlorite based on recovered concentration with respect to Cl (based on methodology by Van Beek and Kooper, 1980<sup>1</sup>)

Process	Relation used (in moles)	Calculated consumption of Na-hypochlorite
<b>Oxidation of Fe-sulphides</b>	$\Delta\text{SO}_4 / \Delta\text{Cl}$	9 % (max 1.3% to $\text{Fe}(\text{OH})_3$ 8-9% to $\text{SO}_4$ )
<b>Oxidation of SOM to <math>\text{HCO}_3</math></b>	$\Delta\text{HCO}_3 / \Delta\text{Cl}$	27 %
<b>Oxidation of SOM to TOC</b>	$\Delta\text{TOC} / \Delta\text{Cl}$	presumably the rest, based on high $\Delta\text{TOC} / \Delta\text{Cl}$

### Installation of new HDDWs at the Groede site

At Groede (Province of Zeeland, Figure 9.1), two attempts were made to install new HDDWs within in the Subsol project, in order to further develop a robust HDDW set-up. The main difference was in the choice of materials:

1. A similar well to the Ovezande site (75 mm HDPE, wrapped in nylon textile, Table 9.3), made by the installer;
2. A more sophisticated PVC wire-wrapped (type: Boode CSS, 75 mm, slot size: 0.3 mm, Figure 9.11 and Table 9.3) selected by KWR and supplied by Boode Zevenhuizen (The Netherlands). This well screen was selected because of its large open area, small slot size, and acceptable costs.

Each well was placed in a perforated 125 mm HDPE pipe in order to pull in the well and protect the well screen (Figure 9.12). This perforated pipe was left behind and should permit sand and water to flow in, the inner well screens were to separate the water and the sand.

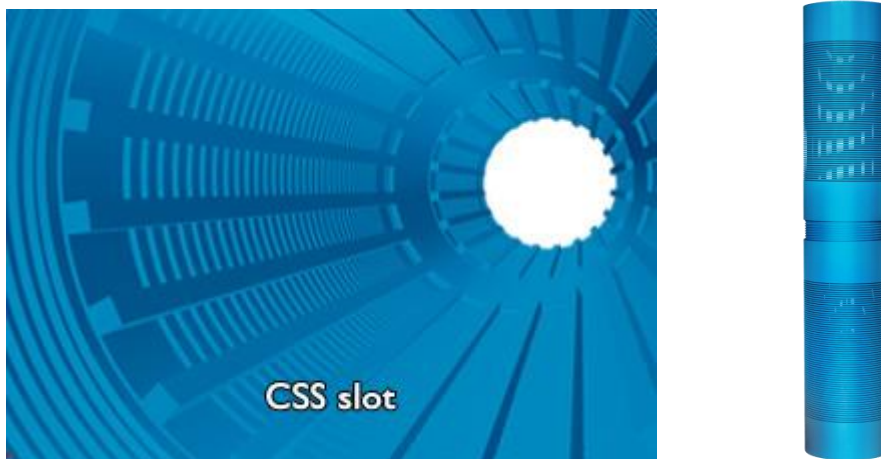


Figure 9.11: The Boode CSS well screen ([www.boode.com](http://www.boode.com))

<sup>1</sup> Van Beek, C.G.E.M en W.F. Kooper, 1980. The clogging of shallow discharge wells in the Netherlands river region. *Ground Water*, 18(6): 578-586.

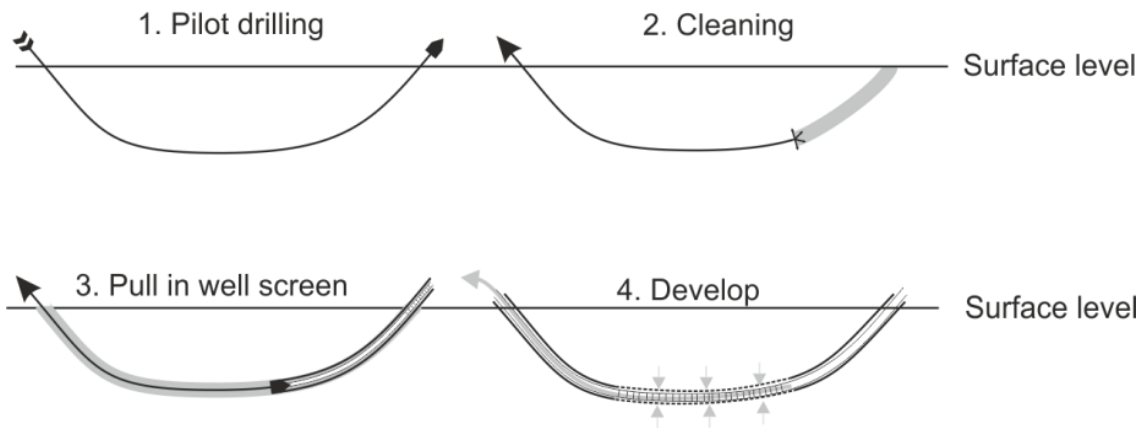


Figure 9.12: Drilling and installation strategy

Table 9.3: Characteristics of the wells applied at the Groede site

Characteristic	1. HDPE in textile	2. Boode CSS (PVC)	Outer HDPE (1 and 2)
<b>Diameter</b>	75	75	125
<b>Slot/hole size</b>	10 mm (8 rows, one hole every 68 mm)	0.3 m	10 mm (8 rows, one hole every 40 mm)
<b>Open area</b>	2%	6%	3.9%
<b>Total length</b>	200 m	130 m	200 m / 130 m
<b>Length well screen</b>	120 m	70 m	200 m / 130 m
<b>Depth</b>	10 m	10 m	10 m

### Attempt 1: HDPE wrapped in simple textile

In September 2016, the simple HDDW wrapped in textile was successfully installed within exactly one working day. During development (clean pumping), however, it was observed that a lot of sand was produced with the water abstracted. During cleanpumping of the well, high and continuous recovery rates were not attained. In order to clarify potential causes, a camera inspection was executed by KWR on December 8, 2016. The camera inspection showed a clear inflow of sand at 2/3 of the HDDW well screen (Figure 9.13). The sand accumulated at the bottom of the HDDW and clearly flowed towards the suction line, which therefore got clogged.

An attempt was made to re-line the HDDW with a 50 mm PVC slotted well screen, after cleaning the well with the drilling rig (like a pilot drill). However, the 75 mm well screen was

largely pushed out of the 125 mm HDPE pipe during this process. This revealed the damaged textile (Figure 9.14), which was the cause of the inflow of sand, but also hampered further successful re-lining. The first HDDW was therefore abandoned.

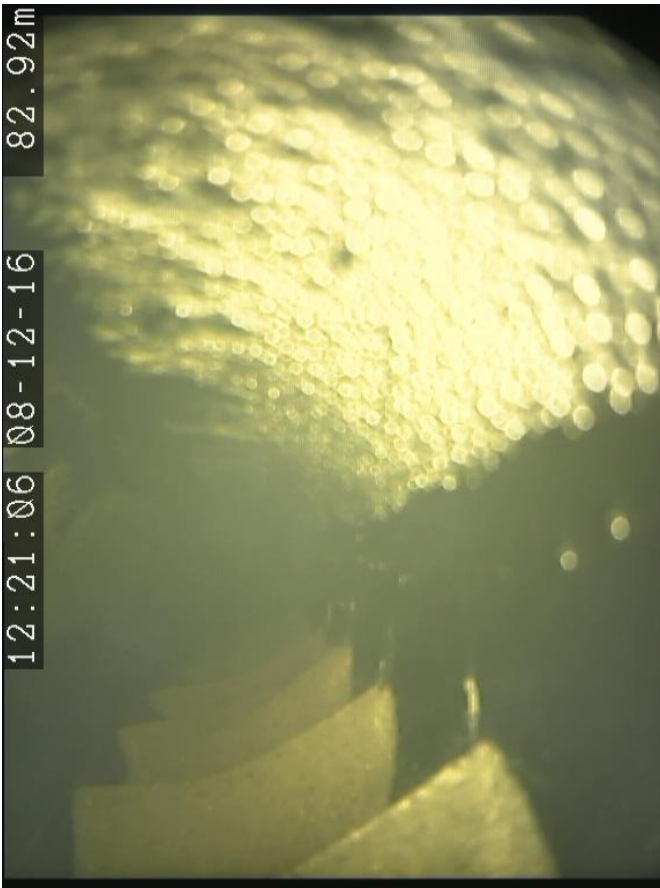


Figure 9.13: Sand at the bottom of the first HDDW in Groede, ripples formed in the direction of the suction line.



Figure 9.14: Damaged textile around the HDDW Groede, creating inflow of sand.

### Attempt 2: The wire-wrapped PVC CSS well screen

On July 5, 2017, the second HDDW well was installed at the Groede site, again within one working day. The PVC well screen segments could be connected and inserted in the outer 125 mm HDPE pipe since they are provided with C-Type female flush butt joints with male adaptors. On July 6, 2017, the well was not able to produce water yet because of the heavy drilling fluid present in the well. The following strategy was applied under supervision of KWR:

- 2 hours of high pressure-cleaning with a conventional drain cleaner;
- introduction of Aqua-Clear PFD (Baroid, USA) dispersant (4 L added to 1 m<sup>3</sup> of water), using the HD-cleaners as tremie line to introduce the product in the screened area (Figure 9.15);
- The well was left like this for 24 h ;
- After 24 h, cleanpumping of the well was started. The water was pumped to waste until the turbidity cleared up. After that moment, the water was pumped to the basin of the local orchard.

After a few days, the capacity reached the maximum capacity of the pump mounted to the suction line (20 m<sup>3</sup>/h) and remained stable for four weeks of pumping. After these four weeks, a minimal presence of sand was observed in the abstracted water. It was concluded that installation of this well was a success.



Figure 9.15: HD-cleaning of the second HDDW (CSS Boode) in Groede on July 6, 2017

### Financial impact of the examined HDDW well screens

In order to further evaluate choices for the different HDDW well screens, the costs of the different options were analysed. Drilling costs were not evaluated here, because they are equal for all choices (approximately 10.000 euro). Same holds for the blind sections from the well screen to the surface level (2700 euro). An alternative to the tested materials is the stainless steel well, which was also evaluated. These wells have been used before in groundwater remediation projects, but there is little data on their long-term functioning.

In Figure 9.16, it is shown that the CSS Boode, which proved itself a viable alternative, is virtually as expensive as the HDPE wrapped in textile. The stainless steel options do not require protection by the 125 mm HDPE perforated casing, but they still come with higher costs.

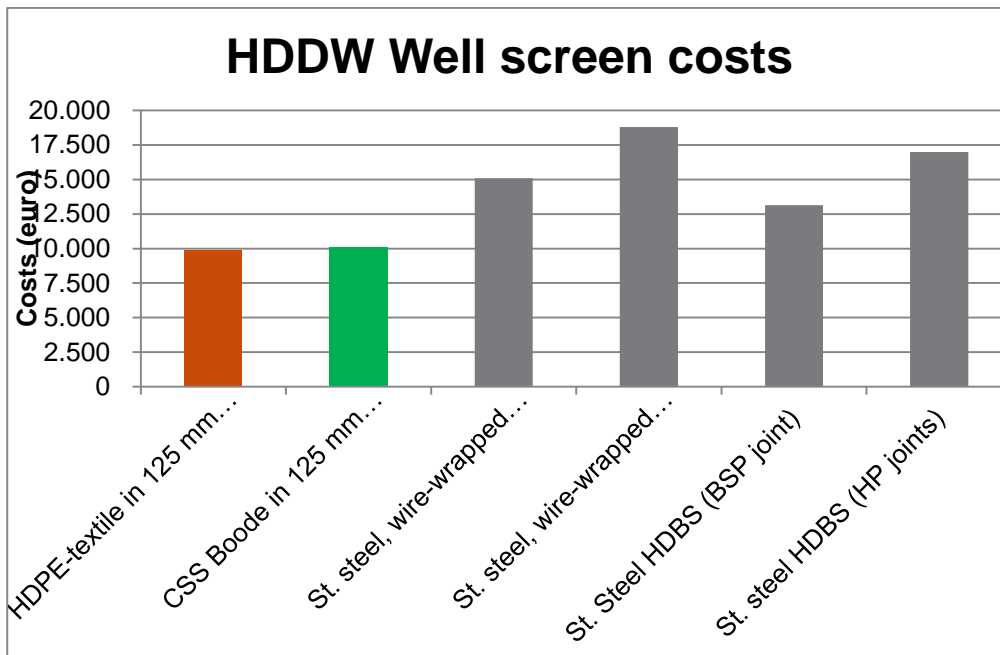


Figure 9.16: Costs for well screen material based on Well 2 in Groede (70 m long, 75 mm).

## Implications for the future use of HDDW technology for the Freshmaker

The observations made from 2013 to 2017 have the following impact for robust, cost-efficient HDDWs, and therefore on the market penetration of the Freshmaker:

1. The well screen type used for the first Freshmaker at the Ovezande reference site (HDPE wrapped in geo-textile) should not be preferred in future Freshmaker projects:
  - a. This well screen seems to be sensitive to clogging during infiltration because complete recovery of the initial capacity by mechanical and chemical regeneration was not attained;
  - b. During installation of this well, damage to the wrapped textile can occur, which will lead to invasion of sand in the well, making the well useless.
2. The wire-wrapped PVC seems to be a viable alternative based on its ease of installation, performance, and costs.
3. Stainless steel has the potential to be another technically viable alternative, but it can be expected that the costs will be significantly higher.

At the Ovezande site, the clogging observed is clearly caused by biogrowth in and around the HDDW, which is caused by the growth potential in the infiltration water (surface water,

high concentrations of nutrients, AOC). It was shown that chemical cleaning (using  $H_2O_2$  and Na-hypochlorite) can be used to partially restore the capacity. Additionally, it was decided that an automated backflush should be introduced to the automated control unit of the Freshmaker to prevent excessive clogging during the infiltration season (Figure 9.7). A 5 m deep drain was added right above the HDDW1 by the fruit grower in Ovezande to ensure sufficient recovery of freshwater in the summer seasons (Figure 9.17). This deep drain provides extra recovery capacity.

It should be noted that the excessive clogging at the Ovezande site is related to the source of the water (surface water). Clogging would have been significantly less with the water from the Dinteloord site (RO-treated waste water) or the ASR-Coastal site (rainwater).



Figure 9.17: Installation of the 5 m deep drain to increase the freshwater recovery in Ovezande in June 2017

## 10. Cost analysis Freshmaker Ovezande

The costs of the Freshmaker in Ovezande were analysed, taking into account:

- The true costs required to build the current installation;
- National subsidies for investment in sustainable technologies like ASR (MIA/Vamil);
- Operational and energy costs;
- Depreciation (in 10 years);
- Re-investments to keep the scheme running (pumps).
- Tax shield: as a consequence of depreciation, less profit tax has to be payed;
- Financing (incl. interest);
- Costs discounted at a discount rate of 3%;
- An economic lifespan of 20 years (wells, pipelines, central control unit should make this without re-investments);
- The total production of freshwater during the lifespan,

The alternative (an aboveground basin) was also analysed with the same model, taking into account the loss of net income by the claim on aboveground agricultural land (fruit orchard: pears) (Table 10.1).

Table 10.1: Input for Freshmaker cost analysis

Parameter	Unit	Input
<b>Freshmaker</b>		
Lifespan Freshmaker	yr	20
Yearly recovery	m <sup>3</sup> /yr	6,000
Yearly infiltration	m <sup>3</sup> /yr	6,000
Depreciation period	yr	10
Discount rate	%	3
Energy price	€/kWh	0.16
Maintenance	€/yr	250
Initial investment	€	55,000
<b>Basin</b>		
Lifespan Basin	yr	15
Depreciation period	yr	10
Loss of net income	€/m <sup>2</sup>	1.2
Surface area	m <sup>2</sup>	0
Basin volume	m <sup>3</sup>	6,000
Basin surface	m <sup>2</sup>	3,740
Costs for realisation	€/m <sup>3</sup>	6.15
Loan duration	yr	5
Interest	%	3

It was found that the Freshmaker produces cheaper water than the current alternative for storage (above ground basins) (Table 10.2), which is primarily due to the longer lifetime and the absence of loss of production by a spatial claim. Initial investments and operational costs are higher, compared to the alternative. Piped river water is locally available in the area, but is also more expensive per m<sup>3</sup>.

Table 10.2: Cost price of the produced irrigation water at the Freshmaker Ovezande site

Water source	Freshmaker	Aboveground basin	Piped water
Costs / m <sup>3</sup>	0.54	1.00	0.58

## 11. Conclusions

The Freshmaker Ovezande site has been operating from 2013 until 2017 (5 cycles). During these cycles, the system was able to store and supply around 5 000 m<sup>3</sup> per year. The system has an estimated maximum storage and recovery capacity of 6 000 m<sup>3</sup>, based on groundwater modelling. The abstraction of this maximum volume has not been required for irrigation to date. Based on measurements, the thickening occurs along the whole length of the HDDW.

Construction and maintenance of HDDWs and pre-treatment was identified as a key aspect for the success of a Freshmaker. A more robust and economically viable alternative for the Ovezande HDDWs was developed and successfully tested at the Groede site. Clogging of the shallow HDDW at the Freshmaker Ovezande was caused by insufficient pre-treatment (2013-2014) and biological growth in the well (2013-2017). Regeneration was successfully applied, but will (slightly) impact the operational costs.

Further automation of the Freshmaker's operation via an automated control unit has been designed and is to be implemented in Ovezande and at future Freshmaker sites to automate the process of infiltration and interception.

It was found based on modelling and field observations that the hydrological impacts of the Freshmaker on the surroundings are limited. The measurements and models suggest there is a stand-still situation or even gradual freshening of the groundwater at the Freshmaker site.

Infiltration of surface water poses water quality risks, mainly related to pesticides in this agricultural area. By limiting the infiltration period to 15 November – 15 April (winter season), potential exceedance of pollutant's maximum concentrations was merely prevented. It does highlight the vulnerability of any MAR solution using surface water in agricultural areas, however. For wide-spread application of MAR it will be vital to keep potential water resources (such as surface water, stormwater) clean such that they can be captured and stored at a local scale without requiring advanced and expensive treatment. The looming transition to more easily-degradable pesticides may contribute to this requirement.

Based on the construction costs, operational and energy costs, and spatial claim on agricultural land, the Freshmaker provides an economically very interesting alternative for irrigation water supply, with an estimated cost price of 0.54 eur/m<sup>3</sup>.



## 12. References

- Ayers, R.S., Westcot, D.W., 1976. Water quality for agriculture, Food and Agriculture Organization of the United Nations., Rome.
- Bear, J., 1972. Dynamics of fluids in porous media. American Elsevier, New York, U.S.A.
- Fipps, G., 2003. Irrigation water quality standards and salinity management strategies.
- Harbaugh, A.W., 2005. Book 6. Modelling techniques, Section A. Ground Water, MODFLOW-2005, The U.S. Geological Survey modular ground-water model - the groundwater flow process. U.S. Geological Survey Techniques and Methods.
- Konert, M., Vandenberghe, J., 1997. Comparison of laser grain size analysis with pipette and sieve analysis: a solution for the underestimation of the clay fraction. *Sedimentology*, 44(3): 523-535.
- Langevin, C.D., Thorne, D.T., Dausman, A.M., Sukop, M.C., Guo, W., 2007. SEAWAT version 4: a computer program for simulation of multi-species solute and heat transport. In: U.S.G.S. (Ed.), Techniques and Methods, book 6, Reston, Virginia, USA.
- McNeill, J.D., Bosnar, M., Snelgrove, J.B., 1990. Technical Note 25: Resolution of an Electromagnetic Borehole logger for Geotechnical and groundwater applications.
- Rowe, D.R., Abdel-Magid, I.M., 1995. Handbook of wastewater reclamation and reuse. CRC Press.
- Van der Linde, S., 2015. Optimizing the performance of the Freshmaker by studying different operational and hydrogeological variables. KWR2015.009, KWR Watercycle Research Institute Nieuwegein.
- Wallis, I. et al., 2011. Process-Based Reactive Transport Model To Quantify Arsenic Mobility during Aquifer Storage and Recovery of Potable Water. *Environmental Science & Technology*, 45(16): 6924-6931.
- Zuurbier, K.G., Kooiman, J.W., Groen, M.M.A., Maas, B., Stuyfzand, P.J., 2015. Enabling Successful Aquifer Storage and Recovery of Freshwater Using Horizontal Directional Drilled Wells in Coastal Aquifers. *Journal of Hydrologic Engineering*, 20(3): B4014003.



## A. Appendix

### Water quality analysis: observed groundwater (MW1)

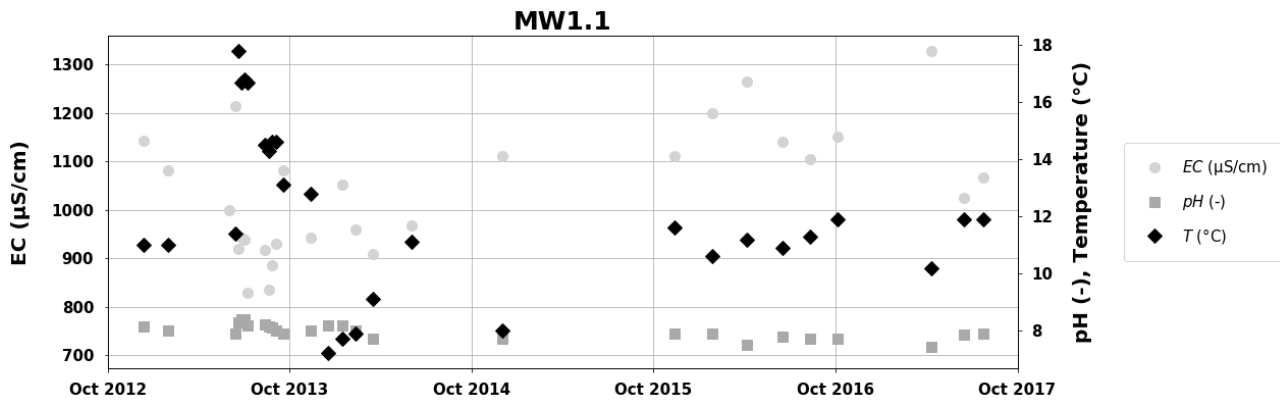


Figure A.1: Electrical conductivity (EC in  $\mu\text{S}/\text{cm}$ ), pH (-), and temperature (Temp in  $^{\circ}\text{C}$ ) of groundwater observed at the first screen of monitoring well 1 (MW1-S1).

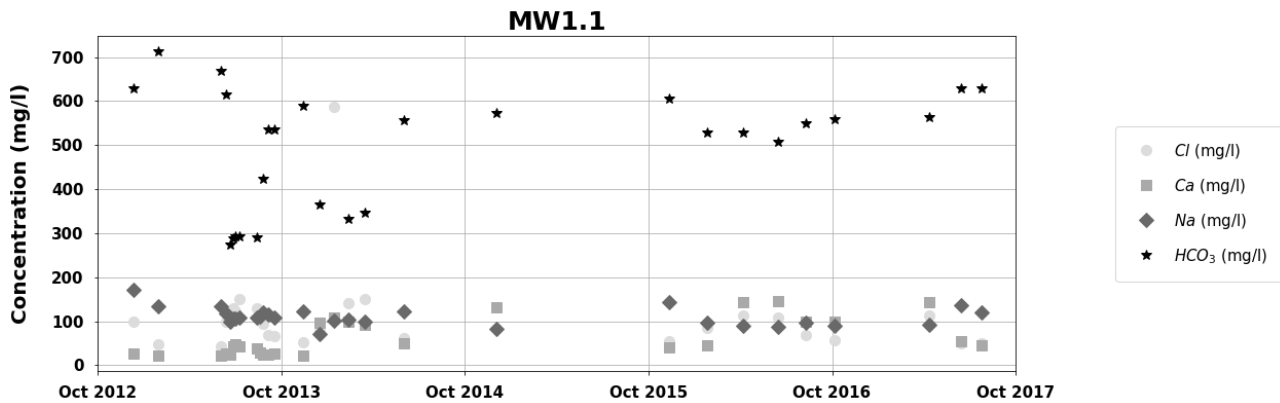


Figure A.2: Concentrations of Cl, Ca, Na, and HCO<sub>3</sub> in groundwater observed at the first screen of monitoring well 1 (MW1-S1).

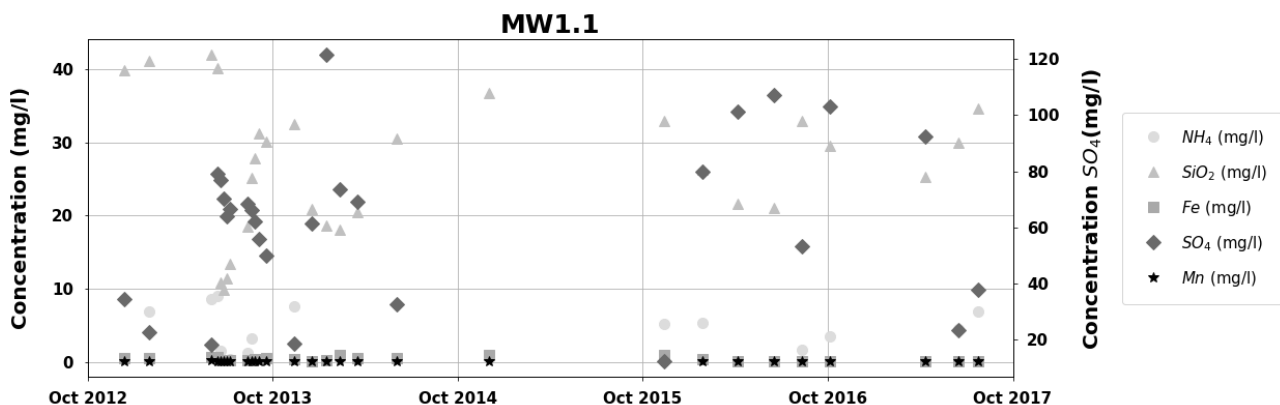


Figure A.3: Concentrations of NH<sub>4</sub>, SiO<sub>2</sub>, Fe, SO<sub>4</sub>, and Mn in groundwater observed at the first screen of monitoring well 1 (MW1-S1). Be aware that the concentrations of SO<sub>4</sub> are plotted on the secondary (right) y-axis.

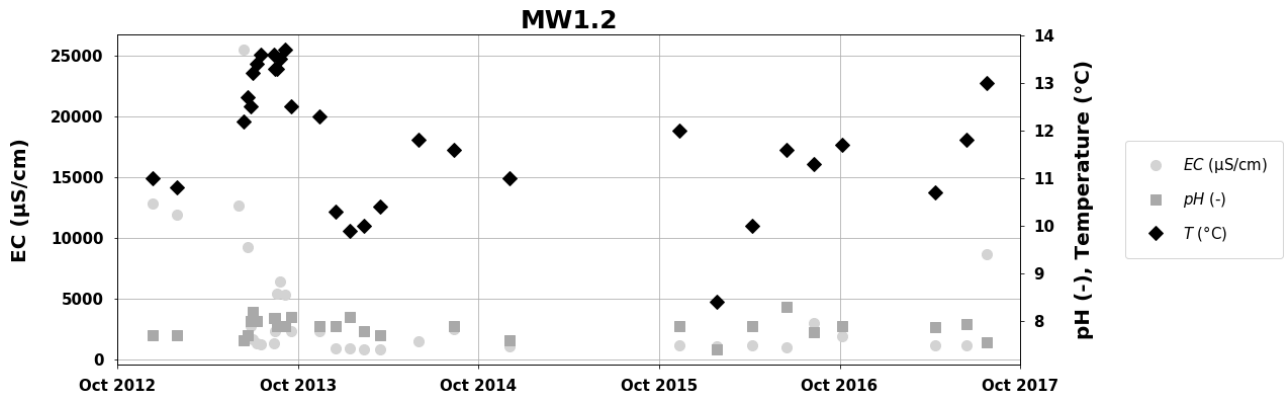


Figure A.4: Electrical conductivity (EC in µS/cm), pH (-), and temperature (Temp in °C) of groundwater observed at the second screen of monitoring well 1 (MW1-S2).

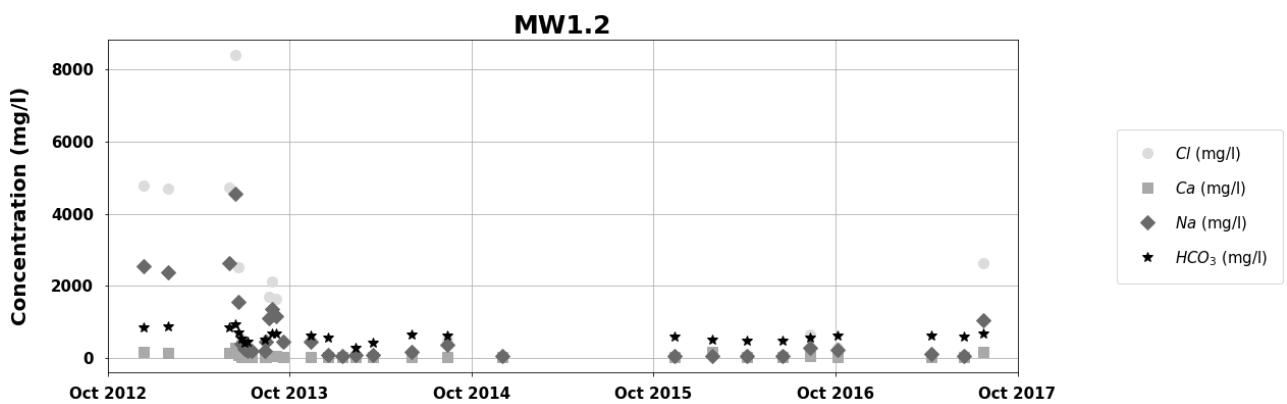


Figure A.5: Concentrations of Cl, Ca, Na, and HCO<sub>3</sub> in groundwater observed at the second screen of monitoring well 1 (MW1-S2).

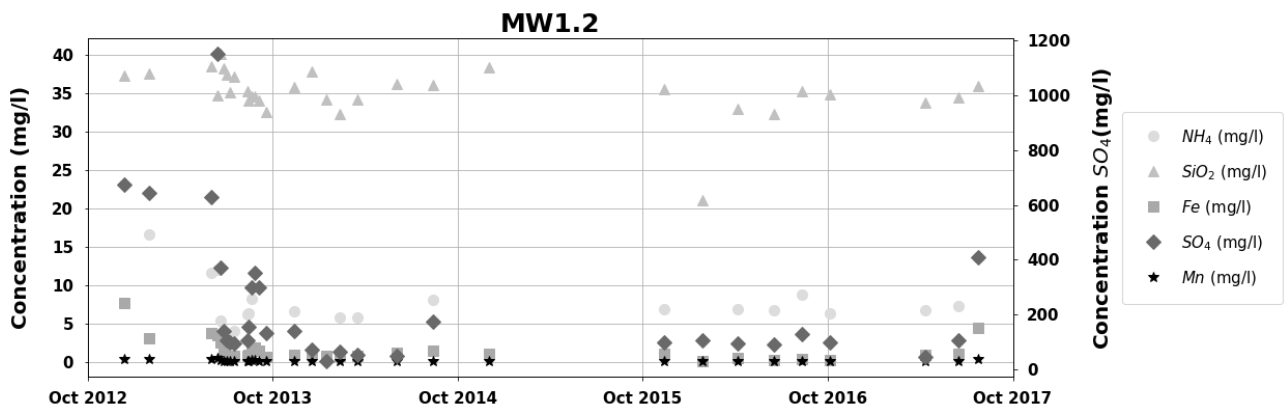


Figure A.6: Concentrations of NH<sub>4</sub>, SiO<sub>2</sub>, Fe, SO<sub>4</sub>, and Mn in groundwater observed at the second screen of monitoring well 1 (MW1-S2). Be aware that the concentrations of SO<sub>4</sub> are plotted on the secondary (right) y-axis.

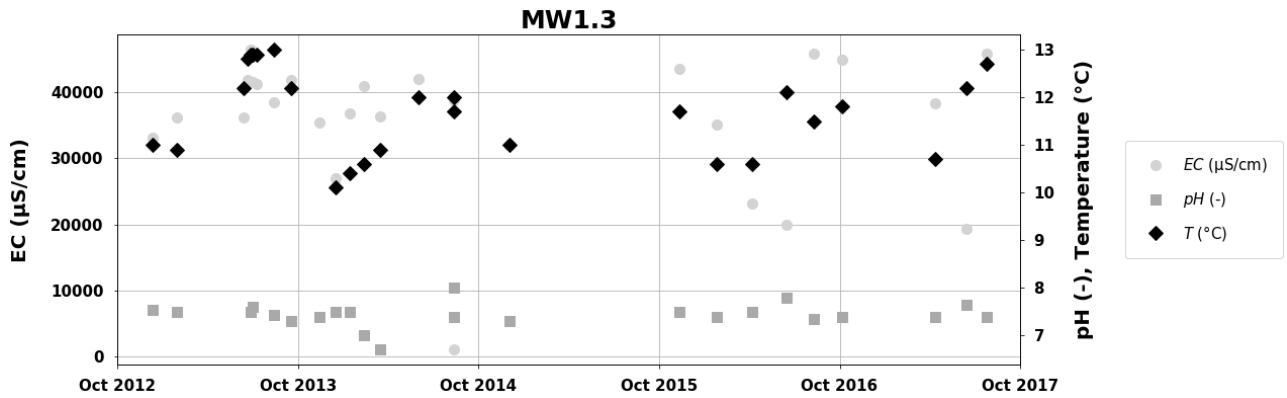


Figure A.7: Electrical conductivity (EC in µS/cm), pH (-), and temperature (Temp in °C) of groundwater observed at the third screen of monitoring well 1 (MW1-S3).

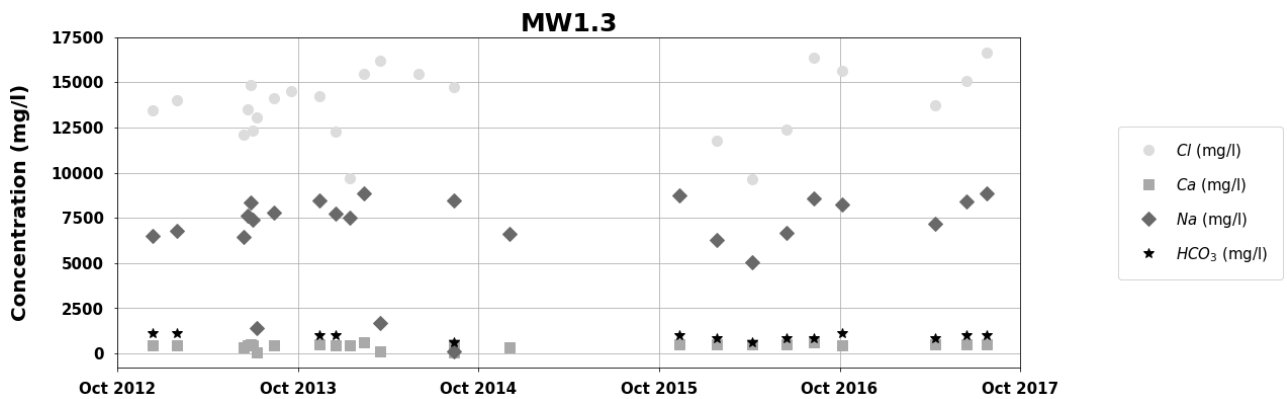


Figure A.8: Concentrations of Cl, Ca, Na, and HCO<sub>3</sub> in groundwater observed at the third screen of monitoring well 1 (MW1-S3).

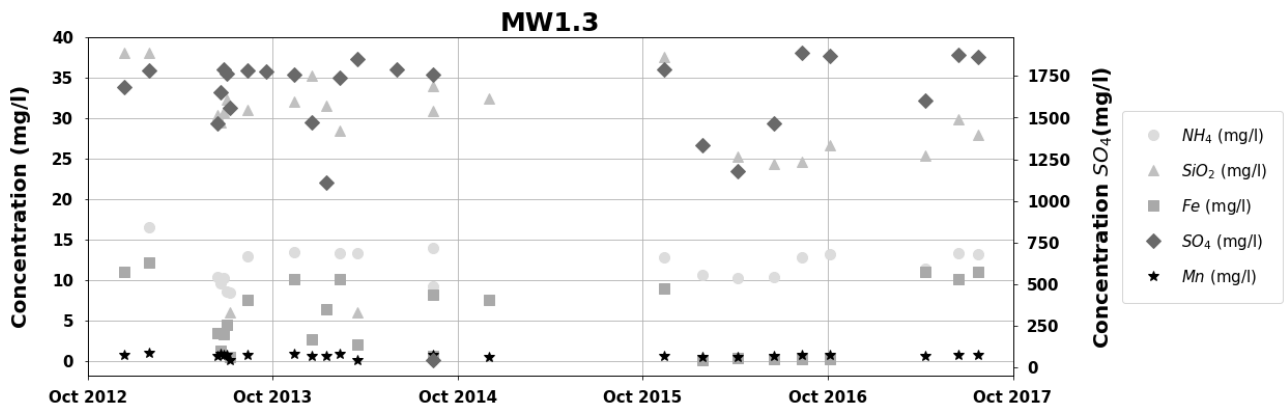


Figure A.9: Concentrations of NH<sub>4</sub>, SiO<sub>2</sub>, Fe, SO<sub>4</sub>, and Mn in groundwater observed at the third screen of monitoring well 1 (MW1-S3). Be aware that the concentrations of SO<sub>4</sub> are plotted on the secondary (right) y-axis.